Spring 2012

Virtual reality visual feedback and its effect on brain excitability

Soha Saleh
New Jersey Institute of Technology

Copyright Warning & Restrictions

The copyright law of the United States (Title 17, United States Code) governs the making of photocopies or other reproductions of copyrighted material.

Under certain conditions specified in the law, libraries and archives are authorized to furnish a photocopy or other reproduction. One of these specified conditions is that the photocopy or reproduction is not to be "used for any purpose other than private study, scholarship, or research." If a, user makes a request for, or later uses, a photocopy or reproduction for purposes in excess of "fair use" that user may be liable for copyright infringement,

This institution reserves the right to refuse to accept a copying order if, in its judgment, fulfillment of the order would involve violation of copyright law.

Please Note: The author retains the copyright while the New Jersey Institute of Technology reserves the right to distribute this thesis or dissertation

Printing note: If you do not wish to print this page, then select "Pages from: first page # to: last page #" on the print dialog screen

ABSTRACT

VIRTUAL REALITY VISUAL FEEDBACK AND ITS EFFECT ON BRAIN EXCITABILITY

by
Soha Saleh

This dissertation examines manipulation of visual feedback in virtual reality (VR) to increase excitability of distinct neural networks in the sensorimotor cortex. The objective is to explore neural responses to visual feedback of motor activities performed in complex virtual environments during functional magnetic resonance imaging (fMRI), and to identify sensory manipulations that could further optimize VR rehabilitation of persons with hemiparesis. In addition, the effects of VR therapy on brain reorganization are investigated. An MRI-compatible VR system is used to provide subjects with online visual feedback of their hand movement. First, the author develops a protocol to analyze variability in movement kinematics between experimental sessions and conditions and its possible effect on modulating neural activity. Second, brain reorganization after 2 weeks of robot-assisted VR therapy is examined in 10 chronic stroke subjects in terms of change in extent of activation, interhemispheric dominance, connectivity network of ipsilesional primary motor cortex (iM1) and the interhemispheric interaction between iM1 and contralesional M1 (cM1). After training, brain activity during a simple paretic hand movement is re-localized in terms of bilateral change in activity or a shift of interhemispheric dominance (re-lateralization) toward the ipsilesional hemisphere that is positively correlated with improvement in clinical scores. Dynamic causal modeling (DCM) shows that interhemispheric coupling between the bilateral motor cortices tends

to decrease after training and to negatively correlate with improvement in scores for clinical scales, and with the amount of re-lateralization. Third, the dissertation studies if visual discordance in VR of finger movement would facilitate activity in select brain networks. In a study of 12 healthy subjects, the amplitude of finger movement is manipulated (hypometric feedback) resulting in higher activation of contralateral M1. In a group of 11 stroke subjects, bidirectional, hypometric and hypermetric,VR visual discordance is used. Both feedback conditions cause small increase in activity of the iM1 contralateral to movement and stronger recruitment of both posterior parietal cortices and the ipsilesional fusiform gyrus (iFBA). Fourth, the effect of mirrored-visual feedback on the activity of the ipsilesional sensorimotor cortex of stroke subjects is examined. While subjects move the non-paretic hand during the fMRI experiment, they receive either veridical feedback of the movement or a mirrored feedback. The results show recruitment of iM1 and both posterior parietal cortices during the mirrored feedback. Effective connectivity analysis show increase correlation of iM1 and contralesional SPL (cSPL) with iFBA suggesting a role of the latter in the evaluation of feedback and in visuomotor processing. DCM analysis shows increased modulation of iM1 by cSPL area during the mirrored feedback, an observation that proves the influence of visual feedback on modulating primary motor cortex activation. This dissertation provides evidence that it is possible to enhance brain excitability through manipulation of virtual reality feedback and that brain reorganization can result from just two weeks of VR training. These findings should be exploited in the design of neuroscience-based rehabilitation protocols that could enhance brain reorganization and motor recovery.

VIRTUAL REALITY VISUAL FEEDBACK AND ITS EFFECT ON BRAIN EXCITABILITY

by
Soha Saleh

A Dissertation
Submitted to the Faculty of
New Jersey Institute of Technology
and University of Medicine and Dentistry of New Jersey
in Partial Fulfillment of the Requirements for the Degree of
Doctor of Philosophy in Biomedical Engineering

Joint Program in Biomedical Engineering

May 2012

APPROVAL PAGE

VIRTUAL REALITY VISUAL FEEDBACK AND ITS EFFECT ON BRAIN EXCITABILITY

Soha Saleh

Sergei V. Adamovich, Dissertation co-advisor — Date
Associate Professor of Biomedical Engineering, NJIT

Eugene Tunik, Dissertation co-advisor — Date
Assistant Professor of Rehabilitation and Movement Sciences, UMDNJ

Alma Merians, Committee member — Date
Chairperson and Professor, Department of Rehabilitation and Movement Sciences, UMDNJ

Richard Foulds, Committee member — Date
Associate Professor of Biomedical Engineering, NJIT

Jason Steffener, Committee member — Date
Assistant Professor, Columbia University
Adjunct Professor of Biomedical Engineering, NJIT

BIOGRAPHICAL SKETCH

Author: Soha Saleh

Degree: Doctor of Philosophy

Date: May 2012

Undergraduate and Graduate Education:

- Doctor in Philosophy in Biomedical Engineering,

  New Jersey Institute of Technology, Newark, NJ, 2012

- Master of Science in Biomedical Engineering
  New Jersey Institute of Technology, Newark, NJ, 2008

- Bachelor of Science in Computer and Communication Engineering

  American University of Science and Technology, Beirut, Lebanon, 2006

- Minor in Biomedical Engineering
  American University of Science and Technology, Beirut, Lebanon, 2006

Presentations and Publications:

Journal Papers

Eugene Tunik, Soha Saleh, Sergei Adamovich. Eliciting Ipsilesional Sensorimotor Areas Activation by Visual Discordance of Paretic Hand Movement in Virtual Reality (manuscript in preparation).

Soha Saleh, Sergei Adamovich, Hamid Bagce, Eugene Tunik. Cortical Reorganization after Robot Assisted Virtual Reality Training of Upper Extremity, (manuscript in preparation).

Soha Saleh, Sergei Adamovich, Eugene Tunik. Dynamic Causal Modeling Reveals a Change in Posterior Parietal Cortex and Motor Cortex Coupling during Mirror Visual Feedback (manuscript in preparation)

Soha Saleh, Sergei Adamovich, Hamid Bagce, Eugene Tunik. Mirror Feedback in Chronic Stroke: Recruitment and Effective Connectivity of Sensorimotor Networks, Brain, (submitted).

Eugene Tunik, Soha Saleh, Sergei Adamovich, Effects of Altered Feedback during Visually-Guided Hand Movement on Sensorimotor Circuits, Transactions on Neural Systems and Rehabilitation Engineering (invited paper, in review).

Hamid Bagce, Soha Saleh, Sergei Adamovich, John Krakauer, and Eugene Tunik, Learning-related corticospinal excitability changes following visuomotor gain adaptation, Journal of Neurophysiology (in review).

Hamid Bagce, Eugene Tunik, Soha Saleh, Sergei Adamovich, Visuomotor Gain Distortion Alters Online Motor Performance and Enhances Primary Motor Cortex Excitability in Patients with Stroke, Neuromodulation (accepted).

Gerard Fluet, Alma Merians, Qinyin Qiu, Ian Lafond, Soha Saleh, Viviana Ruano, Andrea Delmonico, and Sergei Adamovich, Physical therapist management of a patient with upper extremity hemiparesis utilizing haptic robots integrated with virtual reality simulations, Journal in Neurologic Physical Therapy (accepted).

Alma Merians, Gerard Fluet, Qinyin Qiu, Soha Saleh, Ian Lafond, Davidow, A., Sergei Adamovich, Robotically Facilitated Virtual Rehabilitation of Arm Transport Integrated With Finger Movement in Persons with Hemiparesis (2011) Journal of NeuroEngineering and Rehabilitation, p. 27.

Gerard Fluet, Qinyin Qiu, Donna Kelly, Heta Parikh, Diego Ramirez, Soha Saleh, and Sergei Adamovich, Interfacing a haptic robotic system with complex virtual environments to treat impaired upper extremity motor function in children with cerebral palsy (2010) Developmental Neurorehabilitation, 13 (5), pp. 335-345.

Qinyin Qiu, Diego A. Ramirez, Soha Saleh, Gerard Fluet, Heta Parikh, Donna Kelly, Sergei Adamovich (2009), The New Jersey Institute of Technology Robot-Assisted Virtual Rehabilitation (NJIT-RAVR) system for children with cerebral palsy: A feasibility study, *Journal of NeuroEngineering and Rehabilitation*.

Pubmed-Referenced Conference Papers

Soha Saleh, Sergei Adamovich, Eugene Tunik, Resting state functional connectivity and task-related effective connectivity changes after robot-assisted virtual reality rehabilitation, 2012 Annual International Conference of the IEEE Engineering in Medicine and Biology Society, EMBC'12, San Diego, CA, USA. (in review).

Soha Saleh, Hamid Bagce, Qinyin. Qiu, Gerard. Fluet, Alma Merians, Sergei Adamovich, Eugene Tunik, Mechanisms of Neural Reorganization in Chronic Stroke Subjects after Virtual Reality Training,) 2011 Annual International Conference of the IEEE Engineering in Medicine and Biology Society, EMBC'11, Boston, USA.

Hamid Bagce, Soha Saleh, Sergei Adamovich, Eugene Tunik, Visuomotor Discordance in Virtual Reality: Effects on Online Motor Control. 2011 Annual International Conference of the IEEE Engineering in Medicine and Biology Society, EMBC'11, Boston, USA.

Qinyin Qiu, Gerard Fluet, Soha Saleh, Ian Lafond, Alma Merians, and Sergei Adamovich, Integrated versus isolated training of the hemiparetic upper extremity in haptically rendered virtual environments. 2010 Annual International Conference of the IEEE Engineering in Medicine and Biology Society, EMBC'10, Argentina.

Peer-Reviewed Conference Papers

Eugene Tunik, Soha Saleh, Hamid Bagce,; Alma Merians, Sergei Adamovich, Mirror feedback in virtual reality elicits ipsilesional motor cortex activation in chronic stroke patients, 2011 International Conference on Virtual Rehabilitation (ICVR)

Qinyin Qiu, Sergei Adamovich, Soha Saleh, Ian Lafond, Alma Merians, and Gerard Fluet, A comparison of motor adaptations to robotically facilitated upper extremity task practice demonstrated by children with cerebral palsy and adults with stroke, 2011 IEEE International Conference on Rehabilitation Robotics (ICORR).

Qinyin Qiu, Diego A. Ramirez, Soha Saleh, Heta D. Parikh, Donna Kelly, Sergei Adamovich, Design of NJIT-Robot-Assisted Virtual Rehabilitation System to Train the Hemiplegic Upper Extremity of Children with Cerebral Palsy, In Proceedings of the Rehabilitation Engineering and Assistive Technology Society of North America (RESNA) 2009 Conference, 2009, New Orleans, LA, USA.

Soha Saleh, Qinyin Qiu, Sergei Adamovich, Eugene Tunik, fMRI study of the effects of visual feedback manipulation on sensorimotor circuits, (2010) Proceedings of the 36th IEEE Annual Northeast Bioengineering Conference, NEBEC 2010, NY.

Qinyin Qiu, Gerard Fluet, Soha Saleh,, Diego Ramirez, and Sergei Adamovich Robot-assisted virtual rehabilitation (NJIT-RAVR) system for children with cerebral palsy (2010) Proceedings of the IEEE 36th Annual Northeast Bioengineering Conference, NEBEC 2010, NY.

Saleh, S., Adamovich, S., Grafton, S., Tunik, E. FMRI study on the neural mechanisms of sensorimotor transformations (2009), Proceedings of the 35th IEEE Northeast Bioengineering Conference, Boston, MA.

Qinyin Qiu, Diego Ramirez, Soha Saleh, and Sergei Adamovich, NJIT-RAVR system for upper extremity rehabilitation in children with hemiplegia (2009), Proceedings of the 35th IEEE Northeast Bioengineering Conference, Boston, MA.

Abstracts

Soha Saleh, Hamid Bagce, Alma Merians, Sergei Adamovich, Eugene Tunik, Feedback augmented in virtual reality faciliates ipsilesional motor cortex in chronic stroke, Finger and Grasp Control: Age, Pathology, and Physiolog session, Society of Neuroscience 41st Annual meeting, November 12 2011, Washington, DC

Hamid Bagce, Soha Saleh, Sergei Adamovich, Eugene Tunik (November 2011) Effects of visuomotor discordance in virtual reality on online performance and motor cortex excitability in patients with Stroke. Finger and Grasp Control: Age, Pathology, and Physiolog session, Society of Neuroscience 41st Annual meeting, November 12 2011, Washington, DC.

Soha Saleh, Hamid Bagce, Qinyin Qiu, Gerard Fluet, Alma Merians, Sergei Adamovich, and Eugene Tunik, Strengthened Functional Connectivity in Bilateral Sensorimotor Cortex of Chronic Stroke Patients after Robot-Assisted Training in Virtual Reality: A Pilot Study, Motor Cortex Plasticity session, SFN Annual meeting, November 13 2010, San Diego, CA.

Hamid Bagce, Soha Saleh, Sergei Adamovich, John Krakauer, and Eugene Tunik, Exaggeration of visual errors during goal-directed movements enhances primary motor cortex excitability in healthy subjects and stroke patients. Motor Cortex Plasticity session, SFN Annual meeting, November 13 2010, San Diego, CA.

Soha Saleh, Hamid Bagce, Qinyin. Qiu, Gerard. Fluet, Alma Merians, Sergei Adamovich, Eugene Tunik, Strengthened Functional Connectivity in Bilateral Sensorimotor Cortex of Chronic Stroke Patients after Robot-Assisted Training in Virtual Reality: A Pilot Study, UMDNJ 3rd Annual Technology Symposium (Piscataway, NJ), April 12, 2011, Newark, NJ.

Alma Merians, Gerard Fluet, Qinyin Qiu, Soha Saleh, Ian LaFond, and Sergei Adamovich, Improving Hemiparetic Hand Function: Training With Virtual Reality Task-Based Simulations Interfaced With Adaptive Robots. Archives of Physical Medicine and Rehabilitation, Volume 91, Issue 10, October 2010.

Sergei Adamovich, Qinyin Qiu, Diego Ramirez, Soha Saleh, Heta D. Parikh, Donna Kelly, Gerard G. Fluet, Robotically Facilitated Upper-Extremity Task Practice in Complex Virtual Environments for Children With Cerebral Palsy. Archives of Physical Medicine and Rehabilitation, Volume 91, Issue 10, October 2010.

Soha Saleh and Lisa Simone, Identifying Determinants of Hand Posture of Individuals With and Without Movement Disorders. In Proceedings of the 2007 Biomedical Engineering Society (BMES) Annual Meeting, Los Angeles, CA, USA, 2007.

To all who I learned something from

To my parents, siblings, and all my family

To my friends in my beloved country, Lebanon

To my angel

ACKNOWLEDGMENT

I would like to express my deep thanks and appreciation for Dr. Sergei Adamovich for his advice and support throughout the four and a half years in his Neurorehabilitation and Motor Control Laboratory, and for being an understanding and supportive mentor. I also would like to thank Dr. Eugene Tunik for teaching me brain imaging and for being supportive. Both Dr. Adamovich and Dr. Tunik contributed to my PhD training, and I am graduating with pride having them my mentors. Dr. Foulds overwhelmed me with his support since I first joined NJIT in 2006; I would not have joined NJIT if he did not motivate me for that. I acknowledge his support as PhD program director, as a professor, and as an active member of my PhD committee. I would like to thank Dr. Alma Merians for her support, for being a role model as a successful researcher and for being on my dissertation committee. Dr. Jason Steffener is one of the best professors in the department of Biomedical Engineering, who I learned a lot from, and who I highly thank for being member on my committee. I would like to express special thanks to Dr. Gerard Fluet for reading this dissertation and reviewing it for me. I greatly thank him as a friend who I always looked for his advice and opinion. Dr. Qinyin Qiu, is a friend and lab member who I share with very nice memories and who I highly appreciate her assistance in performing part of my experiments, for helping me in many technical issues, and for sharing with me the experience. Another lab member I would like to thank is Hamid Bagce who helped me in performing part of my experiments and he provided lot of help besides being a very good friend. In addition I would to acknowledge the good friends I gained in this journey at NJIT, Jonathan Groth, Yelda Alkan, Abhishek Parasad, Yee-Shuan Lee, Gokhan Ordek, Diego Ramirez, Brooke Odle, Abraham Mathai, David Paglia, Manish Raval, Carlos Rosado, Brad Galego, and Katherine Swift.

TABLE OF CONTENTS

Chapter		Page
1	OBJECTIVE	1
2	INTRODUCTION	6
2.1	Stroke, Stroke Rehabilitation, Hand as a Major Problem	6
2.2	Virtual Reality	7
2.3	A Need for MRI-Compatible VR	8
3	fMRI DATA ANALYSIS	10
3.1	Factors Influencing BOLD Signal	10
3.2	Regression Analysis	11
3.3	Hemodynamic Response	14
3.4	Co-Activation And Correlation	15
3.5	fMRI Functional Connectivity	16
3.5.1	Functional Connectivity	16
3.5.2	Effective Connectivity	16
3.5.3	Dynamic Causal Modeling	18
4	EXPERIMENTAL PROCEDURE (AIM 1)	23
4.1	Data Acquisition	23
4.2	Experimental Setup	24
4.3	Movement Behavior Measures	25
4.3.1	Behavior Measures Statistics	27
4.3.2	Correlation Between BOLD Activity and Behavior Measures	27
5	BRAIN REORGANIZATION AFTER VIRTUAL REALITY REHABILITATION TRAINING (AIM 3)	29

TABLE OF CONTENTS (CONTINUED)

Chapter **Page**

5.1 Background…… 29

5.2 Methods…… 30

5.2.1 Training…… 30

5.2.2 Task During Fmri …… 31

5.2.3 Subjects…… 33

5.2.4 fMRI Data Analysis …… 33

5.3 Results…… 35

5.3.1 Clinical…… 35

5.3.2 Movement Performance During fMRI Experiment…… 36

5.3.3 Change in Extent of Activation…… 36

5.3.4 Change in Signal Intensity…… 40

5.3.5 Change in Connectivity With Ipsilesional M1…… 41

5.3.6 Interhemispheric Balance …… 42

5.3.7 Effective Connectivity Analysis Using DCM…… 45

5.4 Discussion…… 50

6 MANIPULATING FINGER MOVEMENT VISUAL FEEDBACK (AIM 3) …… 55

6.1 Background…… 55

6.2 Methods…… 58

6.2.1 Experiment 1, Healthy Subjects…… 58

6.2.2 Experiment 2, Stroke Subjects …… 60

6.3 Results…… 62

TABLE OF CONTENTS (CONTINUED)

Chapter			Page
	6.3.1	Experiment 1, Healthy Subjects	62
	6.3.2	Experiment 2, Stroke Subjects	67
6.4		Discussion	73
	6.4.1	Contralateral M1 is Facilitated by Discordance in Gain	74
	6.4.2	Processing of Observed Movement Amplitude and the Extrastriate Body Area	76
	6.4.3	Mismatched Feedback Activates Frontoparietal Network	77
	6.4.4	Neural Activity Correlation With Perceptual Judgment of Feedback	79
7		MANIPULATING VISUAL FEEDBACK IN VIRTUAL MIRROR	80
7.1		Background	80
7.2		Methods	82
	7.2.1	fMRI Data Analysis	85
7.3		Results	89
	7.3.1	Experiment 1	89
	7.3.2	Experiment 2	89
7.4		Discussion	98
8		CONCLUSIONS	102
		APPENDIX: SUPPLEMENTARY INFORMATION	105
		REFERENCES	110

LIST OF TABLES

Table		Page
5.1	Subjects' Clinical Information…….....	33
5.2	Subjects' Percent Improvement in Two Main Clinical Measures……	36
5.3	Repeated Measures ANOVA Test of Movement Kinematics……..	37
5.4	Results of Regression Analysis Between LI Values in Eight Main ROIs and the Main Clinical Scores …..……	44
5.5	Bayesian Model Fitting Parameter Estimation in DCM ……..…	45
6.1	Subjects' Clinical Information……..	60
6.2	Behavioral Data Across Conditions ……	63
6.3	Results of Regression Analysis Between T Values in G25>V Contrast And Motor Behavior …...…….	71
7.1	Subjects' Clinical Information ..……...	84
7.2	Correlation Between T Values For Various Regions of Interest (Contrast HANDmirror > (HANDveridical + CTRLmirror + CTRLveridical) And dWMFT Score……..	95
A6.1	Clusters of Activation in the Main Contrasts of Chapter 6 Experiment 1, at p<0.01, K=10……	107
A6.2	Clusters of Activation in the Main Contrasts of Chapter 6 Experiment 1, at p<0.01, K=10……	108
A7.1	Clusters of Activation in the Main Contrasts of Chapter 7 Experiment 2, at p<0.01, K=10……	110

LIST OF FIGURES

Figure		Page
3.1	Example of time series of activity in a selected volume of interest (VOI) in the brain and representation of the movement events convolved with hemodynamic response	12
3.2	Hemodynamic response function with its temporal and dispersion derivatives, these are predictors to the neural activity	13
3.3	Example of a 3 nodes model with A, B and C parameters	20
4.1	A. subject lying in the scanner wearing mri-compatible 5D gloves in both hands. B. Example of a VR environment	24
4.2	Traces of index finger of the active and inactive hands during an experiment, the arrows point to bad trials excluded from the data analysis	25
4.3	Tracking of BOLD signal and joint angles simultaneously	26
4.4	An example of a GLM with 6 sessions, and one task per session. The first column of each block models the movement trials timing and the other three columns model the three parametric modulators 1)Reaction time to move (ReT), Movement angular velocity (MeV), and 3) Movement angular excursion (Peak angle).....	28
5.1	A. B. Robotic arm, data glove and force-reflecting hand system used in the VR therapy. C. VR feedback during the fMRI movement task	32
5.2	Model of interaction between iM1 and cM1 tested in DCM.....	35
5.3	Change in extent of activation after training. This result is at a statistical threshold of $p<0.01$	38
5.4	Correlation between extent of activation in the ROI including BG and thalamus regions, and JTHF, all 10 subjects are included in the figure to the left. In the right figure, data of S4 were excluded	39
5.5	Changes in task related brain activity after training and its relationship with age	40
5.6	Change in PPI connectivity with iM1 after training for each subject. The result is at a statistical threshold of $p<0.01$	41
5.7	Increase in neuro-motor coupling with movement angular velocity.....	42

LIST OF FIGURES (CONTINUED)

Figure		Page
5.8	Changes in LI values in the region including precentral gyrus and postcentral gyrus ……... …….	43
5.9	Difference in DCM B parameters of iM1 and cM1 model after training …...…	47
5.10	Relationship between bilateral motor coupling and Ashworth score (measure of spasticity) …….	48
5.11	Left: correlation between difference in coupling strength after training from iM1 to cM1 and WMFT proximal clinical subtest. Right: correlation between decrease in laterality (LI diff) in the frontal lobe and improvement in the WMFT proximal clinical subtest ……	48
5.12	Regression analyses between change in DCM parameters and re-lateralization of activity in the ROI including precentral gyrus and postcentral gyrus …….	49
5.13	Difference in bilateral motor cortices coupling based on CVA side……	50
5.14	Difference in bilateral motor cortices coupling based on lesion site (cortical, subcortical) ……...……	50
6.1	Feedback conditions of finger movement ……	59
6.2	Evaluation of visual feedback……...……	62
6.3	fMRI activation in veridical compared to hypometric visual feedback……	64
6.4	fMRI activation in veridical compared to mismatched visual feedback……..	65
6.5	BOLD signal correlations with decision time…….……..	66
6.6	Results of PPI connectivity analysis of experiment 1……...……	67
6.7	fMRI activations in G25>V contrast…….……...	68
6.8	fMRI activations inG175> contrast…….…….	68
6.9	Overlap between G25>V and G175 contrasts, at statistical threshold $p<0.05$….	69
6.10	Activity in the precentral gyrus during each of the three conditions, red bar stands for 95% confidence interval……...……	70
6.11	Simple regression analysis of iM1 T values in G25>V and clinical scores……..	72

LIST OF FIGURES (CONTINUED)

Figure		Page
6.13	Simple regression analysis of iFBA T values in G25>V and clinical scores…...	72
6.14	PPI connectivity with the ipsilesional fusiform body area (iFBA) as a seed (V>G25 contrast)……..……	73
7.1	Lesion mapping for 15 subjects……	82
7.2	Different visual feedback manipulations of subject's hand movement in the scanner. Subjects wear the 5DT gloves, and get visual feedback of their movement on the computer screen. Assuming the subject is moving the right hand, the right virtual hand is moving in the veridical condition, the left hand moves in the Mirror condition and in the control conditions, the right (CTRLveridical) or the left (CTRLmirror) ellipsoidal shape rotates at a rate of 1 Hz …….…….	85
7.3	Structure of the main DCM model did not include interhemispheric connections between SPL and M1 areas but included exogenous coupling ……	88
7.4	Effect of mirror visual feedback (HANDmirror > (HANDveridical + CTRLmirror + CTRLveridical) for each of the 15 subjects……	91
7.5	Mirror effect (HANDmirror>HANDveridical+CTRLmirror+CTRLveridical); average of 15 subjects. Right side is the ipsilesional hemisphere ……..…	91
7.6	Conjunction analysis of each subject, results showed overlap in activity when moving paretic hand versus moving non-paretic hand and receiving mirror visual feedback …….	92
7.7	Effective connectivity (PPI) with ipsilesional M1 as VOI……...……	93
7.8	Effective connectivity (PPI) with contralesional SPL as VI……..……...	94
7.9	Regression analysis between FBA T values (HANDmirror > (HANDveridical + CTRLmirror + CTRLveridical)) and dWMFT……..	95
7.10	Results of the fixed (upper) and random (lower) effects Bayesian Model Selection procedures, they both favor Model 18……	96
7.11	The optimal model with the group average parameters derived using Bayesian Parameter average. The asterisk * denotes significant difference between conditions excluding S6……	97

CHAPTER 1

OBJECTIVE

Numerous recent studies have used a variety of methods of brain stimulation (direct electrical current stimulation, high-frequency alternate current stimulation, high- and low frequency magnetic stimulation) to demonstrate that transient changes in cortical excitability can affect the speed of motor learning (Hummel and Cohen 2006; Antal et al. 2008). This approach of temporarily changing brain properties during motor activities could potentially be used in the future to improve the efficacy of existing rehabilitation therapies. One of the objectives of this dissertation is to explore an alternative method to increase the efficacy of rehabilitation therapies. This method involves manipulation of visual feedback that can be used as a tool to facilitate cortical excitability. A large body of literature indicates that action and observation are interlinked (Ghilardi et al. 2000; Ertelt et al. 2007). Several recent studies have demonstrated the effects of visual feedback during limb motion on sensorimotor learning, skill acquisition, and potentially on the motor recovery after brain damage (Brewer et al. 2008). In this dissertation, virtual reality is used as a tool to allow manipulation of feedback during arm/hand motion.

Some visual feedback studies showed strong influence of visual manipulation (illusion) on motor function and on the sensorimotor system. On the other hand; rehabilitation therapies enriched with visual feedback presented in VR, showed promising results in terms of motor recovery (Merians et al. 2011). However, the neural mechanisms of recovery during VR therapy and the specific effects of visual feedback manipulations presented in VR on neural plasticity and brain reorganization are

unknown. According to Hebbian learning theory, a pronounced activation in a group of cells leads to enhanced synaptic strength between those cells. In other words, increased facilitation of select brain regions could possibly induce neural plasticity in that network. This dissertation hypothesizes that VR visual feedback of movement is useful to enhance neural facilitation or increase brain excitability of networks that involve premotor, parietal and occipitotemporal areas. In addition, it is hypothesized that increase of neural facilitation using VR visual feedback would lead to modulation of inter-hemispheric and intra-hemispheric connections between premotor areas, parietal areas, and primary motor cortex in a Hebbian-like manner (Rizzo et al. 2009) leading to neural plasticity.

The first objective of this dissertation (aim 2) is to explore the effects of rehabilitation therapy enriched with VR visual feedback on brain reorganization (neural plasticity). However, the study of VR therapy does not allow for understanding of the specific effects of VR visual feedback on neural facilitation because of the complexity and variety of visual manipulations used during the training. Therefore, the second part of this dissertation (aims 3 and 4) studies VR visual feedback with specific and distinct visuomotor discordances and their effect on brain activity specifically in the sensorimotor cortex.

The main goals of the dissertation are to 1) investigate brain reorganization after rehabilitation therapy enriched with VR visual feedback and 2) explore the optimal ways to use visuomotor discordances presented in VR to enhance brain excitability given its potential effects on neural plasticity. The outcome of this dissertation is expected to increase the knowledge about the neural aspects of brain reorganization after rehabilitation training. In addition, it advances our knowledge of the effective use of VR

visual feedback needed to develop novel neuroscience-based rehabilitation paradigms that will further enhance neural facilitation and brain reorganization and improve motor recovery after a cerebrovascular accident like stroke.

Functional magnetic resonance imaging (fMRI) studies are very relevant to study the neural effect of VR feedback and brain reorganization after therapy; however, one main limitation is the absence of an MRI-compatible VR system. In addition, studying visual feedback during movement task in fMRI studies can add movement confounds and this is another limitation, especially in the case of subjects with motor impairments. Given the need of an MRI-compatible VR system and the importance to understand the influence of VR visual feedback on the sensorimotor cortex activity, the first aim of the dissertation was to develop to this system, and to use the methodology of this system in the experiments of each of the other aims.

The main aims of this dissertation are as follows:

1. Develop a methodology to incorporate virtual reality feedback in fMRI studies: Through tracking hand movement in real time, subjects are provided with VR visual feedback in real time; this tracking limit confounds related to difference in motor performance and it allows analyzing its possible effect on BOLD signal.
2. Use the methodology developed in aim 1 to build an approach to study brain reorganization in a group of chronic stroke subjects participating in the NJIT-RAVR rehabilitation training protocol: It is hypothesized that rehabilitation therapy enriched with virtual reality based visual feedback results in a distinct pattern of brain reorganization. This brain neuro-plasticity is quantified in multiple dimensions by measuring:

a. Regional changes in intensity of activation (regional specialization);

b. Change in inter-regional interactions (functional connectivity)

c. Change in the relationship between neural activity and movement (neuro-motor coupling).

d. Change in coupling strength of primary motor cortices

3. Use the methodology developed in aim 1 to study the neural network sub-serving responses to error-based visual feedback in the sensorimotor cortex of neurologically healthy subjects and stroke subjects: The neural effects of visuo-motor discordances are studied during visually-guided finger movements. An fMRI-compatible data glove is used to actuate (in real-time) virtual hand models on a display. Virtual hand motion is manipulated to simulate either hypometric, hypermetric or unintentional (actuation of a mismatched finger) feedback. It is predicted that veridical (errorless) visual feedback would be associated with stronger activation in regions processing biological action, in addition to the motor system activation, while error-based visual feedback would be associated with activation in regions involved in sensorimotor transformations, such as posterior parietal cortex and premotor cortex.

4. Use the methodology developed in aim 1 to study the effect of mirror visual feedback on the activity of ipsilesional sensorimotor cortex of stroke subjects: Subjects see their paretic hand virtual representation actuated by the motion of the non-paretic hand. It is hypothesized this feedback manipulation would recruit ipsilesional sensorimotor cortex activity. The neural networks sub-serving this

possible effect of mirrored effect are not well understood; therefore, this aim include two main parts:

a. Examine the effect of mirrored feedback of hand movement on the activation of the ipsilesional sensorimotor cortex.
b. Use psychophysiological interactions (PPI) analysis and dynamic causal modeling (DCM) analysis to investigate connectivity among the regions responding to the mirrored visual feedback.

CHAPTER 2

INTRODUCTION

This dissertation investigates virtual reality therapy as a tool to provide visual feedback of movement, as a promising approach in hand rehabilitation. In addition, specific types of VR visual feedback discordances are studied to explore their effect on enhancing neural facilitation. This chapter provides a brief introduction to the main background of this dissertation, where more detailed background research will be provided when discussing each of the four specific aims.

2.1 Stroke, Stroke Rehabilitation, Hand as a Major Problem

Stroke is a leading cause of disability in the United States (Lloyd-Jones et al. 2010) as well as in the world. Majority of stroke survivors live with motor disabilities that affect their quality of daily life. Years of research and clinical practice have produced with interventions that caused some motor recovery and improved stroke survivors' quality of life. Despite the achievements in the improvement of gait and arm movement, little success has occurred in the field of hand rehabilitation. This is mainly due to the complexity of hand movement, which includes 21 degrees of freedom skeleton including the wrist (Balasubramanian et al. 2010), and the highly developed neural system that controls hand movement (Bosecker et al. 2010). Considering the example of shoulder movement rehabilitation, therapy focuses on range of motion of the joint and movement in three dimensions; however, it is much more complex with the hand because of multiple factors including finger range of motion, finger individuation, coordination of the finger wrist and radio-ulnar joints, etc. Therefore, there is a critical need to have

interventions that concentrate on hand rehabilitation and one of these promising interventions can involve virtual reality therapy.

2.2 Virtual Reality

Today, there is an increase interest in using virtual reality games in rehabilitation of movement disorders; virtual reality appears to be very promising for hand rehabilitation specifically, one of the main simple justifications is that gaming in virtual reality gives flexibility to train hand movement more naturally. Daily activities can be programmed in virtual reality as motor tasks, and patients get the chance of training on these tasks intensively and with possible assistance if needed. Many studies were published on rehabilitation studies using commercial devices like Playstation (Golomb et al. 2010) (Yavuzer et al. 2008), or Nintendo Wii (Mouawad et al. 2011). However, the hand is more complex and there is a need for custom-programmed virtual reality simulations that concentrate on hand movement in terms of finger individuation and wrist supination and pronation. This was achieved at the NJIT "Motor control and rehabilitation" lab where virtual reality games like playing piano, catching birds or using a hammer were developed to intensively work on hand rehabilitation (Adamovich et al. 2009; Qiu et al. 2009). In addition to simulating natural activities, virtual reality therapy main advantage over traditional therapeutic paradigms is allowing for increased interest and engagement of subjects during training and for larger intensity of training (Adamovich et al. 2009); in addition, subjects get the chance to get feedback of their movement either online or at the end of the training session, or both. Another possible advantage of VR is its possible effect on the proposed "mirror neural system". Many studies (Iacoboni et al. 1999; Aziz-Zadeh et al. 2002; Maeda et al. 2002; Rizzolatti and Craighero 2004) have shown

increased activity in the premotor areas, inferior parietal areas and superior temporal areas when the subject watches motor activity of another person. In virtual reality, this effect might also be there especially if the subject watches VR hand models and get online feedback of his or her movement in a 1st person perspective (Perani et al. 2001; Adamovich et al. 2009).

The claim about efficiency of VR therapy cannot be justified without better understanding of the neural mechanism of recovery or brain reorganization and the possible effect of visual feedback on the brain activity. This understanding is critical in order to develop more neuroscience-grounded rehabilitation interventions; this dissertation approached this need in aims 2, 3, and 4.

2.3 A Need for MRI-compatible VR

To summarize the background discussed in the previous sections, stroke is a leading cause of disability and virtual reality therapy is promising in terms of interventions and in terms of providing visual feedback that might enrich brain reorganization. Therefore, there is a big need to study virtual reality feedback and test for the efficiency of virtual reality therapy on brain reorganization; this can be best achieved using fMRI. However, there is a lack of an MRI-compatible virtual reality system to test brain activity during manipulated VR visual feedback.

In the literature, some VR-based fMRI studies required watching a VR simulation without any motor interaction (Pilgramm et al. 2010), other studies required doing a simple motor task in a VR environment using a motor rotor (Rice et al. 2007) (Tunik et al. 2009), a precision grip (Begliomini et al. 2008), a digitizing tablet (Ghilardi et al. 2000), a graspable device to control a cursor (Culham et al. 2003) or a joystick.

Researchers have created many designs studying motor function in fMRI by doing grasp and supination/pronation movements to control a cursor or an object. However, none of the studies we know about has integrated visual feedback of individual finger motor task in an fMRI study. In addition, there is limitation in the ability to track hand activity in real time and save this data to correlate BOLD activity with motor performance. A way to track individual finger movement in fMRI can be through an MRI-compatible data gloves. One of these gloves is 5DT glove by Fifth Dimension Technologies (http://www.5dt.com, Irvine, CA) which is also being used for video-game animations in virtual reality based therapy (Golomb et al. 2010). In this dissertation, a 5DT glove is used to track hand movement in real time and provide online feedback.

CHAPTER 3

FMRI DATA ANALYSIS

3.1 Factors Influencing BOLD Signal

Blood Oxygen Level Dependent (BOLD) signal measured in functional Magnetic Resonance Imaging (fMRI) is believed to be directly correlated with neural activity. However, vascularity of different brain areas might also influence the BOLD signal in terms of the properties of the hemodynamic response. The main properties of the hemodynamic response is its amplitude, the latency which is time to the onset of response, the dip amplitude which is the small decrease in BOLD activity that precedes a sudden increase in the BOLD signal, duration, and time to peak. A neurological disorder like brain injury or stroke could have direct influence on the metabolism in certain brain areas and conversely an influence on the hemodynamic response of these areas. This fact increases the challenge to investigate neural response in stroke subjects, with difference lesion locations and sizes.

In fMRI studies that investigate motor movement, the main task of subjects in the scanner is movement task. Herein lays the challenge of motor variability between multiple conditions and multiple sessions, this variability can be in terms of movement amplitude, speed or duration. It is not well know how this variability would affect neural signal and the hemodynamic response measured as a BOLD signal; however, it can be a main confound in fMRI data analysis. As an example of subject with motor impairment, might perform a movement task with speed X and amplitude Y during the first session of the experiment but then this subject might get fatigued or may adapt to the task and move differently in the subsequent experimental session. The factors that might influence motor

behavior are variable and some might not be identifiable. However, they are definitely an important factor that might influence BOLD signal.

The experiments in this dissertation have used even-related designs for fMRI data acquisition while subjects performed movement task. In an event-related design, the trials duration is few seconds, and there is few seconds rest in between, the short duration of events increases the chance of having hemodynamic response affected by the duration of the task or by the reaction time, which is directly related to the duration of the task. In such experiments, subjects are given few seconds to do a task, but they might start within few milliseconds or they might delay the movement onset by a second or more. These possible differences in reaction time within and across subjects might be a confound, this idea is controversial (Grinband et al. 2011) but as a precaution, reaction time and movement performance need to be tracked when doing regression analysis in fMRI data analysis.

In conclusion, there is a great need to develop an MRI-compatible VR system not only to study the neural correlates of VR visual feedback in fMRI but also to get the flexibility to account for factors influencing BOLD signal like variability in motor output. Moreover, understanding the potential power of visual feedback manipulated in VR to modify the activity in the primary and secondary sensorimotor areas may be crucial for developing novel, more efficient neuroscience-based rehabilitation interventions.

3.2 Regression Analysis

Regression analysis is the main technique to analyze fmri data. The acquired data in fmri experiment is the BOLD signal with TR as the sampling rate. The assumption in the field of fMRI is that BOLD signal is a representation of neuronal response to the functional

task through increase in cerebral blood flow during that task (Ogawa et al. 1990; Ogawa et al. 1993). Therefore the relation is BOLD=B*(a model of the functional task). This is the main idea of regression analysis, the regressand is BOLD signal, the regressor is the functional task and B is the parameter estimating the relation between both. While the idea is simple, the application needs to take more parameters into account. Functional task is a simple on/off signal which does not have the properties of the bold signal. However, there are many mathematical models of the brain hemodynamic response which can also be referred to as the impulse response of the system; the best would be the double gamma function(Glover 1999). Convolving the task boxcar with the gamma function gives prediction of the BOLD signal based on the task, and that lead to the statistical model of the measured BOLD signal that can be used in general linear modeling (GLM), a generalized approach of linear regression analysis.

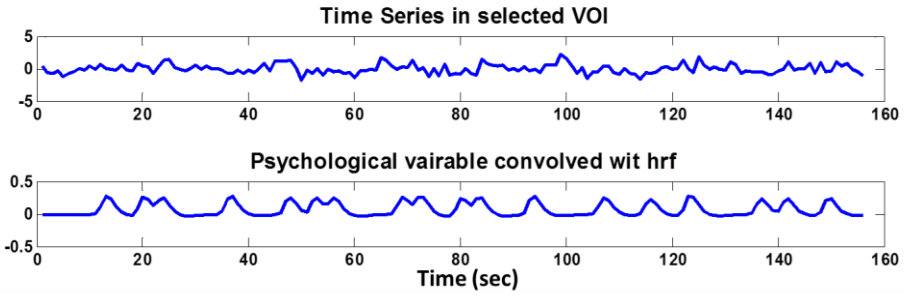

Figure 3.1 Example of time series of activity in a selected volume of interest (VOI) in the brain and representation of the movement events (psychological variable) convolved with hemodynamic response function.

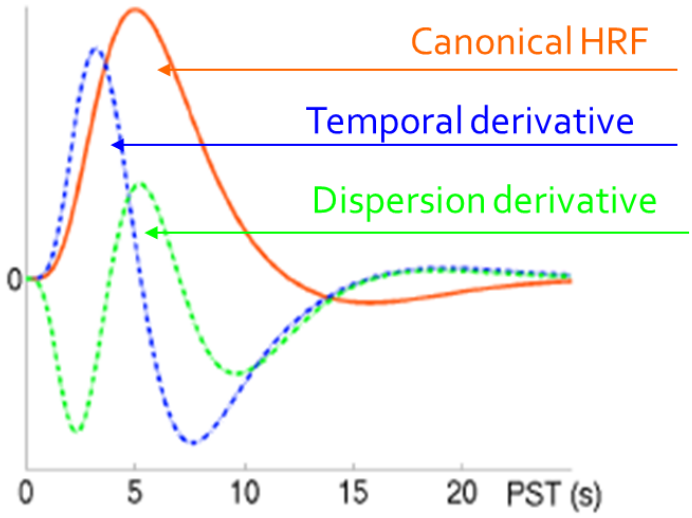

Figure 3.2 Hemodynamic response functions with its temporal and dispersion derivatives. These are predictors to the neural activity.

During an experiment, there would be more than one experimental task (A, B, etc), and it is important to extract the correlates of these tasks from the BOLD signal. Figure 3.2 shows a model of canonical hemodynamic response function (hrf) based on double gamma function equation with its time and dispersion derivative (discussed more in the next section).

In GLM, X_A is task A box car convolved with the canonical hrf, and X_B is task B box car convolved with hrf. Thus, X_A and X_B are predictors of the hemodynamic response to the neural correlates with tasks A and B respectively. Therefore, they can be used in GLM equation as regressor to derive the relationship between BOLD signal and each of the tasks; this is what is called parameter estimation.

$$y_t = \beta_A X_A + \beta_B X_B + \varepsilon \tag{3.1}$$

Equation 3.1 represents the GLM equation to derive the regression analysis. The regressand, y_t is the change in BOLD signal across time t, X_A and X_B are the regressors

discussed above, β_A and β_B are the estimates of correlation between the task and the BOLD activity and ε is the error estimate.

3.3 Hemodynamic Response

The model of hemodynamic response function (hrf) used in statistical parameter modeling software (SPM, http://www.fil.ion.ucl.ac.uk/spm/) is the difference of two gamma functions that model the slight dip after the onset of the response (Friston et al. 1998). On the other hand, the hemodynamic response can be different in different brain regions due to differences in the vascularization, metabolism, hemodynamics etc (Miezin et al. 2000). In addition, the hemodynamic response can vary among subjects (Aguirre et al. 2002) especially in the presence of a neurological disorder like stroke. This difference in hemodynamic response suggests that the double gamma function might not always predict the response to the neural response. One of the solutions to this issue might be to model subject specific hrf. That can be done by extracting the hemodynamic response of V1 in a vision task or from M1 in a simple motor task, as examples. In this case the shortcoming is to model the hrf based on one or two areas, but the rest of brain areas will not necessary have a similar hemodynamic response (Conner et al. 2011).

This lead to the last and possibly best option, which is using the basis, set functions (Figure 3.2) which are the double gamma hrf function and its temporal and dispersion derivatives. It is assumed that this combination would outperform the canonical hrf alone and all together, might better account for variability in hemodynamic response. The canonical response function alone might not be sufficient to capture different BOLD response function especially in the case of stroke subjects where the variability in vascular activity between different regions might be higher than

average(Calhoun et al. 2004). The time derivative of the canonical response function is able to capture BOLD signal with early peak and the dispersion derivative is able to pick BOLD activity with higher dispersion or longer latency (Henson et al. 2002; Steffener et al. 2010). Therefore, in this study the GLM of stroke subjects are created using the canonical hemodynamic response function (hrf) (Friston et al. 1998; Friston et al. 1998) and its partial derivatives as basis functions.

$$y_t = \beta_0 + \beta_1 x_t + \beta_2 \frac{\partial x_t}{\partial t} + \beta_3 \frac{\partial x_t^{\,2}}{\partial t^2} + \varepsilon_t \tag{3.2}$$

Assuming that there is one experimental condition, the GLM regression equation will be similar to equation 3.2. The regressand y_t is the BOLD signal, the regressor x_t is the signal activation model and ε_t is the residual error. β's are the regression coefficients or the activation amplitudes of each condition for each of the basis functions.

3.4 Co-activation and Correlation

Regression analysis provides the beta estimate for each voxel of the brain relative to the task (see equation 3.2). Mapping all voxels of the brain or a group or regions of interest defines areas that are active during a task. Many areas can be correlated with the task; they define a network with nodes that are coactive within the window time of the task. However, regression analysis is incapable of extracting how the areas are related to each other. While this analysis provides answers about the task effect, it does not examine the causal interactions across the sub-served neural networks. In addition, co-activation and correlation analysis does not provide information about the direct modulation of activity in an area by the task or through modulation by other areas during the task. Scientists tried to address these questions using connectivity analysis, which is discussed below.

3.5 fMRI Connectivity Analysis

3.5.1 Functional Connectivity

Functional (seed voxel) connectivity analysis studies the temporal correlation between one region and other regions in the brain. Functional connectivity analysis is mostly popular in studying default neural networks during resting state. However, it can be used to understand development of new neural networks during functional recovery from stroke. Areas with high temporal correlated time-courses are said to be functionally connected. However, this connectivity can be due to sharing neuro-modulatory influences or sharing sensory input and not necessarily an interaction due to a given task.

3.5.2 Effective Connectivity

Effective connectivity studies the interaction of brain regions during a task or the activity in a brain region in the context of another (Paus et al. 1996). Psychophysiological interaction (PPI) is an effective connectivity analysis that studies the connectivity between one area and other areas in the brain during a given experimental task; it was developed (Friston et al. 1997) in the middle 1990's and in less than two decades it gained popularity and validity. In this dissertation, PPI analysis was used to test for change in functional connectivity of the ipsilesional motor cortex with the rest of the sensorimotor cortex after therapy (see chapter 5) and to study difference in brain connectivity with a seed region given different experimental tasks (see chapters 6 and 7). PPI can be summarized in equation 3.3 where the activity in Xi is summation of contributions (C_{ij}) from all other regions (j=1 to N (number of regions)), and X_k is the activity in each of the contribution regions.

$$X_i(t) = \sum C_{ik} . X_k(t) \tag{3.3}$$

Given one region of interest, PPI effective connectivity is defined in equation 3.4 where β_{ik} is the contribution of activity in the seed region (k) to the activity in voxel i , G stands for global activity, and ε for error. In the presence of a psychological input (experiment condition), the input might modulate region i directly or through the input from region k; thus, the contribution of k to the activity of i should also include the interaction with the psychological input; this is modeled in equation 3.5 where g stands for the task demand. In equation (3.5), the interaction between the task demand and BOLD response in a region or interest is defined by the cross product "x".

$$X_i(t) = \beta_{ik} X_k(t) + G\beta_G + \varepsilon \tag{3.4}$$

$$X_i(t) = \beta_i (X_k(t) \times g) + (X_k(t) g G)\beta_G + \varepsilon \tag{3.5}$$

The standard PPI analysis procedure include three main steps: 1) extract seed time series 2) define PPI regressor which is computed as element by element cross product of seed time series and the box car of the specific experimental condition; PPI and time series are in phase during the specific task of interest and out of phase in the rest of experimental session, 3) create a GLM using seed time series and ppi as regressor and estimate the GLM before defining the contrast of interest.

PPI is implemented as a part of the SPM toolbox. It is a well-established procedure however it is long and cumbersome to use the graphic user interface (GUI) for analysis of big data set, however Donald Mclaren developed a gPPI toolbox (Mclaren 2011) which is similar to the SPM GUI but automates all the above steps into a Matlab® code. Using gPPI, the procedure is defining the seed, then defining the conditions of interest and running gPPI code after small modifications to match the studied task. The

gPPI automated and PPI toolboxes, currently implemented in SPM, produce same results; however, gPPI uses a regional mean instead of the eigenvariate of the seed.

3.5.3 Dynamic Causal Modeling

The main objective in Dynamic causal modeling (DCM) is to study coupling of region-specific neuronal activity in a given model. DCM is a well-established methodology (Friston et al. 2003) established to test the validity of model of interactions among multiple neuronal brain areas' time series given an fMRI task. It stems from graph theory where nodes are the time series of a brain area. DCM allows testing three types of interactions among brain regions 1) extrinsic neurophysiological interaction among brain region irrelative to the input (experiment task) 2) intrinsic interactions between brain regions modulated by the input 3) direct influence of the task on brain regions' activity.

DCM is not a methodology to find the true model of interactions among brain regions (Friston et al. 2011), it is a way to assess the validity of a model or to compare a class of valid models. The user has to define an anatomical valid model, and then provide assumptions on the site of activity modulation by the input task. DCM computes the coupling strength between brain areas (in terms of the rate constant of one region activity in response to another) and the probability estimate of this coupling based on its variance. DCM estimates these interactions based on Bayesian estimation method, it also estimates the validity of the parameters and how much the data fits the suggested model.

DCM is very similar to regression analysis described in section 3.2; however, it works backwards from regression analysis. While in regression analysis, the hemodynamic response is defined then the analysis is performed in terms of relationship between the data and hrf, in DCM the BOLD signal is modeled using the balloon model

(section 3.3.3.1), the response is predicted based on the model and at the end, the response is validated based on the data using Bayesian statistics. One of the main concepts of DCM is to predict the BOLD signal based on the model. DCM uses balloon model to define the relationship between regional cerebral blood flow (rCBF) and BOLD signal (Buxton et al. 1998). The relation between blood flow and synaptic activity was studied by (Miller et al. 2001) where they found linear relation between synaptic activity and rCBF flow. The prediction of the response is then validated by the measured BOLD signal. This validation is what provides conclusion about model fitness to the data.

3.5.3.1 BOLD signal model. As discussed earlier in this section, DCM estimates 1) endogenous interactions among the nodes 2) interactions modulated by the task and 3) the direct influence of the task on the regions' response. These three outcomes are known as the A, B, and C parameters of the linear DCM model estimation and together they constitute the model parameters "ϴ" . In a given model, the change of neuronal state of region z is a function of input u(t), current neuronal state z and interaction between brain regions at a neuronal level n, this lead to equations 3.8 and 3.9.

$$\dot{z} = f(\dot{z}, u, \theta^{n}) \tag{3.8}$$

$$\dot{z} = \left(A + \sum_{j=1}^{M} u_t(j) B^{j} \right) z_t + C u_t \tag{3.9}$$

Given a stimuli, the neural activity response varies depending on the strength of the signal, however, the BOLD signal response also depend on the difference in blood flow dynamics across brain regions. Thus, estimation of synaptic activity of region X to region Y depends on estimation of BOLD signal (z). The speed of response of region Y

to region X is in seconds, and it depends on the speed of blood flow (venous properties) and the strength of neuronal activity. Mathematically, this coupling (a) is inversely proportional to the half-life (τ) of z (t). The speed of the half-life response for example can be 1 sec (1 Hz coupling) or 10 seconds (0.1 Hz coupling). In this dissertation the response that takes 10 seconds (0.1 HZ coupling) was considered very weak coupling but a coupling >0.1 Hz was considered. The algorithm to derive the DCM parameters (A, B, C) in equation 3.8 is known as the expectations maximization (EM) algorithm (Friston et al. 2003).

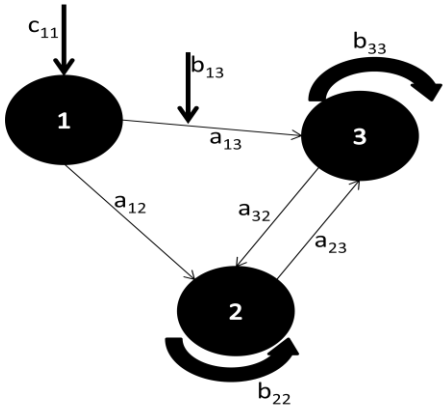

$$\dot{z}_1 = c_{11}u + a_{11}z_1$$

$$\dot{z}_2 = a_{22}z_2 + a_{12}z_1 + a_{32}z_3 + ub_{22}z_2$$

$$\dot{z}_3 = a_{33}z_3 + a_{13}z_1 + a_{23}z_2 + ub_{13}z_1 + ub_{33}z_3$$

$$\begin{bmatrix} \dot{z}_1 \\ \dot{z}_2 \\ \dot{z}_3 \end{bmatrix} = \left(\begin{bmatrix} a_{11} & 0 & 0 \\ a_{12} & a_{22} & a_{32} \\ a_{13} & a_{23} & a_{33} \end{bmatrix} + u \begin{bmatrix} 0 & 0 & 0 \\ 0 & b_{22} & 0 \\ b_{13} & 0 & b_{33} \end{bmatrix} \right) \begin{bmatrix} z_1 \\ z_2 \\ z_3 \end{bmatrix} + \begin{bmatrix} c_{11} \\ 0 \\ 0 \end{bmatrix} u$$

$$\dot{Z} = (A + \sum_j u_j B^j)z + Cu$$

Figure 3.3. Example of a 3 nodes model with A, B, and C parameters.

3.5.3.1 Model Fit and Model selection. Given a DCM model, other than deriving the parameters, the models need to be validated; BOLD signal and synaptic activity are used to predict the response while model fitting involves fitting the data to the predicted response by the model. The validity of the model is the assessment of probability of the model given the data P(y|m); y is the data and m is the model. Inferences about model parameters in Bayesian statistics start by defining the priors of the parameters constituting the model where each parameter model is Gaussian (Penny 2012) (eq. 3.10). These prior distributions are not conditional which means they do not rely on observed

data but are predictors of it. Priors are defined by both the coupling parameters (A, B and C) and the hemodynamic response (h), together priors, expectations, and covariance from the EM algorithm are used to derive the posteriors of the model (Friston et al. 2003).

$$P(\theta|m)P(B|m)P(m|C)P(h|m) \tag{3.10}$$

The probability of the data given the data is known as posterior probability density (q), it is derived using Variational Laplace (VL) method and it takes the covariance of priors into account to derive the model evidence. The three main measures used to assess the validity of a DCM models are free energy (F), Akaike information criterion (AIC), and Bayesian information criterion (BIC). Free energy was found to be the best in validating a DCM model since it accounts for both accuracy of estimation and complexity of the model, on the other hand, BIC favors simpler models with more accuracy and AIC favors models with higher complexity (Penny et al. 2004). Model evidence is a critical step to compare across models and it is calculated as in equation 3.11. The mathematical computations of model accuracy and complexity that help derive free energy, AIC, and BIC are explained in multiple publications (Penny et al. 2004) (Friston et al. 2007; Penny 2012). After deriving model evidence, Bayes factor is used to compare models, it is the ration of the evidence of one model "i" over the other "j" (equation 3.12). Bayes factor of values less than three means there is a weak evidence of model "i" favoring model "j, a factor between 3 and 20 is considered positive evidence, 20-150 is a strong evidence and >150 is a very strong evidence (Penny et al. 2004).

$$P(y|m) = \int P(y|\theta, m)P(\theta|m)d\theta \tag{3.11}$$

$$B_{i,j} = \frac{P(y|m=i)}{P(y|m=j)} \tag{3.12}$$

3.5.3.2 Challenges in DCM. The first challenge in DCM is to define a plausible model which would require basic neuro-scientific background of the regions of interest (ROI) included as nodes in the DCM. To define the model, it is required to define the regions of interest then extract their time series, draw the logical connections among them to have plausible model, then define the interaction and the modulation of the task. The task can be modulating the ROI directly or through input from another ROI. Therefore, it is common to have very high number of possible models given a small number of ROIs or model nodes even with prior knowledge of the function of included ROIs. As an example, if there are three ROIs, it is possible to define at least 8 models of possible endogenous interactions among and there is much higher number of possible exogenous interactions to be modeled (Kasess et al. 2008). The other challenge is to compare models. It is possible to define models that fit the data with high validity, but still model comparison fail to isolate a winning model, especially with big models with high complexity. A possible solution to this issue, is to make inferences based on a group of models or family of models that share same endogenous connectivity but are different in terms of exogenous interactions (Penny et al. 2010).

CHAPTER 4

EXPERIMENTAL PROCEDURE (AIM 1)

The data of the main experiments in this dissertation (chapters 5, 6 and 7) were acquired using a similar procedure and a very similar setup, which was developed as aim 1 of this dissertation. Thus, this chapter discusses procedures for data acquisition, experiment setup and data analysis. All subjects in each of the studies participated after signing informed consent approved by NJIT and UMDNJ Institutional Review Board (IRB) committees.

4.1 Data Acquisition

fMRI data acquisition was performed using a 3-T Siemens Allegra head only scanner with a Siemens standard head coil. High resolution structural images (TR=2000 ms, TE= 4.38, voxel size 0.938x0.938x1, 176 slices, 1 mm slice thickness) and functional images (TR=2000 ms, TE=30 ms, FOV 100 mm, voxel size= 3x3x3 mm, number of slides 32, interslice time 62 ms) were taken for each subject. All functional scans used a T2* weighted echo planar imaging sequence. FMRI data was preprocessed and analyzed using the Matlab® based statistical parameter modeling software (SPM8). Each subject's functional volume was realigned to the first volume and co-registered with the structural image. All images were normalized to the SPM8 Montreal Neurological Institute template, and functional images were smoothed with an 8 mm Gaussian kernel.

4.2 Experimental Setup

Subjects were positioned in the MRI scanner so that they could easily see a back-projected image on semi-transparent screen through a rear-view mirror (see Figure 4.1). During the movement task, bilateral hand movement were measured using an MRI-compatible 5DT Data Glove (Fifth Dimension Technologies, http://www.5dt.com). The glove has 14 fiber-optic sensors that measure the metacarpophalangeal (MCP), proximal interphalangeal (PIP) joints, and finger abduction angles. The gloves were interfaced with a virtual reality (VR) environment developed with Virtools 4.0 software package (Dassault Systems) and a VRPack plug-in that communicated with an open source Virtual Reality Peripheral Network VRPN interface (Adamovich, Fluet et al. 2009). The VR environment was designed to show left and right virtual hand models that are positioned in 1st person view, in semi-pronated positions (thumb toward the viewer), on the left and right side of the display (Figure 4.4.1 B).

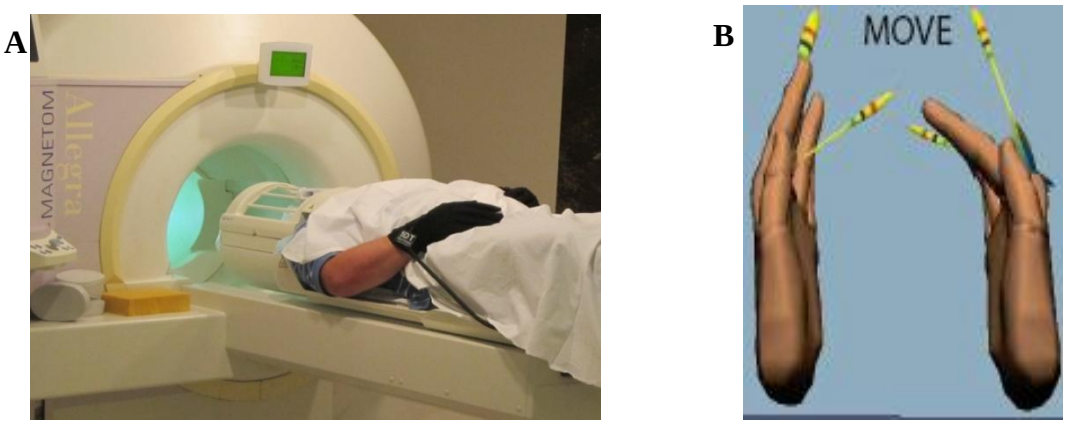

Figure 4.1 A. subject lying in the scanner wearing mri-compatible 5D gloves in both hands. B. Example of a VR environment.

The VR hands were actuated in real-time by data streamed from the 5DT gloves. Previous experiments showed that the 5DT gloves yield reliable measurements and can

be effectively interfaced with VR in an fMRI environment (Adamovich, August et al. 2009). The start of the VR simulation, data glove acquisition, and fMRI data acquisition were synchronized by a back-tick TTL trigger transmitted from the MRI scanner. The VR simulation also included simple instruction text beneath the hand models, which cued subjects to perform the task or rest. The VR simulations were different in the three main experiments in this dissertation (chapters 5, 6 and 7) but the experiment data acquisition and data analysis were similar. Subjects were provided time to practice the task and get familiar with the VR feedback immediately before the experiment, or a day before.

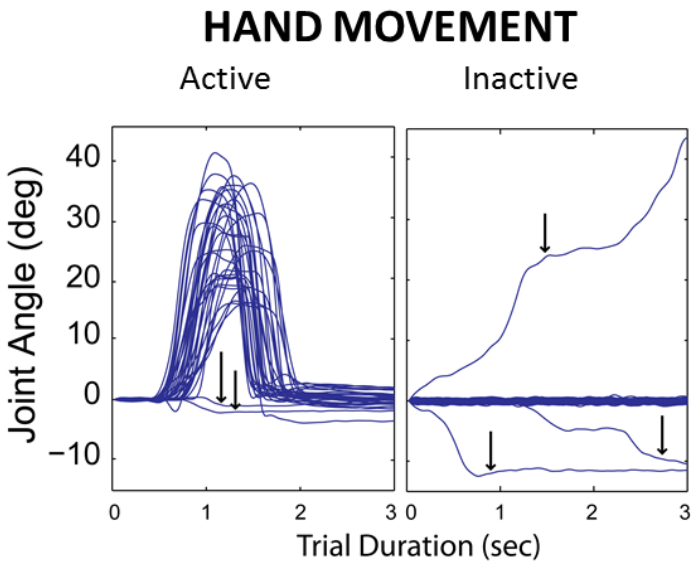

Figure 4.2 Traces of index finger of the active and inactive hands during an experiment, the arrows point to bad trials excluded from the data analysis.

4.3 Movement Behavior Measures

One of the main challenges in analyzing fMRI data taken on different sessions (across sessions or days) is the change in motor performance. Another challenge with stroke subjects is possible mirror movement (unwanted movement) especially if subjects are highly impaired. This dissertation tried to avoid these issues by providing subjects visual

feedback of their movement through a virtual environment. In addition, the finger movements of both hands were monitored tracking movement performance in addition to possible mirror movement. It is novel to monitor the movement kinematics of both hands during the experiment inside the scanner in order to exclude the trials with unintended mirrored movements of the affected hand (Figure 4.2).

Studying the effect of visual effect during a motor task includes confounds related to the effect of difference in motor performance during the fMRI experiment. Researchers tried to limit this effect by restricting the movement duration during the task (metronome) or movement amplitude (define the target). However, it is very difficult to unify all movement parameters across experimental trials or across subjects. Thus, there was a critical need to understand the relationship of hand movement and BOLD activity and regress out this effect when defining the conclusion regarding the main hypothesis of the study.

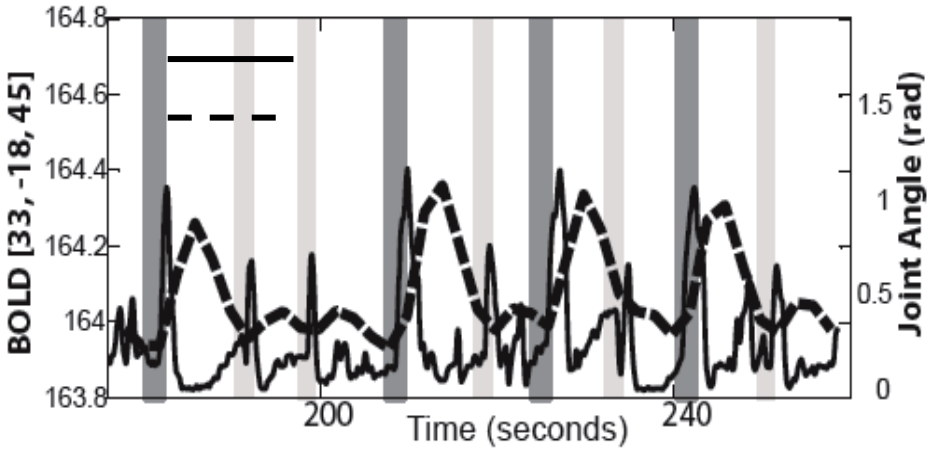

Figure 4.3 Tracking of BOLD signal and joint angles simultaneously.

As mentioned earlier, another issue could be difference in reaction time across trials and sessions in an event-related design. This issue is approached by defining the duration of the task as the time between onset of movement and the offset excluding the

time from the onset of trial and onset of movement. Movement onset and movement time are derived from the glove data using scripts written in Matlab® (Mathworks).

The behavioral measures extracted from the glove data are:

1) Movement time: time between start and end of movement
2) Movement angular excursion : the angle at the peak when subject reached the flexion target
3) Movement reaction time: the time between getting the command to move, and subject's onset of movement
4) Mean velocity: the mean velocity between onset of movement and reaching the target

4.3.1 Behavior Measures Statistics

To verify that movements remained consistent across trials and sessions, all behavior measures data were submitted to a 2-way repeated measures analysis of variance (ANOVA) on all feedback conditions and all experimental runs. For each trial, movement onset and offset were defined as the time at which the mean angular velocity of the four metacarpophalangeal (MCP) joints exceeded and then fell below 5% of the peak mean angular velocity on the corresponding trial. Movement time is the interval between onset and offset. Statistical threshold was set at $p=0.05$ with Bonferroni corrections.

4.3.2 Correlation Between BOLD Activity and Behavior Measures

In the investigation related to aim 2, these behavior measures (except movement duration) were included in the MRI data analysis GLM model as parametric modulators of BOLD activity. This allowed measuring the correlation between change in BOLD

activity and the change in movement kinematics. Figure 4.4 is an example of a GLM design that includes the movement behavior measures as parametric modulators.

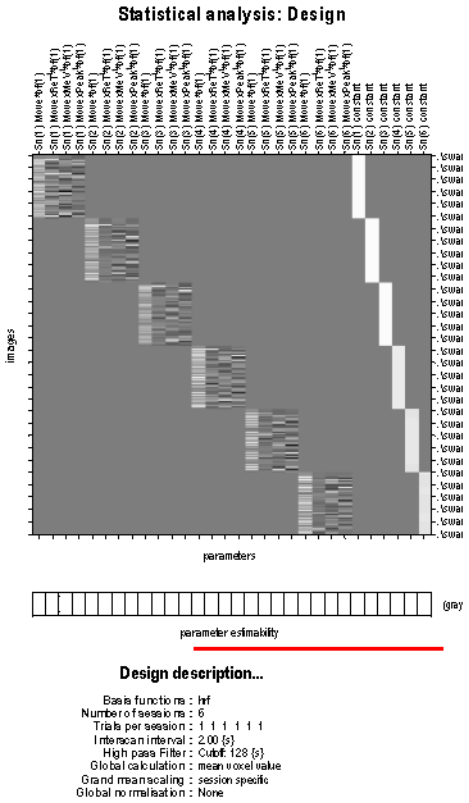

Figure 4.4 An example of a GLM with 6 sessions, and one task per session. The first column of each block models the movement trials timing and the other three columns model the three parametric modulators 1) Reaction time to move (ReT), 2) Movement angular velocity (MeV), and 3) Movement angular excursion (Peak angle).

4.3.2.1 fMRI data analysis. As mentioned earlier, fMRI data were analyzed using SPM8. Basic GLM analysis was performed in each of the three main experiments. Further functional connectivity analysis was performed differently based on the objectives of each of the experiments. Main fMRI data were analyzed using regression analysis (see 3.2), in addition to functional connectivity analysis and effective connectivity analysis (PPI and DCM).

CHAPTER 5

BRAIN REORGANIZATION AFTER VIRTUAL REALITY REHABILITATION TRAINING (AIM 2)

5.1 Background

The main objective of rehabilitative interventions is motor function learning through either recovery or compensation and this can happen due to brain neural plasticity. After stroke and in the case of movement impairment, the brain experiences poor activity in the ipsilesional sensorimotor cortex, this loss is significant in the acute phase after stroke lasting around 6 months. During this period, some form of brain activity reorganization takes place and the contralesional hemisphere tends to compensate for the loss due to the lesion in the other hemisphere (Ward et al. 2003; Butefisch et al. 2005). Brain activity during a simple move versus rest paradigm involves contralateral sensorimotor system, basal ganglia and cerebellum activity (Ghilardi et al. 2000). In longitudinal studies after stroke, increase in contralesional hemisphere activity is experienced, although its dominance starts to decrease during the recovery of the ipsilesional hemisphere (Weiller et al. 1993; Marshall et al. 2000; Pineiro et al. 2001; Carey et al. 2002; Feydy et al. 2002; Small et al. 2002; Butefisch et al. 2005). In the chronic phase, after 6 months, motor recovery slows down and this makes rehabilitation more challenging. However, longitudinal studies still shows possible reorganization with recovery.

Neural plasticity after motor training has been reported as either an increase in BOLD signal amplitude in the sensorimotor cortex or a decrease that might be explained as an increase in efficiency (Seitz 2010). Other than change in signal amplitude (possibly

more synaptic activity), neural plasticity can be in the form of new wiring that develops new neural networks or change in interhemispheric balance.

The main method to evaluate interhemispheric balance is to calculate the laterality index i.e., the ratio of active voxels in the contralesional hemisphere versus the ipsilesional hemisphere. The laterality index equation is $\frac{(C-I)}{(C+I)}$ where "C" stands for active voxels in the specific region contralateral to the moving paretic hand and "I" represents active voxels in the specific region ipsilateral to the moving paretic hand. In this study, LI Matlab® toolbox (Wilke and Lidzba 2007) is used to quantify the shift or change in the balance of activity between two regions, it is used to compare activity in specific areas across movement conditions and across days before and after intervention. This Chapter presents a study of brain neuro-plasticity after two weeks of training, where the extent of change in activation is quantified, in addition to changes in the connectivity of several networks with iM1 as well as re-lateralization of brain activity.

5.2 Methods

5.2.1 Training

Subjects participated in a 2 weeks training program known as New Jersey Institute of Technology Robot-Assisted Virtual Reality training (NJIT-RAVR). Training schedule was 3 hours per day over two weeks, it involved reaching for and interacting with stationary and moving virtual targets, and objects in 3D space (Figure 5.2 A-B). NJIT-RAVR intervention is further explained in other publications (Qiu et al. 2009; Qiu et al. 2009). The main outcome measurements are made two weeks before the start of training

(pretest 1), a day before start of training (pretest 2) and a day after end of training (posttest). Measurements included:

Clinical test: Jebsen Test of Hand Function (JTHF) and Wolf Motor Function Test (WMFT). WMFT and JTHF are standardized clinical tests that quantify motor ability in terms of how fast is the subject to accomplish a set of functional activities. WMFT can be separated into two subcomponents: proximal and distal. Proximal component include six activities that do not require grasping or manipulation of objects while distal component include nine functional activities that require grasping or manipulation of objects. In both WMFT and JTHT, the lower the score the better the performance is.

Kinematic Performance: Change in subject performance on a daily basis in terms of movement speed, movement smoothness, and range of motion.

Neurophysiological activity: fMRI to measure brain activity during a simple paretic hand movement task.

5.2.2 Task During fMRI

During the fMRI experiments, subjects perform whole hand finger flexion with the paretic hand while data of both hands are tracked to monitor possible mirror movements. Prior to the experiment, subject's active range of finger motion is evaluated in order to adjust onscreen targets (arrows) accordingly (40 % and 80% of the active range of motion). The two targets are used to keep the subjects engaged, and to allow analyzing the effects of movement amplitude on the BOLD signal. If active flexion was impossible, the task was finger extension instead, but there is no such issue with any of the subjects. The task trials (16 trials per target) duration is 3 seconds and the trials are randomly interleaved within each run with intertrial rest periods of 3 to 7 seconds. In this

experiment, stroke subjects participated in three fMRI sessions: two weeks before (pretest1), one day before (pretest2) and one day after (posttest) the two-week intensive robot-assisted virtual reality training. The same experimental conditions and parameters were applied on each of the scanning days. Some subjects were not able to do four experimental runs (312 seconds long, 156 TRs) in each of the three testing days due mainly to fatigue; thus, in these cases, three experimental runs were done instead with the same task on each of the three days.

Functional task during fMRI was simple finger flexion movement of the paretic hand. The objective is to compare change in brain activity between posttest and pretests 1 and 2 while subject was doing the same task. Real-time visual feedback was provided by streaming data from an MRI-compatible data glove to animate VR hand models displayed on a screen. The first and second arrows (Fig. 5.1 C.) helped subjects keep same starting position on each trial and do same movement amplitude on every trial. The second arrow was defined randomly at 25 or 45 degrees from the starting position to help reduce the monotony of the task. Non-paretic hand data are also recorded to control for any mirror movement.

Figure 5.1 A. B. Robotic arm, data glove and force-reflecting hand system used in the VR therapy. C. VR feedback during the fMRI movement task.

5.2.3 Subjects

Ten subjects (2 F, 8M, mean age 59.6 ±10.6 years) are included in this study, all are right handed before the stroke (Oldfield 1971) and all suffer from upper extremity impairment. Table 5.1 shows summary of subjects' clinical information.

Table 5.1 Subjects' Clinical Information

subject	Age	Gender	Time Since	CVA side R1 L2	CMA	CMH	Ashworth
1	63	F	53	1	6	4	2
2	55	M	41	2	5	4	7
3	74	M	11	6	6	2	1
4	70	F	96	2	7	5	1
5	58	M	132	1	5	4	3
6	38	M	96	5	4	3	1
7	67	M	90	6	6	0	1
8	51	M	18	1	5	4	6
9	54	M	144	2	6	6	2
10	66	M	15	2	4	5	5

CVA stands for Cerebro-Vascular Accident. CMA stands for Chedockee-Mcmaster scale of Arm movement and CMH is the score for Hand movement.

5.2.4 fMRI Data Analysis

Data of all three days are incorporated in one GLM to compare brain activity during hand movement after therapy versus before therapy. Movement kinematics are included in the GLM as parametric modulators to explore any relationship between BOLD activity and change in motor performance (in terms movement amplitude, velocity, or duration) between testing days.

Main contrast of interest: a) Move>rest, b) posttest > (pretest1 and pretest2), c) (pretest1 and pretest2)>posttest

Connectivity analysis: Change in function connectivity between the ipsilesional motor cortex and the rest of the brain is investigated using PPI analysis (described in Section 3.3.2). The seed voxel for PPI analysis is defined as the most active cluster (8

voxels within the cluster) in the ipsilesional motor cortex (contralateral to the hand moving). Then a new GLM is defined to include PPI vector and seed voxel time series as regressors. The GLM model estimation computes the correlation between all voxels of the brain and the seed voxel. This whole procedure of PPI analysis is performed using gPPI toolbox with customization (see Chapter 3). The output is a regression map between the seed voxel and the rest of the brain for each of the three testing days (pretests 1 & 2 and posttest). The analysis of interest is used to compare the regression maps with iM1 before and after therapy: a) (Regression Map posttest)> (Regression Map pretest 1 & 2) and b)(Regression Map pretest 1 &2)>(Regression Map posttest)

Interhemispheric balance: Interhemispheric balance is computed using the LI toolbox; this analysis is done separately for each of the four lobes (frontal, parietal, temporal and occipital) in addition to the cingulate area, basal ganglia (BG) and thalamus. These areas are defined using the regional masks of the LI toolbox (Wilke and Lidzba 2007). Finally, this analysis is done separately for the ROI that includes precentral gyrus and postcentral gyrus and for the grey matter excluding white matter and central areas of the brain. Both cluster size and variance are used to identify LI (Wilke and Lidzba 2007).

Effective connectivity: Effective connectivity between both M1 areas is analyzed, using the DCM methodology discussed in Chapter 3. The regions of interests are picked from the average move>rest contrast, the regions are of 10 mm radius and a center coordinate as the peak activity within the motor cortex. Dynamic causal modeling is used to study the change in autocorrelation within each of the bilateral motor cortices and their interhemispheric coupling. The tested model is shown in Figure 5.2 and it simply models

the bilateral motor cortices interaction. This model was fitted to the data from each of the testing sessions and days, the next step is to average the DCM models estimated for the sessions in testing days 1 and 2 (pretest=pretest1+pretest2), and testing day 3 separately (posttest). Group average of each subject's model estimated in each of the testing days is performed using Bayesian parameter averaging (BPA) algorithm in SPM. DCM analysis in this dissertation is done using SPM8 , DCM10.

Figure 5.2 Model of interaction between iM1 and cM1 tested in DCM.

5.3 Results

5.3.1 Clinical

In terms of functional outcome, the main outcomes of clinical tests performed are shown in Table 5.2. On average there is improvement in all clinical outcomes; however, some changes are statistically significant (WMFT and distal WMFT) and some are not significant (proximal WMFT and JTHF) at a threshold of p=0.05. S8 is the only subject who does not show improvement in WMFT; however, he showed improvement of 13.9% in the JTHF.

Table 5.2 Subjects' Percent Improvement in Two Main Clinical Measures

subject	WMFT % diff	WMFT proximal % diff	WMFT distal % diff	JTHF % diff
1	0.177143	0.50672	0.151773	0.039438
2	0.104971	0.102314	0.105531	0.096627
3	0.103738	0.131519	0.096527	0.110685
4	0.235164	0.156934	0.245922	0.307438
5	0.031613	0.181179	0.011997	0.063648
6	-0.38795	-0.05964	-0.4414	0.139087
7	0.21232	0.092838	0.18155	0.103433
8	0.397626	0.193691	0.415295	0.10033
9	0.167934	0.208	0.159917	0.162436
10	0.06297	0.050754	0.063726	0.032014
F1,9	2.6	5.5	1.99	17.34
P	0.1414	0.0438	0.192	0.0024

5.3.2 Movement Performance During fMRI Experiment

Repeated Measured ANOVA on the movement kinematics across the testing days shows significant difference (see Table 5.3). The kinematics data for subjects 5 and 9 are corrupted because of technical issues.

5.3.3 Change in Extent of Activation

This is a measure of extent of activation change within each subject after VR training at threshold $p<0.01$ ($T=2.73$). Some of the subjects show increase in the extent of task-related signal (S7), others show decrease in the overall extent of activity (S2, S3, S5, S6) or show both patterns (S1, S8, S9, S10). S4 does not show a significant change in the activation of the sensorimotor cortex at $p<0.01$.

This change of task-related activity suggests some form of brain reorganization, but a direct relationship between direction of change in extent of activation and functional recovery is not apparent. Thus, a regression analysis is performed between extent of activation in 8 main ROIs (the four main brain lobes, cingulate cortex, BG and thalamus, and precentral/postcentral gyrus ROI) with the main clinical scores in Table

5.2. Regression analysis is performed using the statistical package (STATVIEW) to investigate any relationship between change in the extent of activation and clinical scores, Ashworth scale, and age.

Table 5.3 Repeated Measures ANOVA on Movement Kinematics

	Movement duration	Angular excursion	Angular velocity
	Days	Days	Days
S1	$F_{2,14}$=61.87	$F_{2,14}$=78.47	$F_{2,14}$= 29.75
	p<0.001	<.0001	<.0001
S2	$F_{2, 15}$=5.15	$F_{2, 15}$=31.41	$F_{2, 15}$=13.27
	0.012	<.0001	<.0001
S3	$F_{2, 15}$=11.31	$F_{2, 15}$= 85.01	$F_{2, 15}$= 17.43
	0.0002	<.0001	<0.0001
S4		NA	
S5	$F_{2, 15}$= 67.17	$F_{2, 15}$= 77.16	$F_{2, 15}$= 0.77
	<.0001	<.0001	0.472
S6	$F_{2, 15}$= 43.12	$F_{2, 15}$= 2.63	$F_{2, 15}$= 51.07
	<0.0001	0.0885	<0.0001
S7	$F_{2, 15}$= 107.23	$F_{2, 15}$= 138.33	$F_{2, 15}$= 20.32
	<.0001	<.0001	<.0001
S8	$F_{2, 15}$= 114.37	$F_{2, 15}$= 392.40	$F_{2, 15}$= 114.37
	<.0001	<.0001	<.0001
S9		NA	
S10	$F_{2, 15}$= 1423.22	$F_{2, 15}$= 41.2	$F_{2, 15}$= 19.17
	<.0001	<0.0001	0.0006

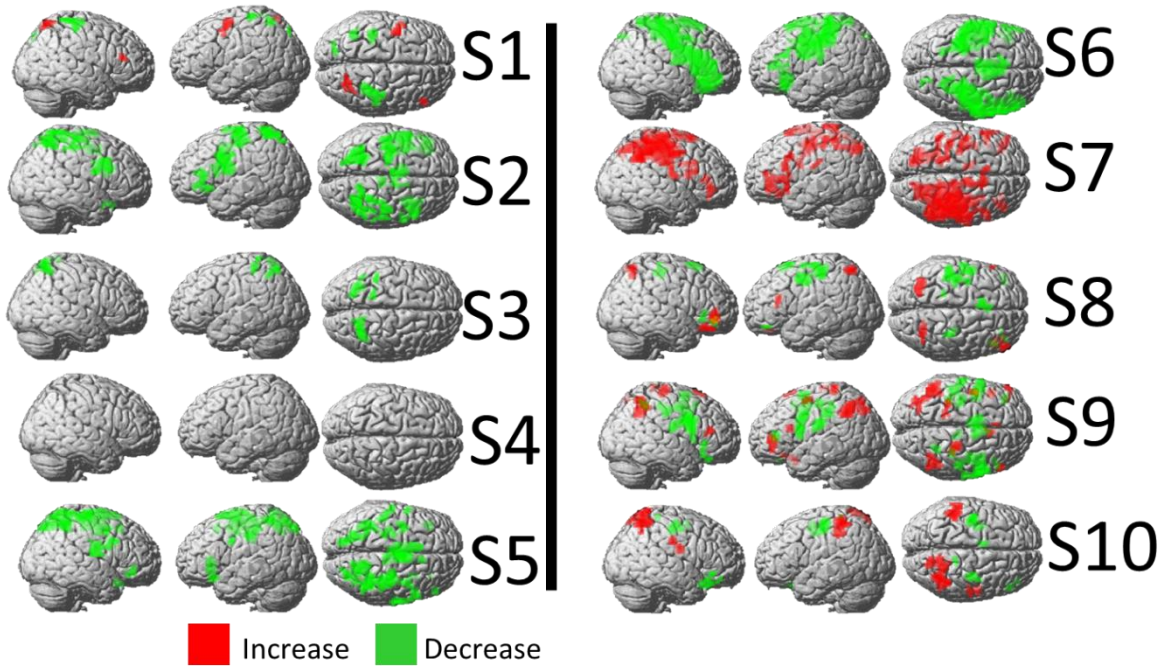

Figure 5.3 Change in the extent of task-related activity. This result is at a statisitcal threshold of p<0.01.

The ratio of change in task-related activity is calculated as the ratio of difference in the number of active voxels in posttest versus pretests normalized to the total number of voxels. There is significant positive correlation between increase in WMFT proximal score and frontal lobe and temporal lobe extent of activation, but one or two subjects drive this correlation. With other scores, the correlation is not significant. Excluding S4 data, there is a significant correlation between the decrease in extent of activation in the basal ganglia and thalamus ROI with increased performance in the JTHF (see Figure 5.4).

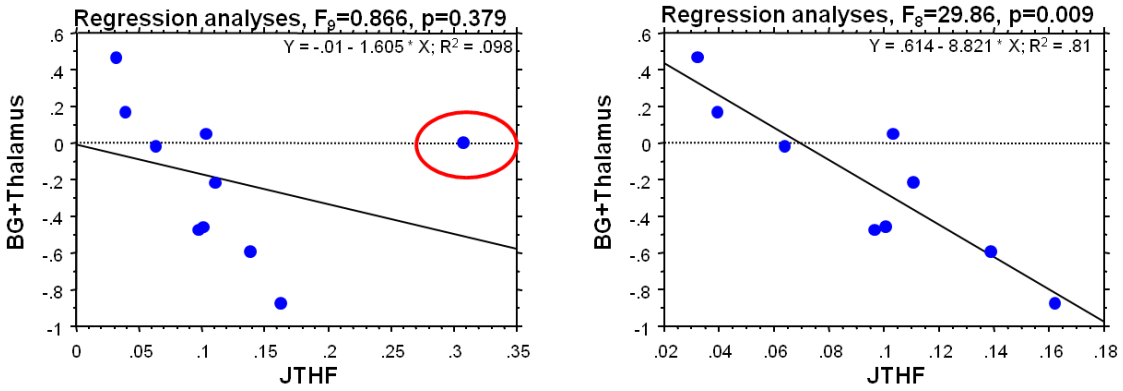

Figure 5.4 Correlation between extent of activation in the ROI including BG and thalamus regions, and JTHF, all 10 subjects are included in the figure to the left. In the right figure, data of S4 is excluded.

In addition to the relationship between change in extent of activity and improvement in clinical scores, there is a relationship between the change in task-related activity and age. Although this relationship is not significant for many of the regions of interest (Figure 5.5), but it seems that older subjects had smaller decreases in extent of activation after training. Previous studies have suggested a relationship between extent of brain activation and lesion location. (Luft et al. 2004) found less brain activation in stroke subjects with cortical lesion when compared to healthy subjects, and more activation in subjects with subcortical lesion; than healthy subjects. In this study, subjects with subcortical lesions demonstrate a decrease in bilateral extent of activation. The ratio of change in extent of activation based on lesion location is analyzed using an Analysis of Variance F test, with hypothesized ratio=1, and lesion location as the grouping variable. S10 is excluded from this analysis because he has both a cortical and subcortical lesion. Combining 8 regions of interests (frontal lobe, parietal lobe, temporal lobe, cingulate cortex, BG+thalamus, and cerebellum), there is a significant difference in decrease of activity between the two group variables ($p=0.0067$, $F_{27,34}=0.361$). Subcortical group had a decrease in extent of action with a ratio -0.295, while the cortical lesion group had a minor decrease (ratio=-0.037).

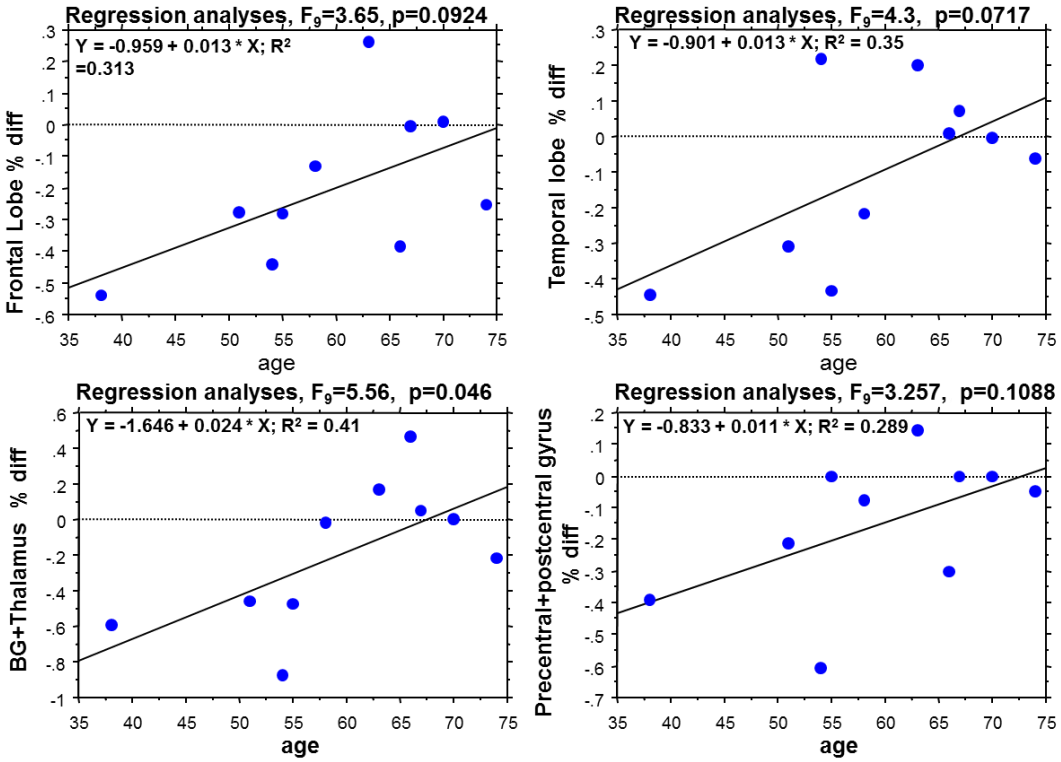

Figure 5.5 Changes in task-related activity after training and its relationship with age.

5.3.4 Change in Signal Intensity

The change in signal intensity is measured as the beta value (regression coefficient between movement and BOLD signal) after training (posttest) relative to pre training (pretest 1 + pretest 2). The ROI of this analysis is the ipsilesional motor cortex, a seed of center coordinate [39 -13 67] and radius 4 voxels. In terms of re-localization of the peak activity in the motor cortex, a simple comparison of the location of the peak activity in iM1 in each of the three testing days shows a small shift between days in terms of location. However, this location changes across the pretesting days as well, suggesting the change at posttest cannot be claimed as a pattern of reorganization due to training.

5.3.5 Change in Connectivity with Ipsilesional M1

Connectivity with ipsilesional M1 is computed using gPPI analysis. Similar to the extent of activation, extent of connectivity either increases or decreases in different subjects. The pattern of change in the connectivity of iM1does not seem to be related to lesion side (right or left), lesion site (cortical or subcortical), or impairment severity.

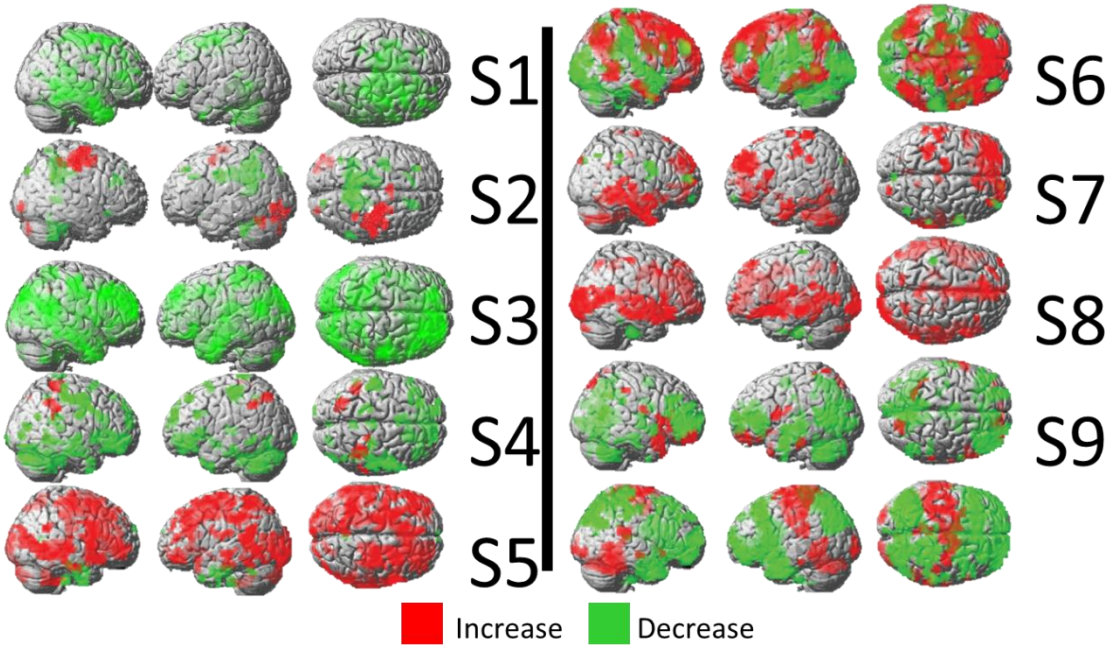

Figure 5.6 Change in PPI functional connectivity with iM1 after training for each subject. This result is at a statisitcal threshold of $p<0.01$.

5.3.5.1 Neuro-motor Coupling. In this dissertation, it is hypothesized that in the presence of consistent movement kinematics across testing days, change in correlation of BOLD signal with movement is due to a change in neuro-motor coupling. It is challenging to perform this analysis since the movement performance is significantly different across testing days; however, for many subjects, the difference is driven by just the pretesting days, meaning that kinematics are similar in posttest compared to either pretest 1 and 2 but pretests 1 and 2 kinematics were different. That is the case in the data

of S2 and S 6 where there is no significant difference in movement kinematics between either pretest1 or pretest2 and posttest. S5 on the other hand shows no significant difference in angular velocity across testing days. Therefore, neuro-motor coupling between movement angular velocity and BOLD signal is compared across testing days showing increase in correlation between angular velocity and BOLD signal in the sensorimotor cortex after training although there is no difference in angular velocity across days (see Figure 5.7).

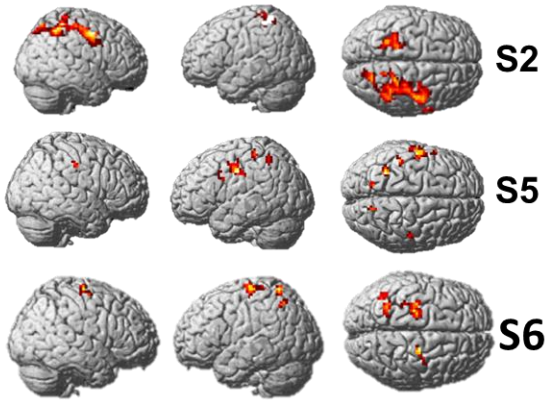

Figure 5.7 Increase in neuro-motor coupling with movement angular velocity.

5.3.6 Interhemispheric Dominance

Laterality Index (LI) is a measure of interhemispheric balance where a value of 1 means complete dominance of the contralesional (left) hemisphere and -1 means complete dominance of the ipsilesional hemisphere. Each of the subjects shows some form of change in interhemispheric dominance, for example S1 shows decease of over-dominance in the contralesional hemisphere. Most of the subjects show variable pattern of change with either a decrease in dominance of the contralesional hemisphere or an increase in dominance of ipsilesional hemisphere; however, there was high variability between subjects. Repeated measures of ANOVA showed significant shift of LI values

toward the ipsilesional hemisphere in the ROI including the precentral and postcentral gyrus (see Figure 5.8) with $F_{1,9}$=9.54 and p=0.013. The difference was not significant in the other ROIs.

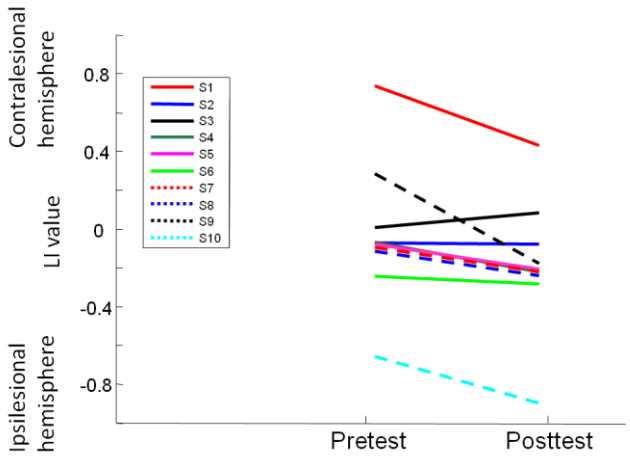

Figure 5.8 Changes in LI values in the region including precentral gyrus and postcentral gyrus.

Change in interhemispheric balance, especially regaining of ipsilesional hemisphere dominance, is expected with recovery, thus, a correlation between decrease in LI value and higher functional score is expected. Simple regression analysis is performed between difference in LI in each of the 9 ROIs previously mentioned and Ashworth scale and the clinical scores presented in Table 5.2. The difference in LI is calculated as ΔLI=(LIpost-LIpre).The results show significant relationship between decrease in ΔLI values of some of the ROIs but not all, and the increase of some clinical scores (mainly the WMFT proximal).

Table 5.4 Results of regression analysis between LI values in 8 main ROIs and the main clinical scores

		Ashworth	WMFT %	WMFT proximal %	WMFT distal %	JTHF %	WMFT pre	WMFT post	JTHF pre	JTHF post
frontal lobe	R^2	0	0.038	0.464	0.033	0.012	0.44	0.33	0.295	0.289
	F	0	0.315	6.92	0.28	0.096	6.25	4.1	3.345	3.25
	P	0.974	0.5902	**0.03**	0.62	0.76	**0.03**	**0.077**	0.105	0.11
parietal lobe	R^2	2.34E-04	4.20E-04	0.003	4.08E-04	0.095	0.483	0.498	0.261	0.286
	F	0.002	0.003	0.027	0.003	0.842	7.46	7.925	2.831	3.21
	P	0.966	0.955	0.874	0.9558	0.3857	**0.0258**	**0.0227**	0.131	0.111
temporal lobe	R^2	0.166	0.066	0.768	0.05	0.008	0.214	0.125	0.127	0.129
	F	1.592	0.566	26.428	0.421	0.066	2.177	1.146	1.126	1.183
	P	0.242	0.473	**0.0009**	0.54	0.804	0.1784	0.2157	0.3125	0.3085
occipital lobe	R^2	0.242	0.003	0.477	1.67E-04	0.01	0.112	0.094	0.042	0.049
	F	2.533	0.02	7.289	0.001	0.078	1.009	0.833	0.352	0.409
	P	0.1488	0.8905	**0.0271**	0.9735	0.787	0.3446	0.388	0.569	0.5403
cingulate cortex	R^2	0.247	0.096	0.144	0.116	0.027	0.003	2.50E-04	0.01	0.005
	F	2.62	0.848	1.341	1.049	0.222	0.023	0.002	0.081	0.037
	P	0.1442	0.384	0.28	0.3358	0.65	0.8837	0.964	0.784	0.8525
BG+ thalamus	R^2	0.249	0.018	0.425	0.009	0.021	0.006	1.30E-05	0.023	0.016
	F	2.647	0.144	5.91	0.071	0.174	0.048	1.09E-04	0.191	0.127
	P	0.142	0.7142	**0.0411**	0.796	0.6875	0.8315	0.99	0.673	0.7306
cerebellum	R^2	0.045	0.019	0.242	0.023	0.036	0.567	0.57	0.429	0.413
	F	0.378	0.157	2.552	0.186	0.3	10.468	10.597	6.011	5.638
	P	0.5558	0.7025	0.1488	0.6778	0.5986	0.012	0.0116	0.0398	0.045
precentral +postcentral gyrus	R^2	0.003	0.002	0.155	0.001	0.041	0.174	0.154	0.082	0.097
	F	0.023	0.016	1.466	0.006	0.344	1.686	1.461	0.717	0.857
	P	0.8828	0.9018	0.2605	0.9416	0.573	0.2303	0.2631	0.4217	0.3815
gray matter	R^2	0.086	0.047	0.601	0.037	0.015	0.264	0.182	0.111	0.121
	F	0.758	0.398	12.033	0.307	0.125	2.867	1.781	0.988	1.098
	P	0.4095	0.547	**0.0085**	0.595	0.733	0.1288	0.2187	0.347	0.325

F degree of freedon = 9

This analysis is challenging since there are two main outliers in the clinical scores, S6 show decrease in WMFT score opposite to all other 9 subjects, and subject 1 show 50% improvement in WMFT proximal score, an improvement that is significantly higher than all other subjects. Therefore, WMFT and JTHF scores in pretest (average of pretest 1 and 2) and posttest days are included in addition to the percentage of change. Interestingly these measures, especially WMFT, show significant negative relationship with the decrease in ΔLI. The slower the subjects are in WMFT, the more functional impaired they are. Therefore, the results show larger improvement in ΔLI for the more impaired subjects.

5.3.7 Effective Connectivity Analysis Using DCM

DCM analysis shows change in coupling between iM1 and cM1 after training. In healthy subjects, it is expected to have negative coupling between these areas, similar to what is known as interhemispheric inhibition. However, before training, many of the subjects showed positive interaction between iM1 and cM1. However, the results of show a decrease or even shift in bilateral motor cortices coupling toward negative in some subjects (see Table 5.5) except for S1 whose data show increase in positive interaction between iM1 and cM1 after training.

Table 5.5 Bayesian Model Fitting Parameter Estimation in DCM

	Pretest											
S	iM1 C		cM1 C		iM1-iM1		cM1-cM1		iM1-cM1-		cM1-iM1	
	CiM1	Pr	CcM1	Pr	BM1-M1	Pr	BcM1-cM1	Pr	BiM1-cM1	Pr	BcM1-iM1	Pr
1	-0.1	0.8	-0.1	0.8	0.3	0.7	0.3	0.7	0.3	0.7	0.3	0.7
2	0.1	1.0	0.5	1.0	-0.4	0.8	0.4	0.7	-0.1	0.6	0.0	0.6
3	0.2	0.8	0.2	0.8	0.4	0.7	0.5	0.8	0.4	0.8	0.4	0.8
4	0.2	1.0	0.2	1.0	0.3	0.9	0.4	0.8	0.2	0.6	0.1	0.9
5	0.1	0.9	0.1	0.9	0.2	0.6	0.2	0.6	0.2	0.6	0.2	0.6
6	0.2	0.7	0.1	0.7	0.3	0.7	0.3	0.7	0.3	0.7	0.3	0.7

Table 5.5 Bayesian Model Fitting Parameter Estimation in DCM (continued)

Pretest												
S	iM1 C		cM1 C		iM1-iM1		cM1-cM1		iM1-cM1-		cM1-iM1	
	CiM1	Pr	CcM1	Pr	BM1-M1	Pr	BcM1-cM1	Pr	BiM1-cM1	Pr	BcM1-iM1	Pr
7	0.1	1.0	0.1	1.0	0.3	0.9	0.4	0.9	0.3	0.9	0.3	0.9
8	0.1	0.8	0.1	0.8	0.0	0.5	0.0	0.5	0.0	0.5	0.0	0.5
9	0.1	0.9	0.1	0.8	0.1	0.5	0.0	0.5	0.0	0.5	0.1	0.5
10	0.1	0.6	0.1	0.6	0.0	0.5	0.1	0.5	0.0	0.5	0.0	0.5
Posttest												
S	iM1 C		cM1 C		iM1-iM1		cM1-cM1		iM1-cM1-		cM1-iM1	
	CiM1	Pr	CcM1	Pr	BM1-M1	Pr	BcM1-cM1	Pr	BiM1-cM1	Pr	BcM1-iM1	Pr
1	0.1	0.9	0.1	0.9	0.5	0.7	0.5	0.7	0.5	0.7	0.5	0.7
2	-0.1	0.9	0.6	0.8	-0.6	0.6	0.1	0.6	-0.3	0.6	-0.4	0.6
3	0.2	0.7	0.2	0.6	0.0	0.5	0.0	0.5	0.0	0.5	0.0	0.5
4	0.4	0.6	0.4	0.5	0.1	0.6	0.0	0.6	0.0	0.5	0.0	0.6
5	0.0	0.6	0.0	0.7	0.2	0.6	0.2	0.6	0.2	0.6	0.2	0.6
6	-0.1	0.7	-0.1	0.7	0.1	0.5	0.1	0.5	0.1	0.5	0.1	0.5
7	0.1	0.8	0.1	0.8	0.3	0.6	0.3	0.6	0.3	0.6	0.3	0.6
8	0.0	0.7	0.0	0.7	0.1	0.6	0.1	0.5	0.1	0.5	0.1	0.6
9	0.0	0.8	-0.1	0.7	0.1	0.5	0.1	0.5	0.1	0.5	0.1	0.5
10	0.2	0.5	0.1	0.5	-0.1	0.5	0.0	0.5	-0.1	0.5	-0.1	0.5

Repeated measures ANOVA is done to investigate the change in DCM parameters in posttest versus pretest (pretest 1 + pretest 2). This analysis does not show a significant difference; however, there is a trend of decrease in coupling between iM1 and cM1 in both directions in addition to change in autocorrelations of iM1 and cM1 (Figure 5.9).

Table 5.5 shows high variability across subjects in terms of iM1 and cM1 autocorrelation and iM1 cM1 coupling strength, this variability is very similar to the variability in motor performance, the variability in performance in clinical scores, and the variability in re-lateralization (LI values). Thus, regression analysis is performed to find any possible relationship between DCM parameters and 1) clinical scores in pretest and

posttest, 2) difference in clinical scores after training, and 3) LI values with the (precentral+postcentral gyri) as an ROI.

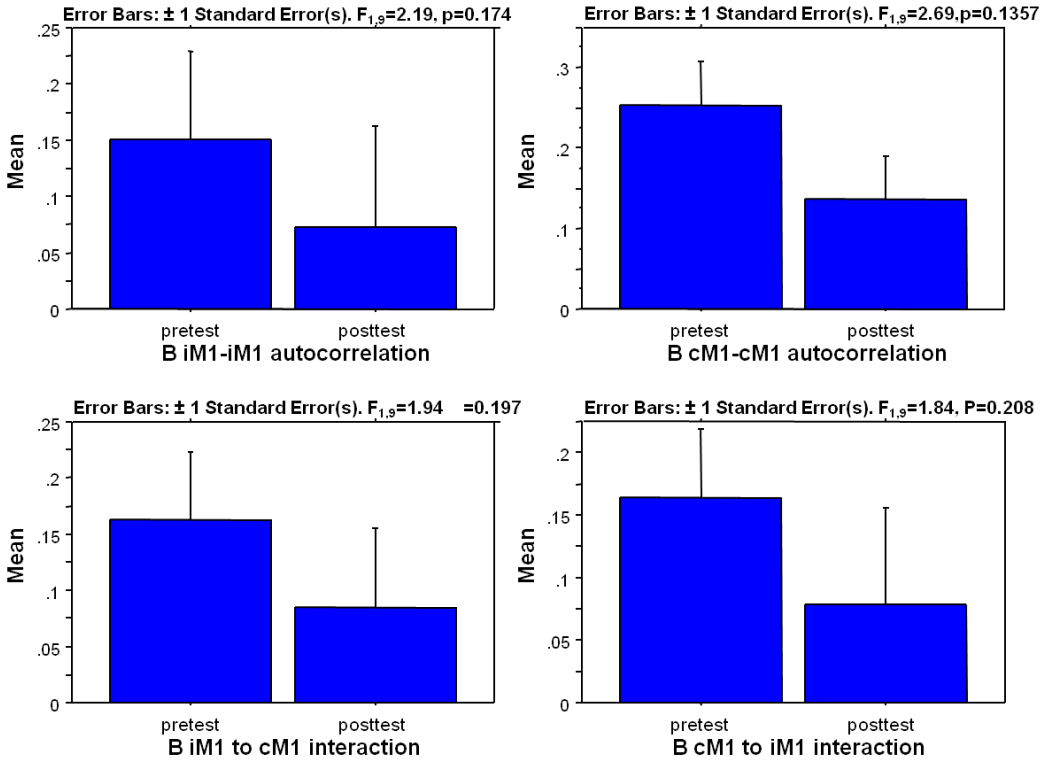

Figure 5.9 Difference in DCM B parameters of the iM1 and cM1 model after training.

There is no relationship between DCM parameters before training and clinical scores or LI values at each of the testing days (pretest and posttest). However, there is relationship between bilateral motor coupling and Ashworth score (measure of spasticity) before training (see Figure 5.10).

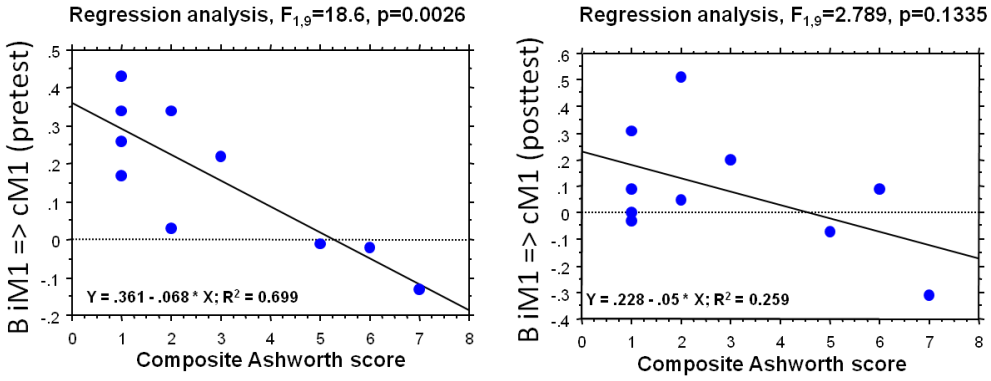

Figure 5.10 Relationship between bilateral motor coupling and Ashworth score (measure of spasticity)

The data show that subjects with weaker performance in WMFT and JTHF, has less decrease in autocorrelation of iM1 and cM1 and in coupling strength among these areas. These results are opposite to the relationship between ΔLI and clinical scores where subjects with weaker movement had less decrease in decrease in LI values. (See Figures 5.11 as an example).

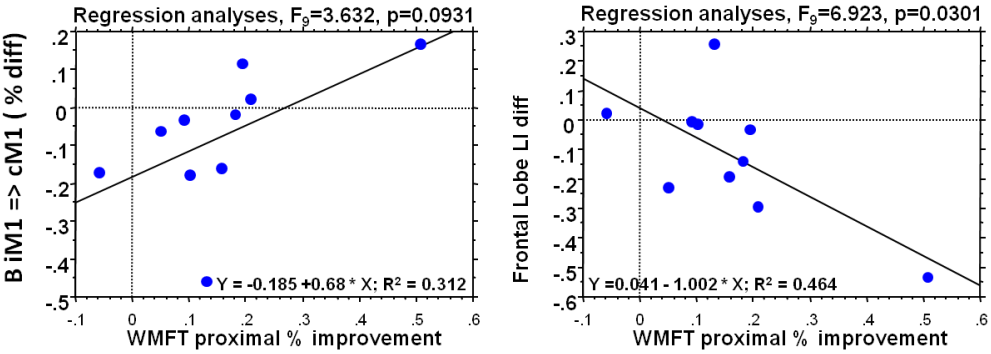

Figure 5.11 Left: Relationship between difference in coupling strength after training from iM1 to cM1 and WMFT proximal clinical subtest. Right: Relationship between decrease in laterality (LI diff) in the frontal lobe and improvement in the WMFT proximal clinical subtest.

In terms of the relationship between re-lateralization and change in DCM parameters, there is a strong negative relationship between difference in DCM parameters and difference in LI values in the precentral and postcentral gyrus after training (see Figure 5.12). A difference in LI and DCM interaction parameters is speculated between

subjects with cortical versus subcortical lesions, however an analysis of variance do not show a significant difference.

While all subjects' motor function improved based on WMFT and JTHF, the variability is high in the patterns of brain activity re-localizations, activity re-lateralization, and iM1-cM1 coupling strength. The negative relationship between ΔLI and DCM parameters changes would suggest that brain reorganization happened either in terms of shift in dominance toward in ipsilesional hemisphere (decrease in LI) or increase interhemispheric inhibition which does not necessary mean dominance of one hemisphere but it does lead to improvement in motor function. These results support the assertion that brain reorganization happens in different directions, and that all should be tracked.

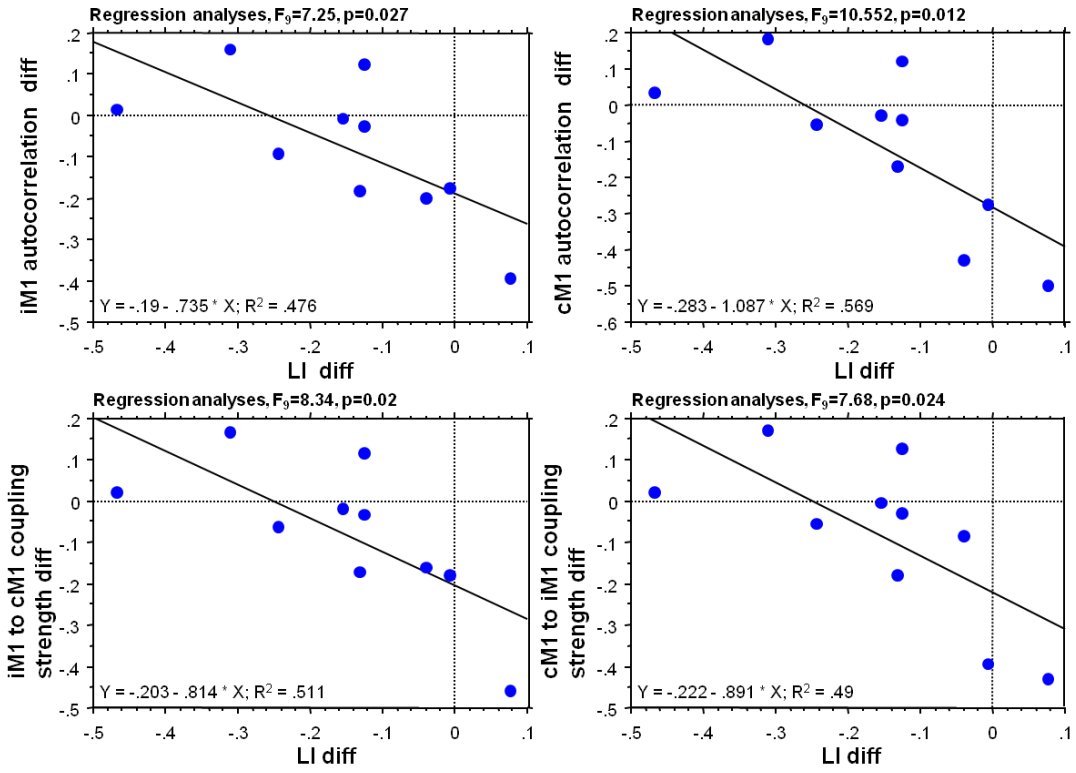

Figure 5.12 Regression analyses between change in DCM parameters and re-lateralization of activity in the ROI including precentral gyrus and postcentral gyrus.

The variability in bilateral motor coupling is also different between subjects with difference CVA sides (L or R) or lesion locations (cortical versus subcortical). Subjects with right CVA show higher bilateral motor cortices coupling strength (see Figure 5.13), and those subjects with cortical lesion show higher bilateral motor cortices coupling strength (see Figure 5.14).

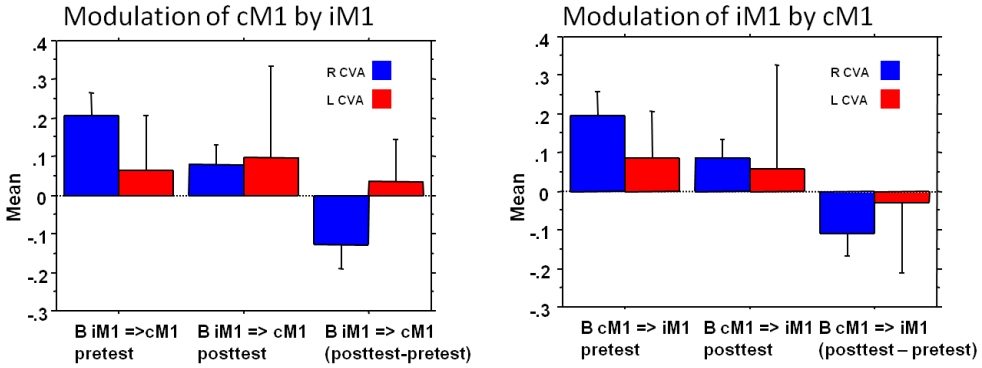

Figure 5.13 Difference in bilateral motor cortices coupling based on CVA side.

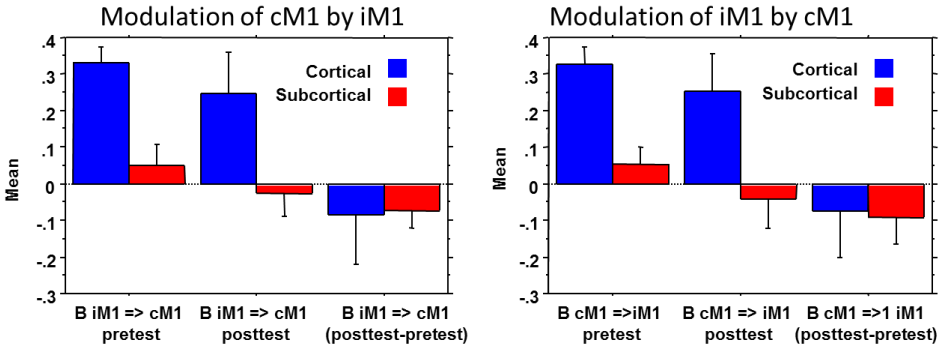

Figure 5.14 Difference in bilateral motor cortices coupling based on lesion site (cortical, subcortical).

5.4 Discussion

In this study, the aim is to quantify patterns of brain reorganization without expecting a discovery of an absolute pattern of brain plasticity. Multiple factors could be contributing to the randomization in reorganization, including age, lesion location, time since stroke, etc. Exploring the literature for imaging studies of interventions, there are 23 studies

which showed either increase in BOLD signal of iM1 after intervention (Butler and Page 2006) (Luft et al. 2004; Szaflarski et al. 2006; Hamzei et al. 2008; Lin et al. 2010; Rijntjes et al. 2011; Kononen et al. 2012; Stark et al. 2012), a decrease (Liepert et al. 2004; Sheng and Lin 2009; Rojo et al. 2011) or no change (You et al. 2005) (Jang et al. 2005; Bhatt et al. 2007; Cho et al. 2007; Murayama et al. 2011). There are few recent studies that showed increased in functional connectivity in brain networks following motor imagery (Sharma et al. 2009), CIMT (Chouinard et al. 2006) and skill retraining (James et al. 2009). There is also a recent study that quantified changes in interaction among three main regions of the brain (iM1, cM1 and SMA) using structural equation modeling (SEM) based on resting state brain activity (Inman et al. 2012).

Besides interventions, few longitudinal studies tried to relate change in brain activity to motor recovery. (Ward et al. 2003) study showed negative relationship between motor recovery and the extent of activation in M1, premotor, prefrontal, SMA, cingulate sulcus, temporal lobe, striate cortex, cerebellum, thalamus, basal ganglia. The Ward study include eight subjects, four of which showed linear relationship between region activations and recovery, this is an example of the difficulty to get a group effect in a stroke longitudinal study. In terms of re-lateralization, (Calautti et al. 2007) reported a negative relationship between recovery and the lateralization of M1 an S1 toward contralesional hemisphere.

Traditional univariate approaches are used to characterize signal intensity in this study, in addition to multivariate approaches to characterize neural dynamics in terms of functional connectivity of iM1. The univariate analysis shows both patterns of change, increase and decrease in brain activation, similar to the multivariate analysis. It is not

easy to relate these changes to motor recovery; however, this spatial re-localization in brain reorganization may be contributing to the improvement in motor function.

Re-lateralization of brain activity is another measure of spatial re-localization of brain activity; this study shows that two weeks of NJIT-RAVR training lead to increase in the dominance of the ipsilesional hemisphere, a spatial re-localization towards normal. In nine ROIs used, there is either a significant relationship or trend of relationship between shift in lateralization toward iM1 (decrease from +1 to -1) and clinical measurements of impairment (Ashworth scale) and performance change after training (WMFT and JTHF). Spatial re-localization of activity and iM1 connectivity may be related to increased efficiency of iM1 brain network leading to functional recovery.

It is interesting to find positive coupling between cM1 and iM1, a maladaptive phenomena that could be unique to chronic stroke. A study by Rehme et al. (Rehme et al. 2011) found that in the chronic phase of stroke, subjects with poorer performance have negative coupling from cM1 to iM1. This would suggest that positive coupling between cM1 and iM1 is a compensation for the absence of efficiency in the ipsilesional hemisphere sensorimotor network.

A novel criterion in this study is modeling trial-to-trial kinematics data of subject movement performance during fMRI scanning. This is crucial not just for exploring neuro-motor coupling but also to identify any possible relationship between difference in motor performance and difference in BOLD activity. Besides, accounting for possible inadvertent movement that would be a confound in data analysis particularly for the measure of re-lateralization. Few studies since 2005 captured some type of motion measurements in fMRI (Bhatt et al. 2007; Stark et al. 2012); however, they did not

address possibility of neuro-motor coupling change after interventions. In this study, it is not possible to track neuro-motor coupling in each subject due to change in motor performance of some of them across testing days; however, it was possible to characterize the amount of BOLD variance, at the single subject level, explained by variability in motor performance.

Due to heterogeneity of the stroke population and to the difference in patterns of brain reorganization after the intervention, it is still necessary to study brain reorganization at the single subject level. In a bigger population, such study would be able to identify patterns of brain reorganization as predictors of motor recovery.

One of the challenges in this study are the heterogeneity of the subjects as mentioned before, which include heterogeneity in lesion characterization, time since stroke and motor performance. This situation creates a challenge to run regression analysis between brain activity spatial re-localization and re-lateralization with the clinical scores. For example, S8 shows a decrease in WMFT test after training being the only subject not responding to the training in that specific test, although he shows improvement in the JTHF. In addition to this variability, there is the challenge of having subjects perform consistent finger movement in the scanner. As found in this study, even visual feedback of movement does not help all subjects to keep consistent movement across testing days. In addition to the heterogeneity of subjects, several subjects could not produce any finger movement in the scanner, so they were unable to participate in this study.

Measuring resting-state functional connectivity (rsFC) is an alternative approach not used in this study that might have avoided this shortcoming. The subject does not

have to produce any movement to acquire a resting state signal, which would have allowed us to examine brain connectivity in subjects with higher impairment. Connectivity of brain activity with iM1at rest can be a good measure of brain activity and brain reorganization after intervention in the absence of task-related fMRI measurements. DCM analysis is possible on resting-state data to investigate interhemispheric connectivity of bilateral primary motor cortex at rest (endogenous connectivity). Besides, this data can be used as a measure of baseline BOLD activity to predict individual task-induced changes in BOLD activity (Liu et al. 2011) and as a means of scaling the task-induced BOLD activity to obtain more accurate BOLD signal measurements during activity (Kannurpatti and Biswal 2008; Kannurpatti et al. 2010; Kannurpatti et al. 2011).

CHAPTER 6

MANIPULATING FINGER MOVEMENT VISUAL FEEDBACK (AIM 3)

6.1 Background

The significant feature of virtual reality therapy is getting feedback of one's own movement. Visual and haptic feedback of person's motor performance can have a strong influence on motor training. Numerous studies have investigated the role of haptic feedback (Wise et al. 1998; Patuzzo et al. 2003; Mattar and Gribble 2005; Bray et al. 2007) and visual feedback (Ghilardi et al. 2000; Culham et al. 2003; Pilgramm et al. 2010) in the motor control of upper extremity. The question is how would the presence of visual feedback during movement improve or change the activity in the sensorimotor cortical system and if it would emphasize motor learning (Patton et al. 2006; Reinkensmeyer and Patton 2009).

Error-less feedback means veridical feedback without distortion while error-based feedback involves distortion of feedback like scaling, or implementing incongruency. Both errorless and error-based feedback have been investigated; some post-stroke arm rehabilitation studies showed promise with errorless feedback on recovery (Macclellan et al. 2005) (Finley et al. 2005), other studies have shown superior benefits of error-based learning on retention of motor skills (Prather 1971), (Mount et al. 2007). Patton and coworkers (Patton et al. 2006; Patton et al. 2006) studied visual feedback during a motor task and showed learning facilitation with exaggerated error. (Mancini et al. 2011) study found that enlarged feedback of subjects hand modulated the thermal heat pain threshold, suggesting that hypermetric feedback would increase the analgesic effect of seeing the hand. (Brewer et al. 2008; Brewer et al. 2009) found that both implicit and explicit

distortion of visual feedback of the movement goal enhanced movement performance of subjects with neurological disorder.

(Feys et al. 2006) studied the role of visually-guided hand movement feedback on reducing intention tremor in multiple sclerosis; they found that averaged visual feedback of movement over time windows of 150, 250, and 350 ms reduced hand intention tremor amplitude. (Coombes et al. 2010) studied the role of visual feedback during isometric force production. A small increase in the visual gain (<1°) leads to reduction in force error and activation of left M1, bilateral V3 and V4 and left PMv. However, visual gain increases above 1° leads to activity in bilateral dorsal and ventral premotor areas in addition to right IPL. It can be concluded from Coombes and colleagues results that different forms of visual feedback bolster activity in distinct neural networks.

Other than motor and premotor areas, multiple studies showed change of activity in the occipito-temporal and occipito-parietal areas in response to feedback manipulation. (Saxe et al. 2006) found that right extrastriate body area (EBA) responds to allocentric visual feedback of body image while activity in MT, left EBA and right lateral occipital cortex were both active with allocentric and egocentric visual feedback. While this difference is interesting it should be noted that what the authors referred to as allocentric perspective can also be regarded a mirror of the egocentric perspective; referring to the feedback of the foot and the palm hand in their experiment. This would suggest a role of EBA in judgment of mirrored feedback of body image (see also chapter 7). Right dorsolateral prefrontal cortex responded more to egocentric versus allocentric visual feedback of body image, right postcentral gyrus showed suppression of activity in the egocentric feedback.

(Yomogida et al. 2010) studied movement to target using a joystick. They found that mismatch of feedback, distorting the sense of agency, is associated with activity in right EBA, bilateral SMA and right IPL, while mismatched feedback was associated with activation in the bilateral insula, bilateral premotor areas, left IPL, right preSMA, and the right middle temporal gyrus.

(David et al. 2007) study showed increased activity in the right EBA and PPC during visual feedback incongruent with real executed movement; moreover, PPI analysis using EBA as the seed showed an increased functional connectivity of the EBA with right postcentral gyrus and bilateral SPL regions during incongruent feedback. On the other hand, Kontaris study (Kontaris et al. 2009) reported equal activity of EBA, fusiform body area (FBA) associated with incongruent and congruent feedback of hand movement while posterior superior temporal gyrus activity was higher with incongruent feedback. (Kontaris et al. 2009) further discussed the activation of right EBA as response to incongruent feedback. (David et al. 2007) study proposed that this activity might be in the MT and not the EBA since there is overlap based these two areas (based on the findings of Downing et al) and the fact that the task involved moving a cursor and not moving a body part.

(Stanley and Miall 2007) investigated effects of incongruent visual feedback of the hand. The incongruency was in the hand position (palm up or down) and it was correlated with the activity in left SPL and dorsal premotor cortex. Stanley and Miall study did not report EBA activity, probably because the visual feedback was using hand imagining instead of hand movement that would induce a sense of agency.

In summary, many forms of visual discordance have been studied showing influence on activity of distinct brain networks. While the above-discussed studies mostly tried to understand the role of select brain regions and networks, this dissertation aims to understand the potential of using visual discordance in recruiting brain regions that are critical for enhancing brain plasticity after a neurological disorder like stroke. If manipulating the hand movement feedback in terms of amplitude or side (see chapter 7) recruits select brain regions especially motor cortex and premotor areas, then these manipulations could be exploited in developing VR therapy paradigms for hand rehabilitation.

6.2 Methods

This study includes two experiments with two groups, healthy subjects and stroke subjects with upper extremity hemiplegia.

6.2.1 Experiment 1, Healthy Subjects

Subjects: Twelve right-handed (Oldfield 1971) and healthy subjects (mean age ± 1 standard deviation: 27.3 ± 3.5 years).

Task: Subjects performed single right hand finger movement while watching feedback of their movement through the above-discussed virtual environment.

Feedback manipulation: the correspondence between subject movement and the motion of the VR hand model viewed on the display is manipulated randomly on a trial-to-trial basis in one of four ways 1) Veridical (V): The fingers of the VR hands move one degree for every degree of subjects' movement; i.e., in a perfect correspondence to the actual movement such that subjects are provided with high fidelity feedback of their

motion. 2) G65: The fingers of the VR hands move 0.65º for every one degree of actual movement produced by the subject. Thus, the amplitude of the VR hands' motion is 65% that of the subjects' actual motion. 3) G25: The fingers of the VR hands move 0.25º for every one degree of actual movement produced by the subject (i.e. 25% of the subjects' actual motion). 4) The amplitude of finger flexion/extension between the VR hands' and the actual hands motion is maintained at a 1:1 ratio but the finger on the VR hand that is actuated is not the same as the actual finger performing the movement (i.e. mismatched finger condition, MF).

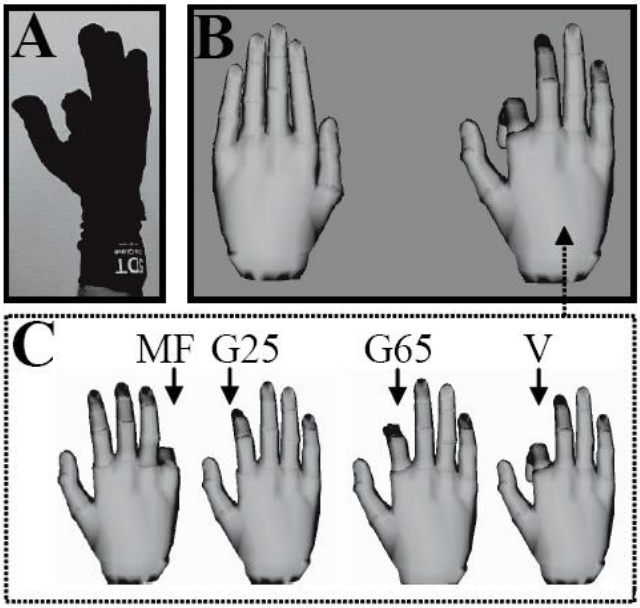

Figure 6.1 Feedback conditions of finger movement.

Conditions 1, 2 and 3 are designed to parametrically investigate effects of varying levels of hypometric feedback such as those that may occur due to paresis (i.e. after stroke), while MF condition is designed to simulate feedback of unintentional movements such as those that may occur due to spasticity (i.e. after stroke). Movement task duration is 3 seconds and it occurs 10 times within a functional imaging run with interleaved rest periods of 3 to 7 seconds.

Main contrasts of interest are: a) Move>rest b) Veridical>G25, c) Veridical >G175, d) Veridical>MF, e) G25>Veridical, f) G65>Veridical, g) MF>Veridical

6.2.2 Experiment 2, Stroke Subjects

Subjects: Eleven right-handed subjects with unilateral hemiplegia due to stroke (see Table 6.1 for subjects' information) participated in this part of the study.

Table 6.1 Subjects' Clinical Information

Pt	Age	Sex	Months since CVA	CVA side L/R	CMA	CMH	Ashworth	Lesion Location
1	55	M	41	L	5	4	7	thalamic nuclei
2	41	M	158	L	6	6	2	frontal, parietal and temporal lobes
3	53	M	156	R	6	6	2	pons
4	41	F	70	R	6	6	0	frontal parietal and temporal lobes
5	74	M	9	R	6	6	1	frontal lobe
6	70	F	96	R	7	5	1	corona radiata
7	58	M	132	R	5	4	3	frontal, parietal and temporal lobes
8	37	M	92	R	4	3	3	pons
9	69	F	18	R	7	7	1	pons
10	68	M	78	R	6	6	1	occipital lobe
11	66	M	15	R	2	4	5	thalamus

CVA stands for cerebrovascular accident; CMA for Cherokee-McMaster motor assessment arm scale; CMH is Chedokee-McMaster motor assessment hand scale; dWMFT stands for distal wolf motor function test. L stands for left and R for right

The data of the healthy subjects (experiment 1) show greater effect of conditions Veridical and G25. Thus, just these two experimental conditions are included in the experiment on the stroke subjects in addition to hypermetric condition G175 where the VR hands move 1.75º for every one degree of actual movement produced by the subject.

Main contrasts of interest: a) Move>rest,) b) Veridical>G25 c) G25> Veridical, Veridical>G175 d) G175>Veridical e) Veridical> (G175+G25), and f) (G175 + G25)>Veridical.

Movement Kinematics: Kinematic analysis was used to verify that movements of the paretic hand (the active hand involved in Experiment 2) are consistent across feedback conditions. For each trial, movement onset and offset are defined as the time at which the mean angular velocity of the four MCP joints exceed and then fall below 5% of the peak mean angular velocity on the corresponding trial. Movement time is the interval between onset and offset. Movement onset and time are modeled in the GLM on a trial-by-trial basis to give a more temporally accurate convolution of the BOLD events with the hemodynamic response function. To verify that movements kinematics remained consistent, the peak angle attained (angular excursion), movement time on each trial and mean velocity from movement onset to reaching the target (angular mean velocity) were submitted to a 2-way (feedback condition by experimental run) repeated measures analysis of variance (ANOVA). Statistical threshold was set at 0.05 with Bonferroni correction.

6.3 Results

6.3.1 Experiment 1, Healthy Subjects

6.3.1.1 Movement behavior measures. Inspection of subject's MCP joint angle trace for each finger and condition recorded during fMRI suggests that subjects complied with the task. Statistical analysis of reaction time, movement duration, and movement extent reveals no significant main effects for FINGER, CONDITION, or SESSION ($p>0.05$ with Bonferroni correction) (see Table 6.2). In addition, estimation of feedback quality performed by the subjects in the scanner shows that subjects' perception of the feedback manipulation is correlated with the amount of feedback distortion (see Figure 6.2A). It is worth mentioning here that subjects perceived the mismatched condition as a condition with the most distorted feedback.

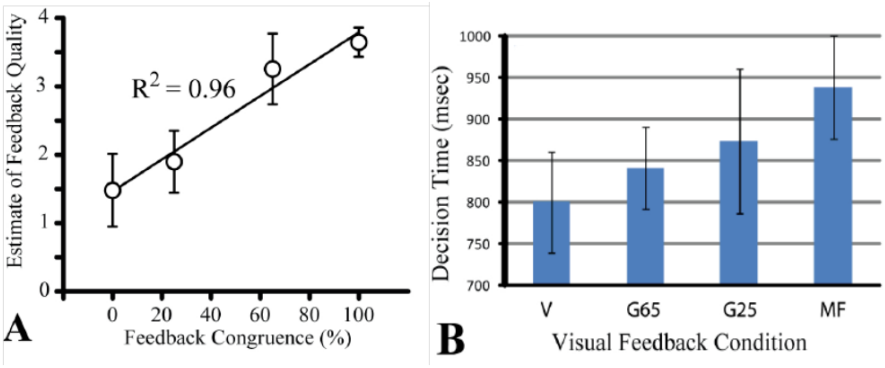

Figure 6.2 Evaluation of visual feedback.

6.3.1.2 fMRI. Veridical compared to hypometric feedback. The main contrast V>G65 does not reveal the main difference between the two conditions; however, the G65 compared to Veridical (G65>V) contrast shows activation in the contralateral primary motor area. Despite the manipulation of visual feedback, subjects complied in keeping their executed movement amplitude constant; assuring that any differences in

activation between these conditions cannot be attributed only to visual feedback of the VR hand model.

Table 6.2 Behavioral data across conditions

Condition	**Peak Amplitude**		**RT**	**MT**	**DT**
Veridical	I	0.53 (0.21)	434 (95)	2498 (218)	833 (227)
	M	0.56 (0.33)			
	R	0.66 (0.21)			
	P	0.55 (0.21)			
G65	I	0.54 (0.19)	438 (102)	2499 (221)	860 (176)
	M	0.57 (0.34)			
	R	0.67 (0.21)			
	P	0.50 (0.16)			
G25	I	0.55 (0.22)	448 (116)	2465 (234)	871 (288)
	M	0.56 (0.31)			
	R	0.66 (0.21)			
	P	0.52 (0.16)			
MF	I	0.54 (0.21)	453 (89)	2445 (181)	921 (213)
	M	0.52 (0.29)			
	R	0.64 (0.18)			
	P	0.51 (0.17)			
p		0.841	0.235	0.122	0.814
F		0.31	1.49	2.08	0.32

Veridical compared to hypometric feedback (V>G25) is associated with activation in the bilateral superior parietal lobule, and bilateral occipitotemporal cortex and bilateral middle occipital cortices. The reverse contrast, hypometric compared to Veridical feedback (G25>V) is associated with activation in the contralateral precentral

gyrus. This region is adjacent with some overlapping to the precentral gyrus activation recruited in the reverse (G65>V) contrast. Figure 6.3 shows the negative and positive correlation with visual gain distortion combining G65 and G25 conditions.

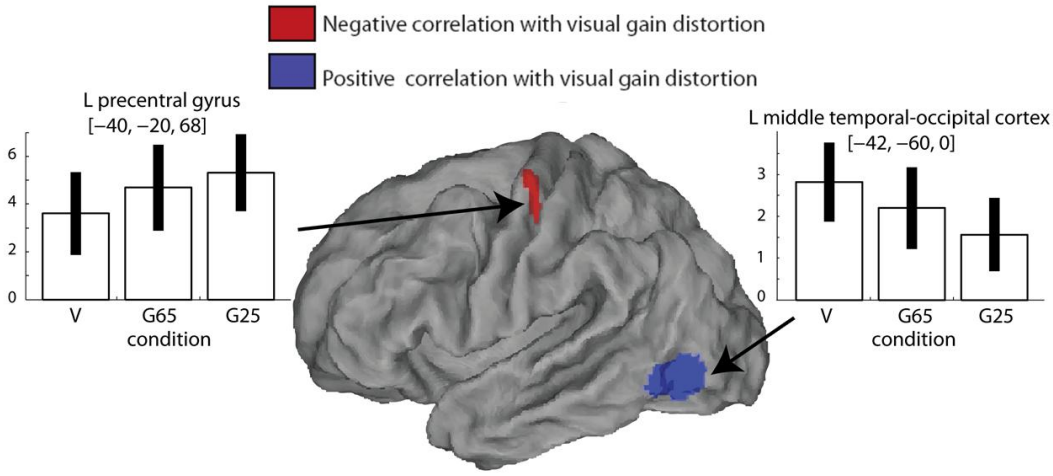

Figure 6.3 fMRI activation in veridical compared to hypometric visual feedback.

6.3.1.3 fMRI. Veridical compared to mismatched feedback. In mismatched feedback (MF) trials, the actuated virtual finger never corresponded to the real finger that the subjects moved. Importantly, the amplitude of VR hand motion corresponded to actual motion (unlike in the hypometric condition above); only the mapping between the virtual and real fingers is altered. Activation in the V>MF contrast is noted only in the ipsilateral pre- and postcentral gyri, ipsilateral rolandic opercularis, superior temporal gyrus, and calcarine and contralateral inferior and middle occipital cortex. The reverse contrast, MF>V, is associated with activation in the bilateral ventral precentral gyri extending into caudal middle frontal gyri, left frontal operculum and superior frontal gyrus, left parietal operculum, left superior parietal lobule extending into the postcentral gyrus, and left occipitotemporal cortex (see Figure 6.4).

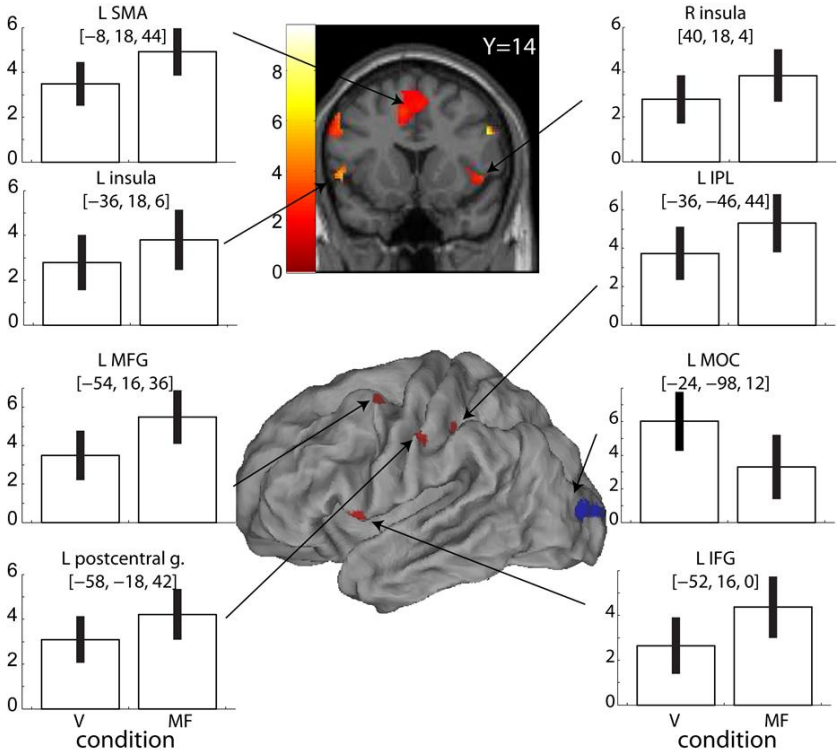

Figure 6.4 fMRI activation in veridical compared to mismatched feedback.

6.3.1.4 fMRI. BOLD signal correlation with movement decision time. Decision time was measured as the time it took subjects to rate the perceived amount of correspondence between their actual movement and the VR hand's movement (i.e. decision-making time). Figure 6.2B shows that subjects took increasingly longer to evaluate the perceived distortion as the degree of correspondence decreased (i.e., they were quicker to recognize veridical feedback). Interestingly, subjects took the longest to evaluate the feedback of the MF condition, which is arguably the most distinct feedback condition. Figure 6.5 shows that BOLD activity positively correlates with the decision time in bilateral insula, bilateral superior parietal lobules, contralateral caudal middle frontal gyrus (dorsal premotor area, Broadmann area 6), bilateral supplementary motor area and bilateral inferior occipital lobe (see Table A6.1).

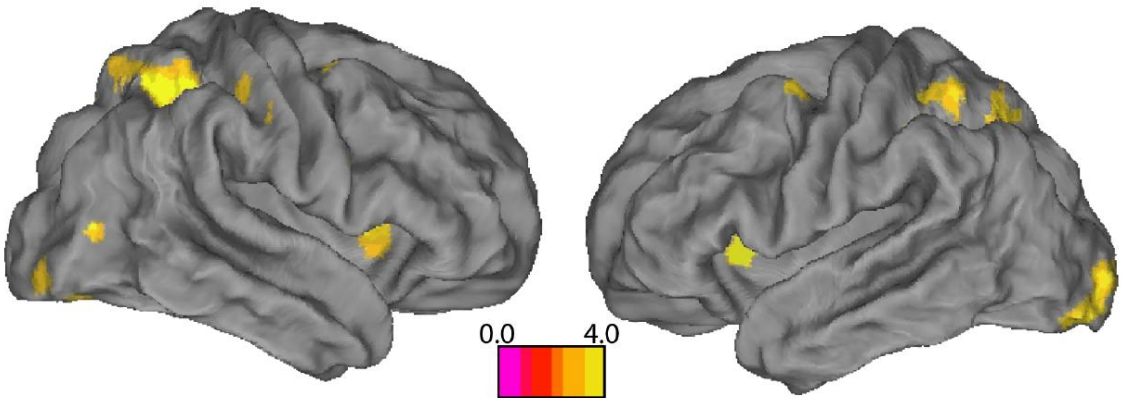

Figure 6.5 BOLD signal correlations with decision time.

6.3.1.5 PPI connectivity analysis. This PPI analysis was performed using contralateral (left) M1 as the ROI. This region was selected using the G25>V contrast (see Figure 6.3) as a sphere with the center coordinates [-40 -20 68] and 8 mm radius. This ROI is the hand region in the precentral gyrus. In G25>V and MF>V contrasts, contralateral M1 is correlated with areas within the central sulcus ([-48 8 34] for G25>V and [-45 -6 30] for

MF>V). However, in G25 versus V, M1 regression map includes central sulcus and prefrontal cortex activity. MG>V PPI regression map includes central sulcus in addition to occipitotemporal area and inferior temporal gyrus, this suggests a distinct network of connectivity of M1 in each of the two conditions. In V versus both G25 and MF (V>G25, and V>MF), PPI analysis shows higher correlation of M1 with frontal areas, insula, occipitotemporal and occipitoparietal areas (Figure 6.6).

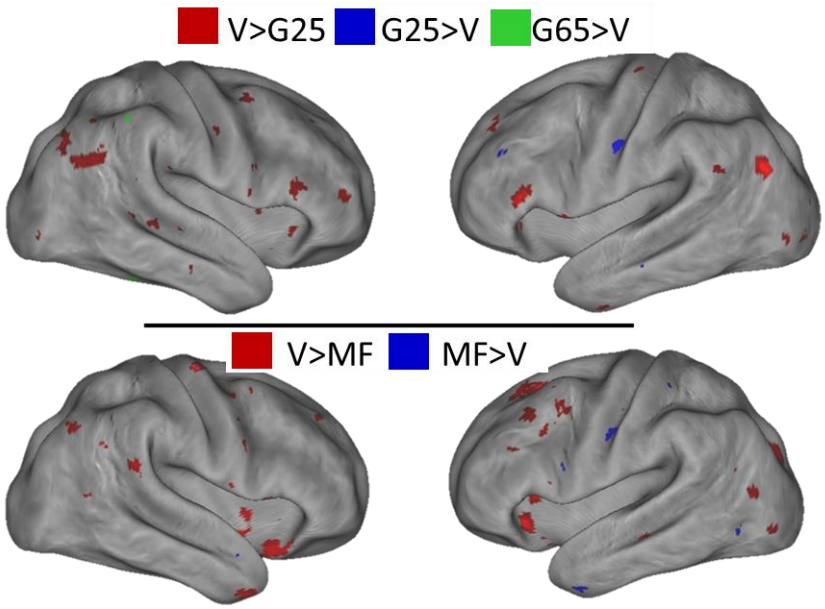

Figure 6.6 Results of PPI connectivity analysis of experiment 1, at statistical threshold $p<0.01$.

6.3.2 Experiment 2, Stroke Subjects

6.3.2.1 Movement behavior measures. Repeated measures ANOVA of angular excursion shows no difference between runs ($F_{3,10}=0.96$, $p=0.4241$), but there is a difference between conditions ($F_{3,10}=16.284$, $p<0.001$), the mean amplitude in G175 condition is 0.744 (0.26) radians, but it is higher in V conditions (0.817(0.28)) and lower

in G25 condition (0.904 (0.337)). Although the difference in angular excursion is significant between conditions, the actual difference does not exceed 0.1 radians. In terms of movement time, it is not statistically different between runs ($F_{3,10}$=0.322, p=0.0809) and conditions ($F_{3,10}$=0.138, p=0.872). Similarly, angular velocity is not different between runs ($F_{3,10}$=0.771, p=0.519) and conditions ($F_{3,10}$=0.738, p=0.4905).

6.3.2.2 Response to visual discordance. It is interesting to find that both G25 and G175 induce changes in excitability of sensorimotor cortex in addition to occipitoparietal and occipitotemporal areas. At p<0.05, iM1 is significantly active in both contrasts G25>V but weaker in the G175>V. G25>V contrast induces significant increase in activation of ipsilesional posterior parietal cortex (PPC), in addition to the middle occipital cortex, this activity extends to the temporal lobe. G175>V contrast similarly induces increase in activation of bilateral PPC, but it involves more inferior parietal lobule (IPL) than superior parietal lobule (SPL).Both G25>V and G175>V contrasts reveal higher activation in the ipsilesional hemisphere fusiform gyrus (fusiform body area). (See Figures 6.7, 6.8, and 6.9 and Table A6.2).

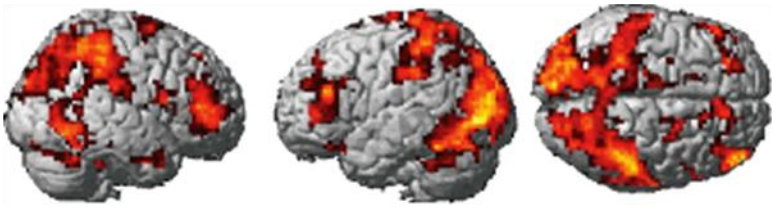

Figure 6.7 fMRI activations in G25>V contrast, at statistical threshold p<0.05.

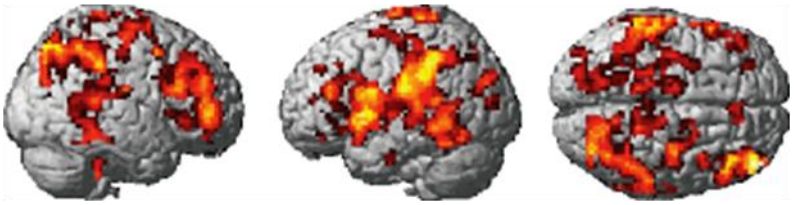

Figure 6.8 fMRI activations in G175>V contrast, at statistical threshold p<0.05.

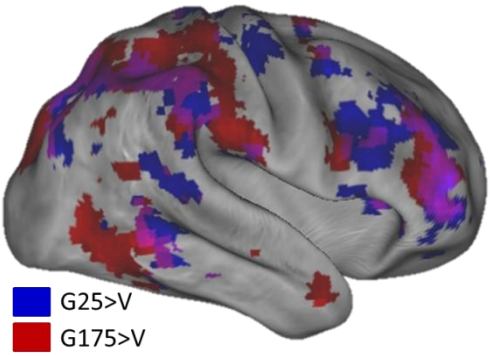

Figure 6.9 Results of the main contrasts, G25>V and G175>V contrasts, at statistical threshold p<0.05.

6.3.2.3 Regression analysis. In healthy subjects, the effects of visual discordance are uniform across subjects. On the other hand, there is more variability in the response to visual discordance in the stroke subjects. The variability can be attributed to the impairment level or to the lesion location. For example, in S10 brain lesion is in the occipital cortex; similarly, S4 has vision problems and a lesion that involves the right posterior parietal cortex. In these two subjects, there is no response to the visual discordance in the sensorimotor cortex**.**

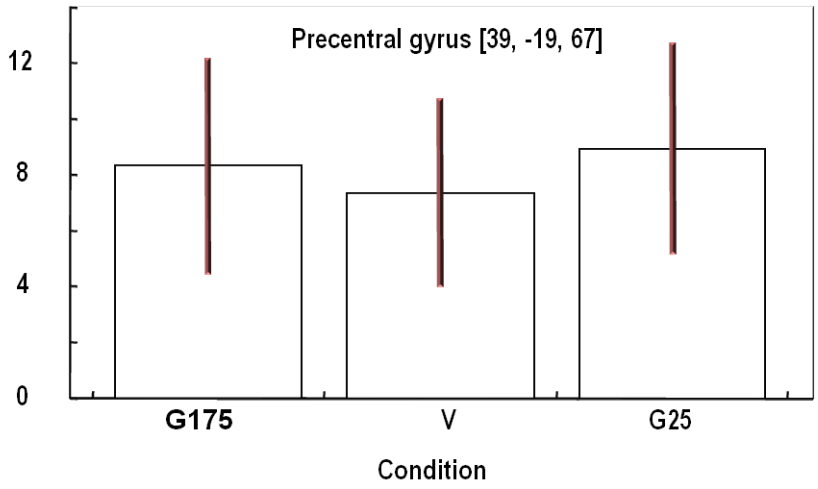

Figure 6.10 Activity in the precentral gyrus during each of the three conditions, red bar stands for 95% confidence interval

Hypometric conditions (G25 and G65) in healthy subjects demonstrate a strong correlation with activity in the motor cortex; however, in stroke subjects hypometric and hypermetric conditions are more effective in recruiting parietal and temporal areas with activation in the precentral gyrus but these correlations are not as strong. Figure 6.9 shows the average recruitment of a voxel in the motor cortex in response to visual feedback. The activity in this area is higher in both hypometric and hypermetric conditions when compared to veridical condition.

On the other hand, regression analysis was performed between the strength of response to the visual feedback discordance (T values of the main contrasts) and 1) Ashworth scale of spasticity and 2) the clinical scores WMFT and JTHF clinical scores. The purpose was to study correlation between the response in eight specific ROIs to hypometric and hypermetric feedback conditions relative to veridical condition and the clinical scores. The T values of G25>V and G175<V in each of the regions for each subject were extracted using a customized MATLAB® code.

Table 6.3 Results of regression analysis between T values in G25>V contrast and motor behavior

G25>G100		**iM1**	**cM1**	**iPMv**	**cPMv**	**I ipl**	**C ipl**	**I inf temp**	**C postcentral**
Ashworth scale	R^2	0.44	0.50	0.41	0.20	0.46	0.44	0.19	0.35
	$F_{1,10}$	6.16	8.05	4.23	2.01	6.91	6.24	1.92	3.77
	p	0.04	0.02	0.09	0.19	0.03	0.04	0.20	0.09
WMFT	R^2	0.48	0.85	0.76	0.35	0.52	0.32	0.51	0.41
	$F_{1,10}$	7.45	45.36	18.67	4.36	8.72	3.72	8.38	4.77
	p	0.26	0.00	0.01	0.07	0.02	0.09	0.02	0.07
JTHF	R^2	0.52	0.76	0.70	0.14	0.54	0.33	0.62	0.61
	$F_{1,10}$	8.54	14.16	3.76	1.29	9.20	3.99	13.10	10.90
	p	0.02	0.00	0.01	0.29	0.02	0.08	0.01	0.01

i stands for ipsilesional, c stands for contralesional hemisphere. M1 denotes primary motor cortex, PMv is ventral premotor area, ipl is inferior parietal lobule. Inf stands for inferior and temp for temporal lobe.

Regression analysis shows no significant correlation of T values for regions active in the G175>V contrast with the clinical scores. However, there is a significant positive correlation of activity in the selected ROIs in the G25>V contrast with the WMFT and JTHF clinical scores. This means that the slower (worse) is the performance, the higher is the activation in the G25>V contrast. Results of the regression analysis are shown in Table 6.4. Figures 6.11 and 6.12 show the correlation between the clinical scores and T values in iM1 and ipsilesional fusiform body area (iFBA) respectively.

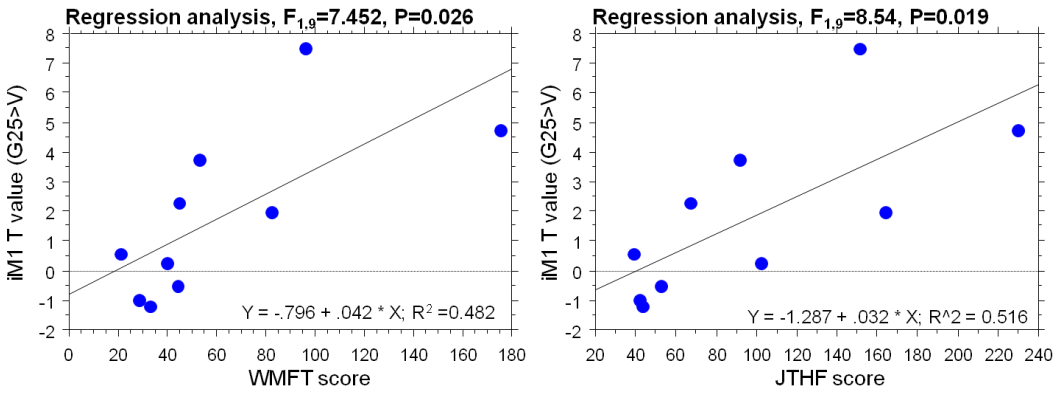

Figure 6.11 Simple regression analysis of iFBA T values in the G25>V contrast.

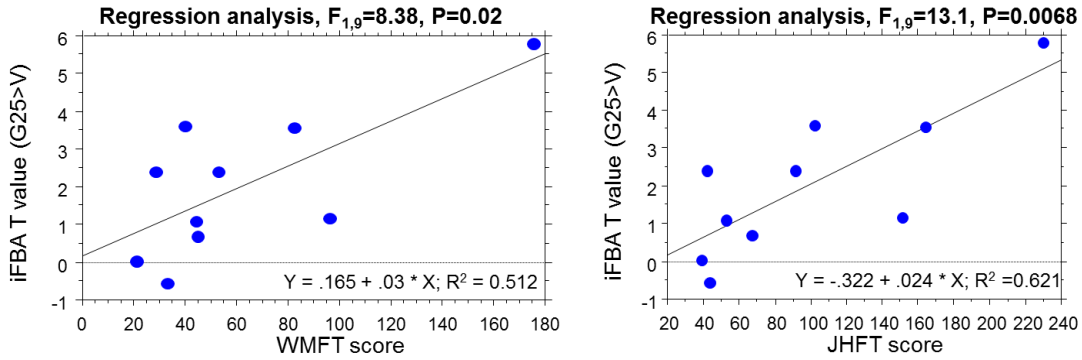

Figure 6.12 Simple regression analysis of iFBA T values in the G25>V contrast.

6.3.2.4 PPI connectivity analysis. Effective connectivity analysis was performed with iM1 as a seed and another analysis was performed with iFBA region as a seed, where the cluster was defined as a seed is more active in G175 and G25 than Veridical condition. The network of iM1 connectivity does not show any difference between conditions, however, iFBA shows higher connectivity with cSPL and iM1 in the Veridical condition versus G25 condition although the activity in these areas is higher in the G25 condition.

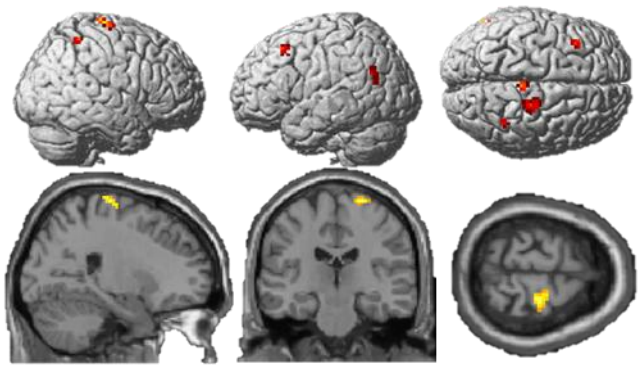

Figure 6.14 PPI effective connectivity with the ipsilesional fusiform body area (iFBA) as a seed (V>G25 contrast), at statistical threshold p<0.01.

6.4 Discussion

Visual feedback is dissociated from movement to study effects of visual feedback on neural circuits. Behavioral data during fMRI experiment indicate that subjects were able to follow instructions and to maintain consistent movements across different visual feedback conditions, despite the altered feedback.

Feedback manipulation of healthy subjects' movement shows a strong linear relationship between the feedback congruence and subjects' estimation of feedback quality confirming that subjects attended to the visual feedback throughout each trial. The task is associated with activation in a typical distributed network of sensorimotor regions sub-serving visually guided sequential action. Experiment 1 of this study shows that different forms of altered feedback have unique effects on brain activity within a task-related mask. One could conclude that these differences are driven entirely by visual feedback manipulations rather than by potential discrepancies in motor output since movement kinematics are similar across conditions and movement-based activation is subtracted out in each contrast. Unlike healthy subjects, stroke patients (Experiment 2)

had difficulty maintaining consistent movement kinematics across conditions, a finding that was expected (Viau et al. 2004). However, movements were slower and faster in G175 and G25 respectively relative to veridical and cortical activation is comparably higher in G175 and G25 relative to veridical. This suggests that difference in movement behavior was not a confounding factor in brain activations.

6.4.1 Contralateral M1 is Facilitated by Discordance in Gain

The most notable finding is that quantitative discordance in gain between executed movement and observed feedback is associated with a parametric increase in activation in contralateral M1 (iM1 in experiment 2). Analysis of movement kinematics confirms that actual movement performance does not confound this result. This finding is consistent with a model in which M1 was involved in on-line processing of error-based information for visual guidance of movement. This data fits previous imaging work integrating gain manipulations into isometric force production tasks (Coombes et al. 2010) and sinusoidal line tracing with finger flexion-extension movements (Carey et al. 2006). In these studies, activity in contralateral M1 is found to be increasing with accuracy demands that required subjects to modify their motor output in order to reduce error. The experiments of this chapter add to this knowledgebase by (1) ruling out the possibility that feedback-based modulation of M1 is affected by performance changes (since performance in this study was clamped), (2) showing that M1 can be modulated even in the absence of an explicit target or goal, and (3) demonstrating that this modulation can occur at a single trial level rather than after adaptation that occurs over the course of a block of training, as in the above mentioned studies.

There is no facilitation of the contralateral M1 in MF>V contrast. Suggesting that the modulation is feedback-error specific. A parsimonious explanation is that low-gain feedback in the G25 and G65 conditions relative to veridical (in Experiment 1) and G175 relative to veridical (in Experiment 2) up-regulates neural activity in the motor system as if M1 is acting to reduce the discrepancy between the intended action and the sluggishly moving virtual finger, irrespective of the direction of discrepancy (higher or lower amplitude). Such up-regulation would not be necessary in the MF condition (since the observed amplitude of the incorrect finger motion matched the actual movement) and may be the reason why no M1 modulation is noted in the MF condition. In a recent imaging study, subjects lifted objects whose weight was unpredictably lighter or heavier than expected (Jenmalm et al. 2006), the authors noted that M1 activity increased only when the object weighed more than predicted, but not in the opposite condition. They concluded that this M1 modulation reflected the gradual increase in lift force (above predicted levels) after the object was grasped. Collectively, these data suggest that low-gain feedback manipulations may serve as a useful therapeutic tool during training by having a facilitatory effect on the motor system. Like the haptic feedback manipulation used by(Jenmalm et al. 2006), this study demonstrates that visuomotor discordance may also bolster the motor system. However, the data in Experiment 2 shows that both hypermetric and hypometric feedback may bolster activity in the ipsilesional motor cortex of stroke patients (Figure 6.10) suggesting that both high-and low-gain discordance may have excitatory effects on the lesioned motor system although hypometric feedback might be more efficient (Figure 6.9).

Since visual manipulations can be easily implemented into virtual reality-based systems, VR can be an ideal platform for delivering interventions with visuomotor discordances (Adamovich et al. 2009; Merians et al. 2011; Merians et al. 2011). These conclusions are of course to be taken with caution given the limited number of patients in this study and the lack of other published data in this regard. However, this study indicates the need to further investigate the interesting potential that the application of visuomotor discordance may have on recovery and brain reorganization after stroke, and in a broader spectrum of patients.

6.4.2 Processing of Observed Movement Amplitude and the Extrastriate Body Area

There is an ongoing interest in the role that higher-order visuomotor processing areas, such as the extrastriate body area (EBA), play in action observation. A recent meta-analysis study by (Nelson et al. 2010) elegantly demonstrated that EBA is overwhelmingly recruited for activities involving task-level control and focal attention. More specific to motor control, the EBA is repeatedly identified for its role in higher order visual processing of observed biological movements (Astafiev et al. 2004; Kontaris et al. 2009) (Jackson et al. 2006). An interesting proposition by Downing and co-workers (Peelen and Downing 2005; Kontaris et al. 2009) is that activity in EBA reflects observed actions independent of efferent motor signals. This suggests a role of EBA in reconciling discordance between intended and observed motor outcomes. In this study EBA is more active in veridical versus G25 in experiment 1, however, in experiment 2, EBA is more active in G175 and G25 versus veridical condition. On the other hand, there is an equal increase in BOLD in EBA for both veridical and mismatched finger conditions, in which the amplitude of physical and observed movement are clamped in spite of the

incongruency. Importantly, EBA activity decreased as the amplitude of the observed movement decreased from the V to the G25 in experiment 1 and increased in experiment 2 with stroke. Urgesi et al. (Urgesi et al. 2007) found that functional disruption of EBA using repetitive transcranial magnetic stimulation (rTMS) impaired the ability to visually distinguish between subtle differences in human body posture configurations of the same body part. In the context of this work, experiment 1 and experiment 2 findings suggest, therefore, that activity in the EBA may be modulated by the amount of observed body motion of the same body part, whether it is congruent with the executed movement or not. Besides, this study shows difference in response of the EBA to visual discordance in healthy compared to stroke subjects, suggesting a difference between these two populations that needs to be further investigated. In this regard, regression analysis of activation in ipsilesional inferior temporal cortex and the clinical scores, shows more activation in this area in subjects with poorer performance and higher degrees of motor impairment, suggesting a relationship between motor impairment and response to the visual feedback. The connectivity between ipsilesional fusiform gyrus with cSPL and iM1 in Veridical compared to G25 supports the idea that the neural correlates of visual discordance involves interaction between areas that area responsible to understand the visual input in terms of body schema or agency (FBA and EBA) in addition to the visuomotor areas.

6.4.3 Mismatched Feedback Activates a Frontoparietal Network

Virtual hand motion in the mismatched feedback condition is both amplitude- and phase-locked to the subject's movement so that only the mapping between fingers is altered, creating a discrepancy between the intended action and the visual feedback of that action.

Mismatched feedback is perceived by the subjects to be more discordant than the gain feedback manipulation. Arguably, this is the only condition in which the subjects' body schema are violated. The contrast between the mismatched and veridical feedback reveal activation in the bilateral insula, inferior frontal gyrus (pars opercularis), postcentral gyrus, supplementary motor area, contralateral anterior intraparietal sulcus, and dorsal premotor cortex. No significant motor cortex activation is noted in this contrast, as in the case of the hypometric and hypermetric conditions relative to the veridical condition. Recent work demonstrated that observation of actions with the intention to imitate the observed movements results in activation of similar parietal and insular networks (Adamovich et al. 2009). Given these regions' involvement in a wide variety of sensorimotor processes including the processing percepts of agency / ownership of actions (Farrer and Frith 2002), intentional action observation of action (Fogassi et al. 2005) (Rizzolatti et al. 2006), the remapping of body image to incorporate tools (Iriki 2006), the maintenance of connectivity with the premotor cortex (Rushworth et al. 2006), it is likely that observing motion of a mismatched finger condition elicited a salient discordance in the self-other representation of the body, bolstering activity in the parietal and insular areas as it reconciled this discordance.

An interesting finding is the significant activation of bilateral premotor areas in the mismatched relative to veridical feedback conditions. Previous work has identified premotor areas to be recruited during action observation, particularly when sensorimotor transformations between executed and observed movement were necessary (Manthey et al. 2003; Buccino et al. 2007). For example, in one study, subjects observed either correct or incorrect pairings between hand postures and objects, having to analyze whether the

hand posture was appropriate for functionally grasping the object. Similar to this study, the authors noted bilateral ventral premotor activation in the “incorrect pairing” versus “correct pairing” contrast. In another study, however, (Buccino et al. 2007) in which subjects observed intentional and unintentional actions, the authors noted stronger activation in the lateral premotor areas for the intentional (relative to the unintentional) condition. This and previous studies suggest a role of lateral premotor cortex in processing visuomotor transformations.

6.4.4 Neural Activity Correlation with Perceptual Judgment of Feedback

This experiment is the first study in this dissertation that include discordance of visual feedback, thus it is interesting to understand how subjects’ perception of the feedback in VR affected BOLD activation. Subjective ratings of the quality of feedback (the degree to which the observed motion of the VR hand matched the subjects’ action) are significantly correlated with the altered feedback, with mismatched feedback being reported to correspond the least with the performed action. In other words, subjects perceived mismatched feedback, though similar in amplitude to their physical motion, to be more disruptive than the hypometric (G65 and G25) feedback.

Correlation between BOLD activity and the time taken by subjects to evaluate the feedback (decision time) is significant in bilateral insula, bilateral superior parietal lobules, contralateral caudal middle frontal gyrus (dorsal premotor area, Broadmann area 6), bilateral supplementary motor area and bilateral inferior occipital lobe. The insula activity is unsurprising given its role in self-agency distinction. However, it is interesting that this rather extensive sensorimotor network is correlated with this phase in which subjects were evaluating the degree of correspondence.

CHAPTER 7

MANIPULATING VISUAL FEEDBACK IN A VIRTUAL MIRROR (AIM 3)

7.1 Background

Mirror feedback was first suggested as a rehabilitation tool (Altschuler et al. 1999) to reduce phantom limb pain after amputation. Later it showed promise in patients with motor impairments, especially if patient's movement was very limited so that they could not participate in conventional therapeutic protocols. The main idea is to have subjects move both hands symmetrically, moving the affected side as best as they can, while watching the mirror reflections of their healthy hand in a sagittally oriented mirror. The reflection is overlapped with their affected hand hidden behind the mirror. Several small clinical studies have demonstrated efficacy of this approach for hand rehabilitation (Sathian et al. 2000; Yavuzer et al. 2008) and lower extremity rehabilitation (Dohle et al. 2009).

Knowing the results of these rehabilitative studies, one can suggest that mirror visual feedback might have a facilitatory effect on the impaired hemisphere. However, the neural effects of this visual illusion are not well understood. An fMRI study with a sagittally oriented mirror showed that movement with mirror visual feedback recruited sensorimotor cortex (SMA, M1 and S1) ipsilateral to the hand moving in healthy subjects and amputees without phantom limb pain, (nPLP) but not in subjects with phantom limb pain (PLP) (Diers et al. 2010). This difference in the mirror effect on sensorimotor activations in the PLP and nPLP groups, the effect might be correlated with recruitment of sensorimotor areas. Conversely, in a recent study with mirror feedback provided by a sagittally oriented mirror (Michielsen et al. 2010), stroke subjects showed activation in

the precuneus and posterior cingulate cortex but did not show recruitment in the sensorimotor areas of the lesioned hemisphere during bimanual hand motion. Similarly, Matthys et al (Matthys et al. 2009) study showed increased activation in the superior temporal gyrus and right superior occipital gyrus in response to mirror visual illusion, with no additional recruitment of the sensorimotor areas or frontoparietal mirror neural system.

Furthermore, a study of lateralized readiness potentials (Touzalin-Chretien and Dufour 2008) showed recruitment of the primary motor cortex contralateral to the inactive hand during mirror lateral and mirror frontal visual feedback of hand movement. In another TMS study (Garry et al. 2005), facilitation in the primary cortex contralateral to the inactive hand was observed during unilateral hand movement and mirror visual feedback. (Tominaga et al. 2009) reported significant suppression in the stimulus-induced 20 Hz activity in response to visual feedback of hand movement directly or as a mirror reflection (stimulus-induced 20-Hz suppression was considered an indicator of primary motor cortex activation (Hari et al. 2000)).

While mirror visual feedback has been studied using a mirror, in this study mirror feedback is provided to stroke subjects using an interactive virtual environment instead. Virtual reality is advantageous over a real mirror due to the flexibility to manipulate the visual feedback (Adamovich et al. 2009). Moreover, since hand movements were not measured and recorded during the scanning with the real mirror setup, it was impossible to exclude the potential effect of unintended mirrored movements in the hemiparetic arm that are common in hemiparesis on the activation of the ipsilesional sensorimotor cortex. It was also impossible to control for the effect of gaze.

7.2 Methods

Subjects: Fifteen right-handed (Oldfield 1971) subjects, with hemiparesis due to stroke (5 right-hemiplegics, 5F, mean age 54 ± 12 years, range 37-74 years old) participated in the study after signing informed consents approved by the University of Medicine and Dentistry in New Jersey and the New Jersey Institute of Technology Institution Review Boards. All subjects are independent in basic activities of daily living; four of the subjects used a cane as an assistive tool. As an assessment of subjects' functionality, the WMFT clinical test is performed for each of the subjects (except for subjects 8 and 15 due to their restricted time schedule). See table 7.1 for more detailed clinical information about each of the subjects.

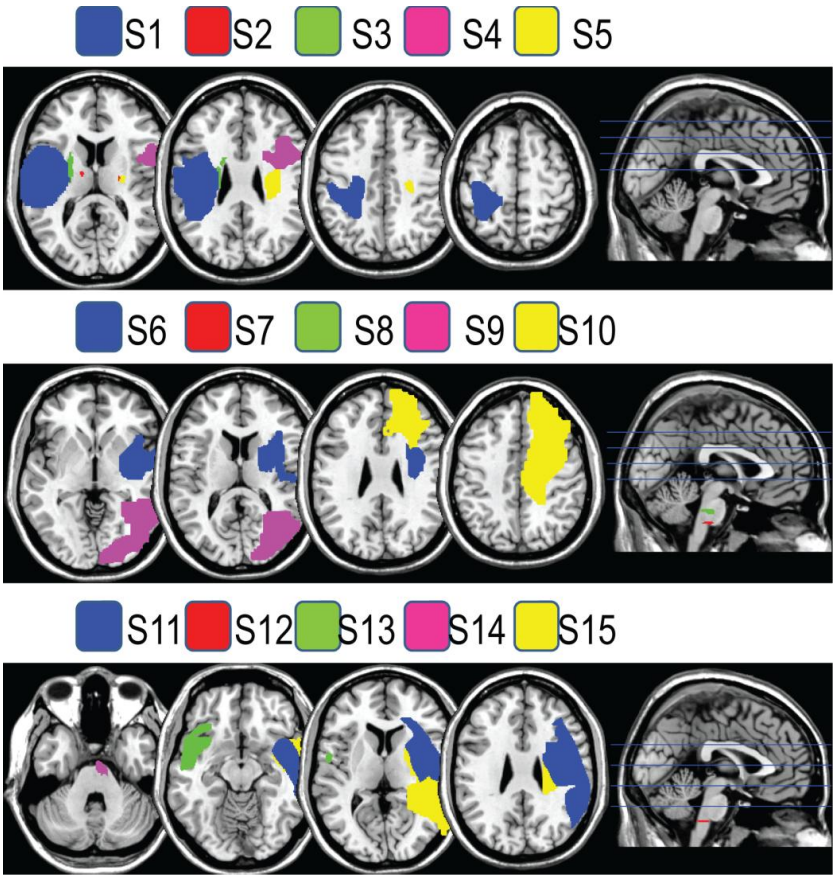

Figure 7.1 Lesion mapping for 15 subjects using mricron.

Task: The task is to perform whole hand finger movements with the paretic (Experiment 1) and non-paretic (Experiment 2) hand. Similar to all experiments previously discussed, real-time left and right glove data were continuously streamed and used to animate the motion of the VR hand models. This study includes two main experiments:

Experiment 1*:* Subjects perform the task only with the paretic hand, leaving the non-paretic hand at rest. The correspondence between data streamed from the gloves and the VR hands remain veridical. Three of the subjects were not able to do this experiment due to severity of impairment.

Experiment 2: Subjects perform the task only with the non-paretic hand, leaving the paretic hand at rest. The correspondence between data streamed from the gloves and VR hands remained either veridical (as in Experiment 1) or flipped (mirrored feedback) such that motion of the fingers on the left hand actuates the fingers of the right VR hand, or the opposite. The movement of the virtual hand corresponds either to the veridical moving hand or, in the case of mirrored-feedback, to the resting paretic side. A control feedback condition (CTRL) is included to subtract out potential confounds of visual field position, gaze direction, and motion. For the control condition, the VR hands are replaced with a non-anthropomorphic object (ellipsoid) that is similar in size and color to the VR hands. The left or right control object rotates about an oblique axis (1 Hz) while the subjects move their non-paretic hand, such that it either corresponds to the veridical or mirrored side (Figure 7.1).

Table 7.1 Subjects' Clinical Information

Pt	Age	Gender	Months since CVA	CVA side L/R	CMA	CMH	dWMFT score	Lesion Location
1	63	F	53	L	6	4	175.5	L frontal and parietal lobes
2	55	M	41	L	5	4	53	L thalamic nuclei
3	49	M	144	L	5	4	85	L basal ganglia
4	74	M	9	R	6	6	21.4	R frontal lobe
5	70	F	96	R	7	5	40	R corona radiata
6	58	M	132	R	5	4	96.5	R frontal, parietal and temporal lobes
7	37	M	92	R	4	3	82.5	R pons
8	69	F	18	R	7	7	NA	R pons
9	68	M	78	R	6	6	33.1	R occipital lobe
10	48	F	148	R	4	3	102.67	R frontal and parietal lobes
11	41	F	70	R	6	6	28.7	R frontal parietal and temporal lobes
12	43	M	11	L	4	4	120.4	L pons
13	41	M	158	L	6	6	44.7	L frontal, parietal and temporal lobes
14	53	M	156	R	6	6	44.1	R pons
15	39	F	14	R	4	3	NA	R parietal and temporal lobes

CVA stands for cerebrovascular accident; CMA for Chedokee-McMaster motor assessment arm scale; CMH is Chedokee--McMaster motor assessment hand scale; dWMFT stands for distal wolf motor function test. L stands for left and R for right

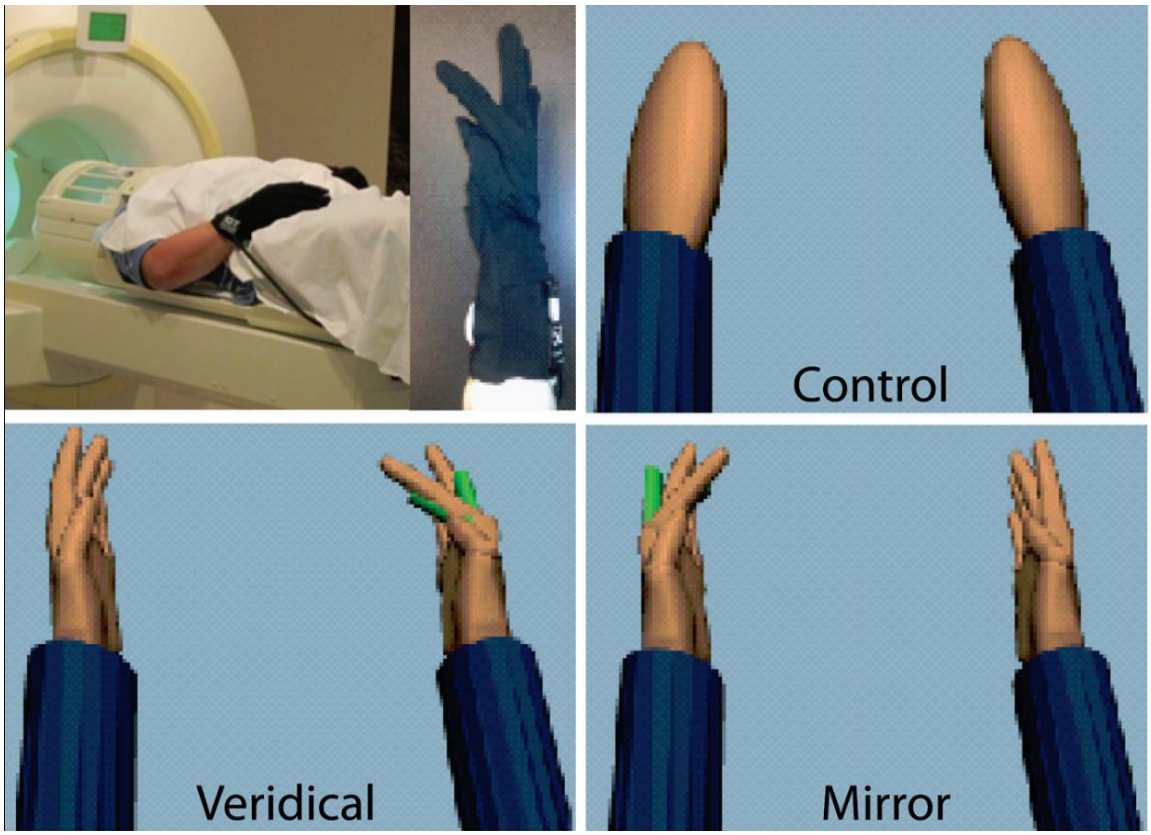

Figure 7.2 Different visual feedback manipulations of subject's hand movement in the scanner. Subjects wear the 5DT gloves, and get visual feedback of their movement on the computer screen. Assuming the subject is moving the right hand, the right virtual hand is moving in the veridical condition, the left hand moves in the Mirror condition and in the control conditions, the right (CTRLveridical) or the left (CTRLmirror) ellipsoidal shape rotates at a rate of 1 Hz .

The four visual feedback conditions (HAND [veridical, mirrored], CTRL [veridical, mirrored]) are presented in an event-related fashion and randomly interleaved with each other in each functional imaging run (8 trials per condition for four subjects and 10 trials per condition for one subject). Each subject performed four runs. Movement events (5 seconds duration) are separated by an inter-trial rest period that randomly varied between 3-7 seconds.

7.2.1 fMRI Data Analysis

The fMRI data are preprocessed as described in chapter 3.

7.2.1.1 Main effects. The main effect of mirror visual feedback is investigated based on the following contrasts: a) Move>rest, b) HANDmirror>CTRLmirror, c) (HANDmirror + HANDveridical) > (CTRLmirror + CTRLveridical) and c) HANDmirror > (HANDveridical + CTRLmirror > CTRLveridical).

7.2.1.2 Movement behavioral measures. The analysis of behavioral measures follows the procedure described in chapter 4 section 4.2.2. In addition, to verify that any mirror feedback-based effects in the fMRI data cannot be accounted for by inadvertent motion of the paretic hand, the above mentioned analysis is also performed on the glove data acquired from the non-moving (paretic) hand. fMRI data corresponding to trials on which subjects moved their paretic hand are excluded from the GLM (see Figure 4.2 for an example).

7.2.1.3 Connectivity analysis. There is no connectivity analysis for experiment 1. In experiment 2, the effective connectivity between the ipsilesional motor cortex and the most active voxels in the HANDmirror condition is examined using gPPI analysis (discussed in Chapter 3). The procedure is as follows:

1) The main contrast (HANDmirror>(HANDveridical + CTRLmirror +CTRLveridical) is used to screen for active cluster in the ipsilesional motor cortex and to select the volume of interest (VOI).
2) A new GLM including the BOLD signal at the VOI of interest, and the interaction values as regressors is evaluated. A univariate contrast is computed to find the contribution map, or the effective connectivity between the (VOI) and the rest of the brain. Clusters correlated with the seed VOI are identified as new seeds.

3) Psychophysiological Interaction between each of the identified VOIs in step 2, and the ipsilesional motor cortex is plotted as a regression plot

In addition to PPI analysis, Dynamic Causal Modeling (DCM) is performed to investigate the interactions between sensorimotor cortex regions in HANDveridical versus HANDmirror feedback. DCM methodology is discussed in Chapter 2.

7.2.1.4 Dynamic causal modeling. DCM analysis is performed to investigate the network driving the excitability of iM1 during the HANDmirror feedback. The main stimulus of iM1 recruitment in the HANDmirror condition must be through visual feedback, thus, three main regions are included in this analysis 1) superior parietal lobule (SPL) because of its role in visuomotor processing, 2) supplementary motor area (SMA) because of its possible effect in directly manipulating M1 and 3) M1. These regions are modeled bilaterally to find out if the driving modulation of iM1 was within ipsilesional hemisphere or from the contralesional hemisphere through interhemispheric interactions.

Two subjects are excluded from the DCM analysis (S3 and S9) because they did not show any activity in the sensorimotor cortex (S3 and S9). The center coordinates of the main six ROIs are defined based on the group average results. Then, individual ROIs of each subject are defined; the peak coordinate of each subject ROI was the closest to the group average coordinate of that area. The ROIs are defined as spheres with a radius of eight mm. After the ROIs are defined, two additional subjects, S8 and S13, are excluded from this analysis at this stage since they do not show activity in SMA even at a low statistical threshold.

Figure 7.3 shows the main anatomical structure of the model. If the activity of iM1 in the HANDmirror condition is modulated by activity in the contralesional

hemisphere, this would be driven by cM1, or from cSPL or cSMA. This influence of cSPL on iM1 can be through, iSPL, cM1 or cSMA but it also can be direct; an interhemispheric exogenous connection between SPL areas and M1 areas is possible. This possibility is modeled even in the absence of physical connection between cSPL and iM1 or iSPL to cM1. Thirty nine possible interactions between the 6 nodes are modeled; the main concentration is modulation of iM1. The modulations of activity by HANDmirror and HANDveridical are suggested to be on the same sites in each model, hypothesizing that the strength of modulation will be different between conditions.

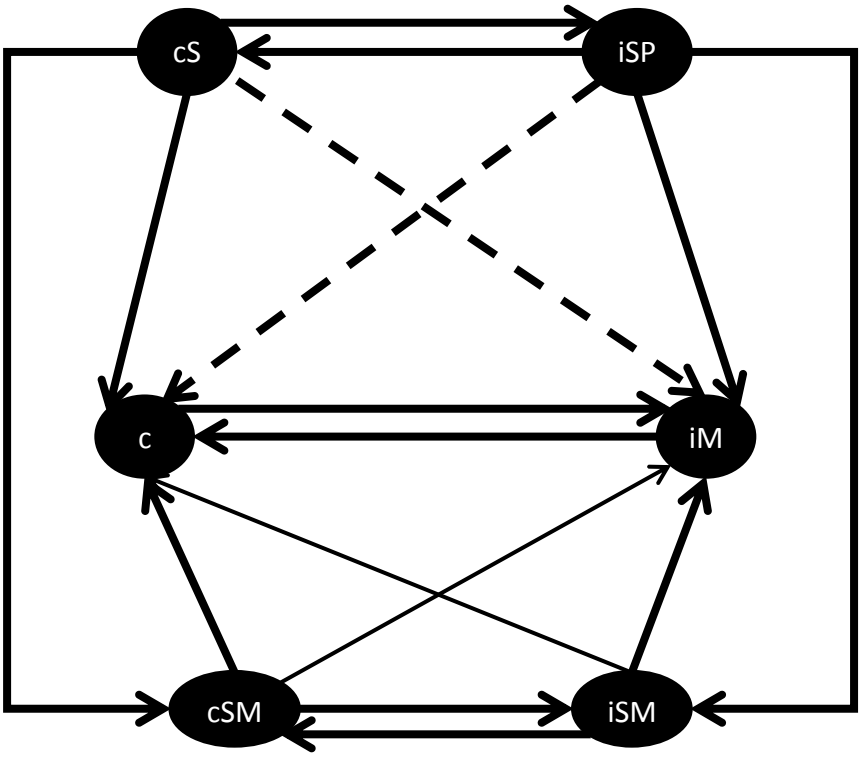

Figure 7.3 Structure of the main DCM model did not include interhemispheric connections between SPL and M1 areas but included exogenous coupling.

After defining all 39 models, with different sites of modulation of HANDmirror feedback and HANDveridical feedback, Bayesian statistics of the models are estimated using DCM and a customized Matlab® code. Bayesian model selection is used to look for

an optimal model that has the highest evidence based on Bayes factor. Bayesian parameter averaging is extracted for the winning model of each subject and ANOVA was used to compare the parameters in HANDmirror versus HANDveridical conditions. The significance of connections is evaluated at a threshold of $p<0.05$ with Bonferroni correction for multiple comparisons based on the number of connections in the model.

7.3 Results

7.3.1 Experiment 1

fMRI: Regions activate during motion of the paretic hand*:* The contrast move>rest shows significant activation in a typical cortical network sub-serving visually guided hand movement. Significant activation is noted in the contralateral precentral and postcentral gyri, the contralateral superior and inferior parietal lobules, the ipsilateral insula, and to a lesser degree in the ipsilateral sensorimotor areas.

7.3.2 Experiment 2

7.3.2.1 Movement Behavior measures. Subjects generally maintained consistent movements with the non-paretic hand. Occasionally, subjects either exhibited inadvertent motion of the paretic hand or missed required motions of the non-paretic hand. Such trials are excluded from behavioral and imaging analyses. Repeated measures ANOVA does not show a significant effect of feedback condition or functional run of movement mean velocity (condition; $p=0.1698$, $F_{3,39}=1.765$, power=0.415, run; $p=0.3117$, $F_{3,39}=1.23$), and movement duration (condition; $p=0.0743$, $F_{3,39}=4.97$, power=0.892, run; $P=0.2484$, $F=1.431$). Same test does not show difference in movement amplitude across

conditions (p=0.1611, $F_{3,39}$=1.8115) but there is a difference across runs (p=0.0051, $F_{3,39}$=4.97). Post-hoc analysis reveals that these effects are caused by a slight increase in movement amplitude across the fMRI runs in the Control conditions (CTRL) (from a mean [±1 standard deviation, SD] 0.7 ±.39 radians in run 1 to .89 ±.41 radians in run 4); this difference is not attributed to changes across the HAND conditions.

7.3.2.2 FMRI: Regions activated during mirror-based feedback. Figures 7.4, shows regions with significant activation in the (HANDmirror > HANDveridical + CTRLmirror + CTRLveridical) per subject, Figure 7.5, shows the group average of the 15 subjects. Significant activation is noted in the sensorimotor system of the ipsilesional hemisphere (ipsilateral to the moving hand) of most subjects. The mirror visual feedback also leads to recruitment of the superior and inferior parietal lobes (SPL, IPL), precuneus, supplementary motor area (SMA), and cingulate gyrus.

7.3.2.3 Group average. The one sample t test of the contrast images (HANDmirror>HANDveridical + CTRLmirror + CTRLveridical) shows activation in the sensorimotor cortex (motor and premotor areas) and strong bilateral posterior parietal activity that includes SPL, IPL and part of the postcentral gyrus (see Figure 7.5, Table A7.1).

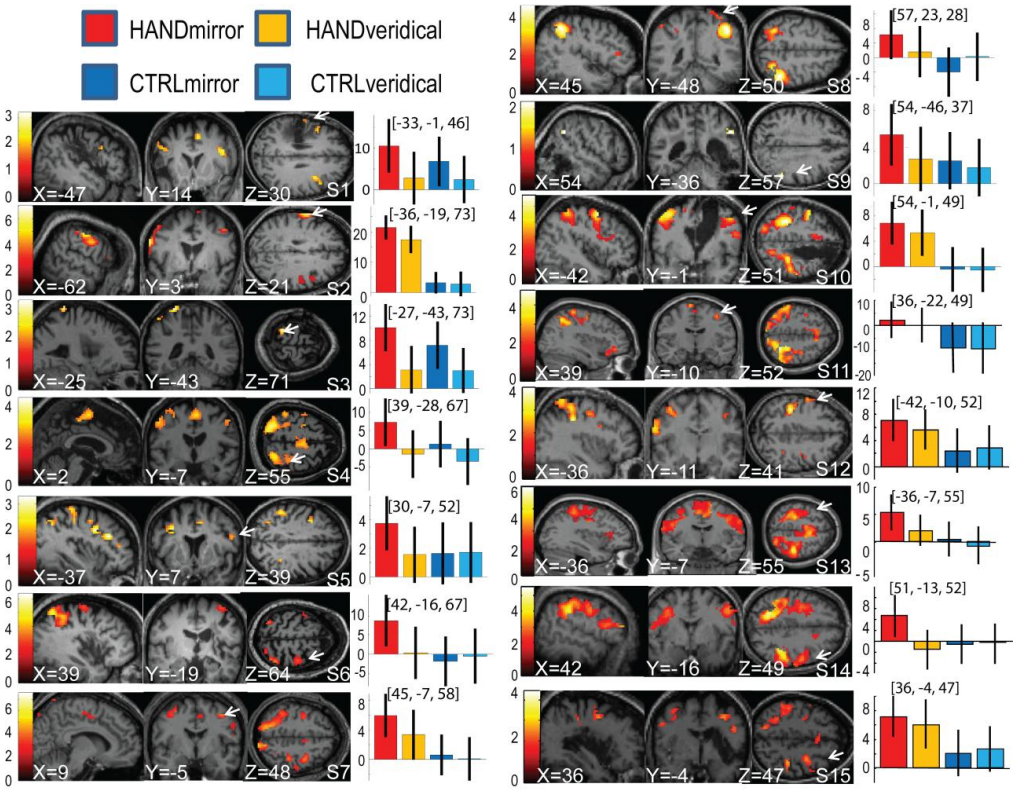

Figure 7.4 Effect of mirror visual feedback (HANDmirror > (HANDveridical + CTRLmirror + CTRLveridical) for each of the 15 subjects.

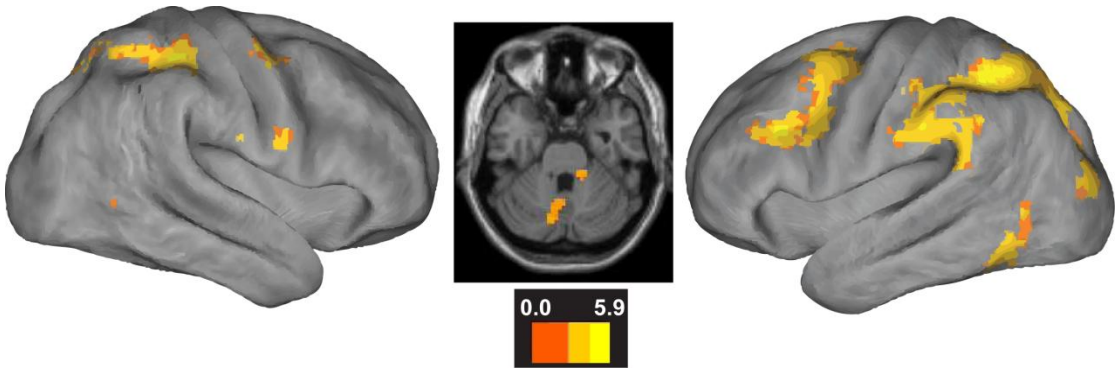

Figure 7.5 Mirror effect (HANDmirror > (HANDveridical + CTRLmirror + CTRLveridical); average of 15 subjects. Right side is the ipsilesional hemisphere.

7.3.2.4 Topographic overlap between motor - and feedback-based representations.

A conjunction analysis is performed between Experiments 1 and 2 to test if motor regions activated by mirrored visual feedback overlapped with motor centers engaged in producing movement of the paretic hand. An affirmative finding would suggest that

mirrored feedback of the unaffected hand could be used to selectively activate relevant motor command centers giving rise to corticospinal projections to the paretic hand. Three of the subjects were not able to do experiment 1, but 11 out of the 12 subjects who did experiment 1, show a cluster in the lesioned motor cortex with distinct topographic overlap across the two experiments. Figure 7.6 shows this result of each of the 12 subjects.

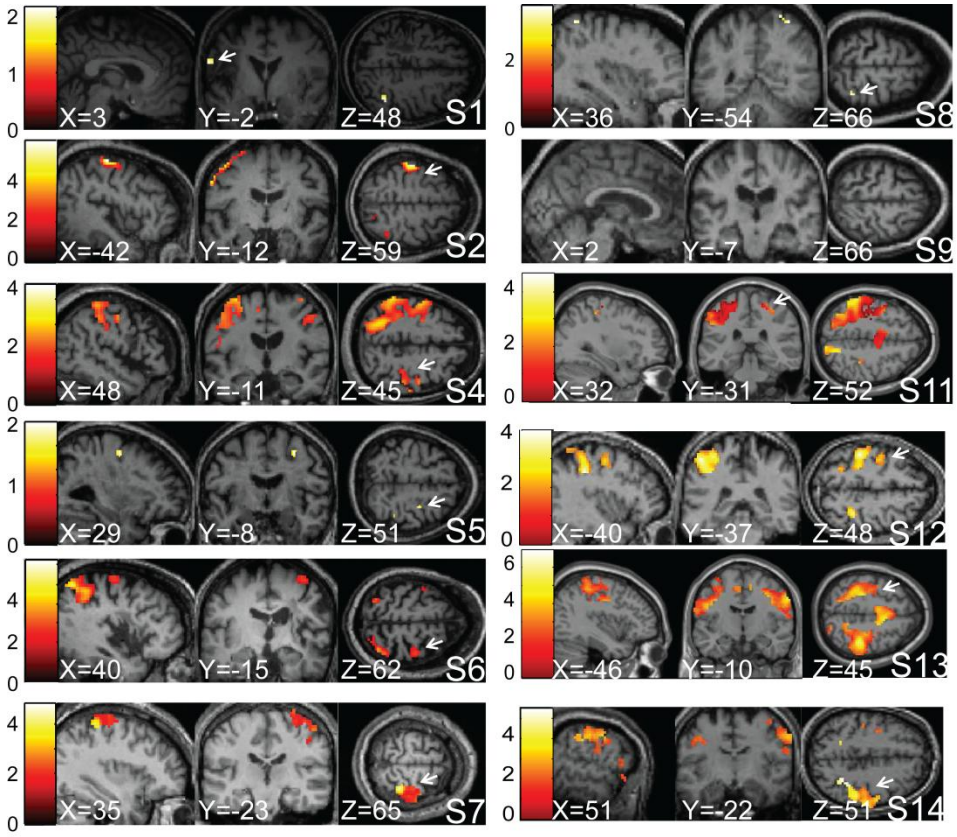

Figure 7.6 Conjunction analysis of each subject, results showed overlap in activity when moving paretic hand versus moving non-paretic hand and receiving mirror visual feedback.

7.3.2.5 PPI Connectivity Analysis. The main contrast (HANDmirror > (HANDveridical + CTRLmirror + CTRLveridical) shows very strong activation in the bilateral superior parietal lobule, especially contralesional SPL. Therefore, PPI analysis is done using contralesional SPL (cSPL) as the region of interest and another PPI analysis

with ipsilesional M1 (iM1) as the region on interest. Figures 7.7 and 7.8 show that cSPL and iM1 are strongly correlated with activity in the fusiform body area (peak voxel coordinate [45, -40, -8]).

A recent study by Kontaris et al (Kontaris et al. 2009) defined the center coordinate of the FBA region as [40.5 -42 -22], this mapping of FBA overlapped with FBA activity in figures 7.7 and 7.8. FBA correlation with cSPL and iM1 was much higher in HANDmirror than HANDveridical and CTRL conditions (see figures 7.7B, 7.8B). Besides, the contrast (HANDmirror + HANDveridical) > (CTRLmirror + CTRLveridical) shows recruitment of the same cluster in FBA regions. Interaction vectors between FBA and iM1 (Fig. 7.7C) are stronger (slope a=0.63) in HANDmirror than HANDveridical (a=0.43), CTRLmirror (a=0.32) and CTRLveridical (a=0.42). Interaction vectors between FBA and cSPL (Fig. 7.8C) are not different between mirror and veridical conditions; however, the bigger slope in hand feedback versus CTRL feedback suggests that FBA and cSPL interaction is biased to anthropomorphic shape (hand) versus a non-anthropomorphic shape (ellipsoidal CTRL shape).

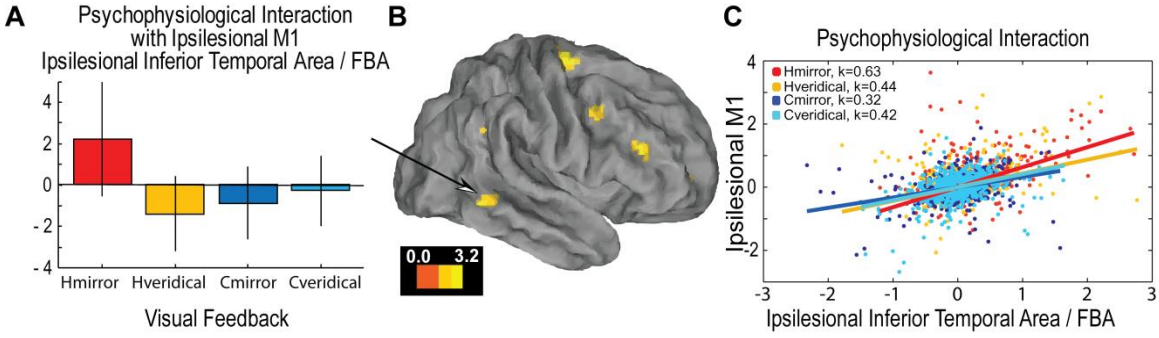

Figure 7.7 Effective connectivity (PPI) with ipsilesional M1 as VOI.

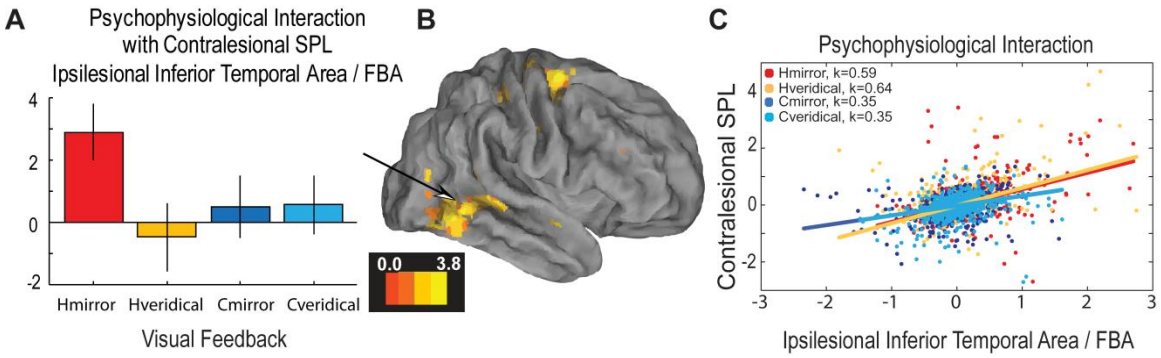

Figure 7.8 Effective connectivity (PPI) with contralesional SPL as VOI.

iFBA strongly interacts with cSPL and iM1 during the mirror condition based on the PPI analysis. The fusiform gyrus is not significantly active at the group level although many of the subjects showed FBA activity, Thus, a relationship between neural response in this area and subjects' motor function could be assumed. Therefore, regression analysis is performed between the T values (in FBA and other regions) and with the WMFT scores (proximal and distal components). The T values of the contrast (HANDmirror > (HANDveridical + CTRLmirror + CTRLveridical) of each of the 15 subjects are extracted from the regions of interests (FBA, ipsilesional PMv, IM1, CM1, ipsilesional precuneus, cSPL and iSPL). Regression analysis between the T values in bilateral M1 and ISPL subjects with clinical scores shows no interaction. There is a trend of negative correlation between cSPL, ipsilesional PMV and ipsilesional precuneus with dWMFT, but this correlation is not significant. There is a tendency of negative correlation between ipsilesional superior temporal region T value and dWMFT and a significant correlation between correlation of FBA T values and dWMFT (R^2=0.48, $F_{1,12}$=10.1, P=0.0087) (Table 7.2, figure 7.9).

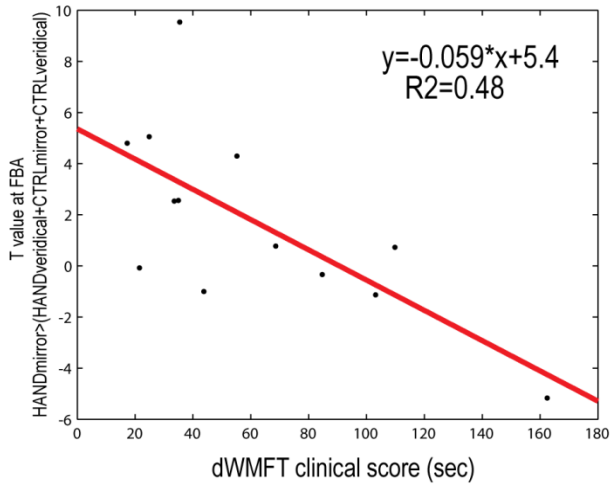

Figure 7.9 Regression analysis between FBA T values (HANDmirror > (HANDveridical + CTRLmirror + CTRLveridical)) and dWMFT.

Table 7.2 Correlation between T values for various regions of interest (contrast HANDmirror > (HANDveridical + CTRLmirror + CTRLveridical) and dWMFT score

	I M1	C M1	I PMv	I SPL	C SPL	I precuneus	I sup temporal	I FBA
R^2	0.024	0.014	0.107	0.016	0.156	0.197	0.260	0.48
$F_{1,12}$	0.274	0.157	1.325	0.181	2.034	2.695	3.86	10.134
p	0.61	0.7	0.274	0.678	0.181	0.129	0.075	0.0087

7.3.2.6 Dynamic causal modeling analysis. Bayesian Model Selection: Both random effects (RFX) and fixed-effects (FXX) model selection are used to compare the evidence of the 39 tested models. Model 18 is found to be the optimal model in both procedures with very high evidence (see Figure 7.10).

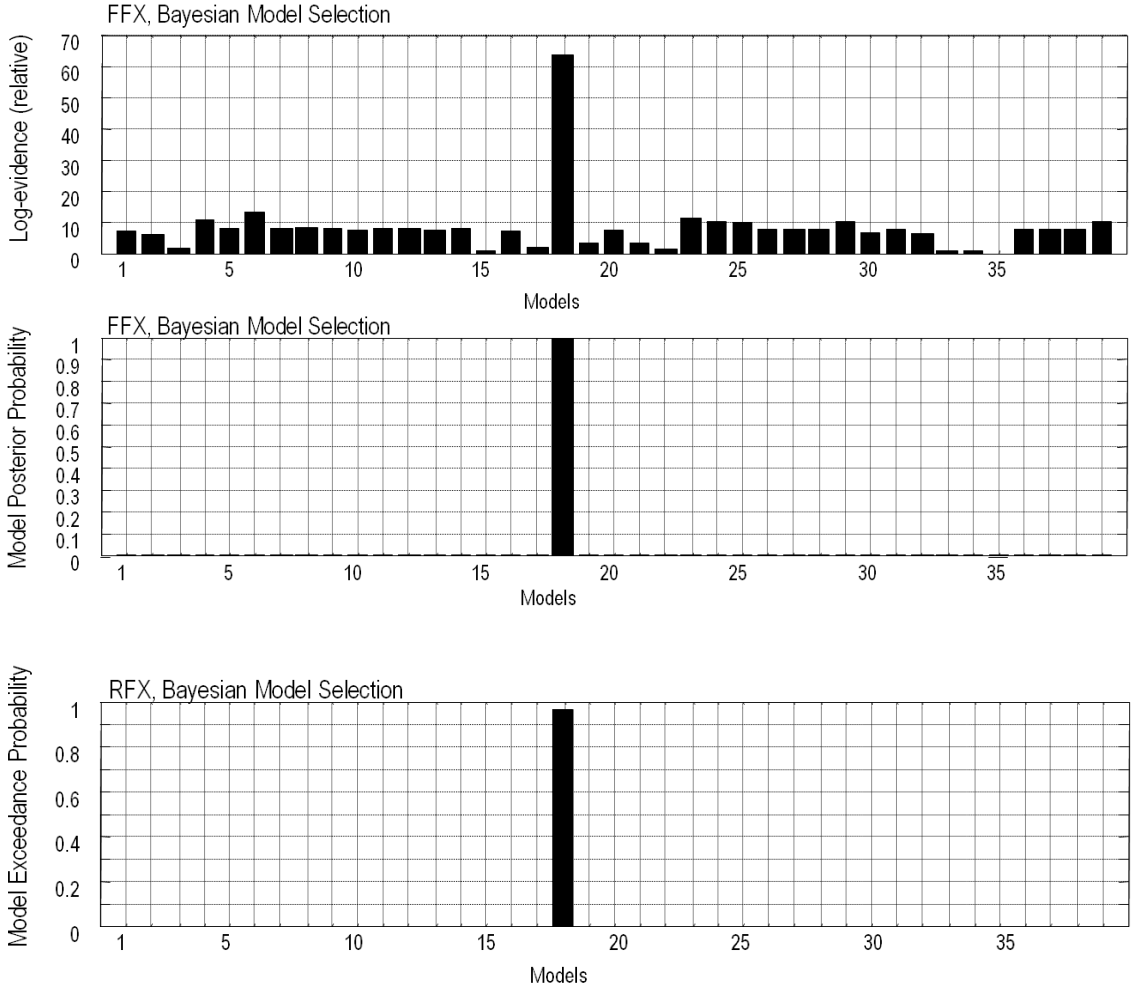

Figure 7.10. Results of the fixed (upper) and random (lower) effects Bayesian Model Selection procedures, the both favor Model 18.

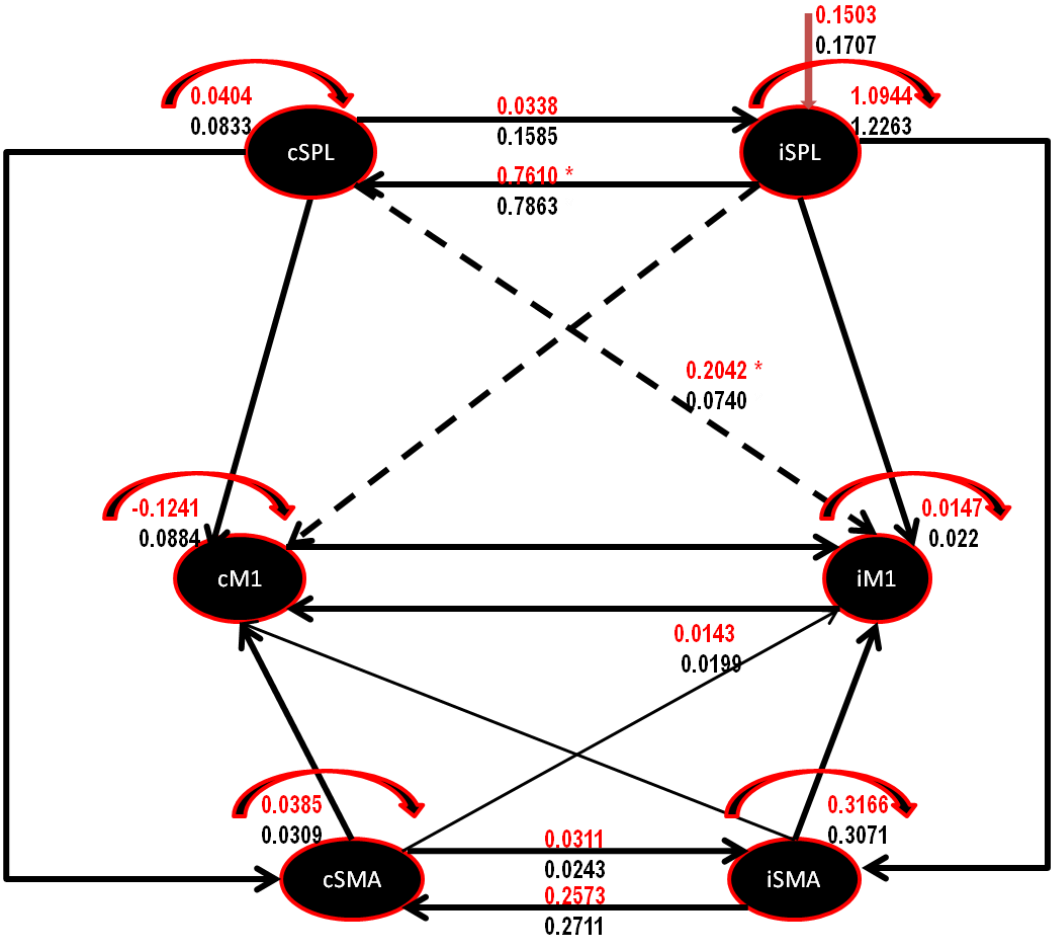

Figure 7.11. The optimal model with the group average parameters derived using Bayesian Parameter average. The asterisk * denotes significant difference between conditions excluding S6. The parameters of mirror feedback condition are in red and those of veridical condition are in black.

Inferences on optimal model parameters: Group average of the optimal model is derived using Bayesian Parameter Averaging (BPA) for each of the two conditions HANDmirror and HANDveridical (see Figure 7.11). Model 18 includes seven main connections across the nodes, and six autocorrelation connections. BPA of the sessions for each subject ae also derived to study the significance of difference, between modulations in the two conditions, across all seven connections. Repeated measures ANOVA shows a significant difference between HANDmirror and HANDveridical ($F_{1,10}$=6.732, P=0.0276) for all seven connections. ANOVA on each of the connection

does not show significance with Bonferroni correction ($p<0.007$). However, excluding S6, the difference in parameters between the two conditions shows significance in the cSPL=>iM1 connection ($F_{1,9}=12.44$, $p=0.0064$) and iSPL=>cSPL connection ($F_{1,9}=18.585$, $p=0.002$).

7.4 Discussion

This study is very important given the promise of mirror therapy for stroke patients; movement-based interventions for hemiparesis are limited by the amount of remaining volitional motion after stroke, mirror therapy may be particularly useful for severely paretic patients or in the early stages post-stroke.

The experimental design in this study demonstrates that mirror visual feedback during unimanual motion of the unaffected hand can significantly activate the motor cortex of the lesioned hemisphere. Further, the data show that this effect cannot be accounted for by arbitrary confounds related to visual motion, gaze effects, position of objects in a particular hemi-field, differences in movement kinematics, or especially to movement production (since activation attributed to these confounds are subtracted out). Finally, data show that regions showing mirror-based effects are topographically overlapping with those involved in producing movement of the paretic hand.

The results are consistent with recent findings, that the motor cortex can be modulated by action observation or perception, irrespective of overt movement. As mentioned in section 7.1, other mirror visual feedback-based studies in healthy neural systems (Matthys et al. 2009; Diers et al. 2010; Michielsen et al. 2011) have noted similar effects on motor cortex. Strangely, this data does not agree with the results of the only fMRI mirror feedback study conducted in stroke subjects (Michielsen et al. 2011) in

which the authors did not note significant sensorimotor activation in response to mirror feedback. However, the critical differences between their design and this design may explain the discrepancy in the results, VR mirror feedback might be more focused than a physical mirror. The discrepancy in the results might be also due difference in the impairment level of the subjects; the relation between severity if movement impairment and the neural response is justified in this study by the negative correlation between dWMFT clinical score and activity in FBA, and sensorimotor cortex areas (see Table 7.2. and Figure 7.8).

Functional MRI (fMRI) in healthy subjects revealed that mirrored feedback using a sagittally oriented mirror-box setup can be associated with increased activity in sensorimotor cortex (SMA, M1 and S1) ipsilateral to the moving hand (however, (Matthys et al. 2009) found no activation in ipsilateral motor cortex). Matthys study showed activation in the right superior temporal gyrus (STG) (coordinates [52 -48 14, k=100) and right superior occipital cortex. Matthys et al reporting of STG with k=100 voxels overlap with FBA region in this study. The data of this study show FBA activity negatively correlated with dWMFT score; the better the movement the more activity in FBA. Besides PPI analysis shows strong interaction of FBA with IM1 and CSPL, which are active in the HANDmirror>(HANDveridical+CTRLmirror+CTRLveridical); the absence of sensorimotor cortex activation in Matthys et al study could be again due to unfocused illusion which makes FBA and occipital cortex interaction with the sensorimotor cortex weaker. Subject 9 has a big infarction in the occipital cortex, and this subject does not show any response to visual feedback. This can be due to loss of focus from the subject but it also can mean a critical role of the input from the occipital cortex

or from the occipito-temporal and occipito-parietal junctions in bolstering activity in the sensorimotor cortex. The latter claim is supported by the fact the PPI analysis showed interaction of contralesional SPL areas with occipito-parietal and occipito-temporal junctions' areas (figure 7.8) and it is also supported by the fact that iM1 was positively modulated by input from cSPL during the HANDmirror condition as demonstrated via DCM.

Interestingly, individuals who have undergone amputation of the upper limb, but do not exhibit phantom limb pain, showed recruitment of sensorimotor cortex activity similar to healthy subjects while those who do experience phantom limb pain did not (Diers et al. 2010); this suggests that sensorimotor regions (which are thought to play a role in phantom sensations) may be mediated by the mirror effects. Similarly, electrical (Touzalin-Chretien and Dufour 2008) and neuro-imaging work in healthy subjects revealed increased lateralized readiness potentials and stimulus-induced 20-Hz suppression of the primary motor cortex contralateral to the inactive hand, both effects are indicative of increased excitability of the motor cortex, during mirrored feedback. Direct facilitation of the healthy corticospinal system has been demonstrated as increased motor evoked potentials (relative to baseline) in the motor cortex ipsilateral to the moving hand during mirrored feedback (Garry et al. 2005).

The contrast HANDmirror>(HANDveridical+CTRLmirror+CTRLveridical) recruits activity in ipsilesional EBA at $p<0.05$. Interestingly Saxe and colleagues (Saxe et al. 2006) found that right EBA responds to allocentric visual feedback of body image versus egocentric visual feedback; which the authors referred to as allocentric perspective is actually a mirror of the egocentric perspective. This would suggest a role of EBA in

judgment of mirrored feedback of body image similar to its role in judging art novelty in (Huang et al. 2011) study. The data in this study shows high EBA interaction with cSPL during mirror feedback, and DCM shows modulation of cSPL to iM1 activity. Therefore, both EBA and FBA must be contributing to the modulation of cSPL which in turn positively modulate activity in iM1.

In conclusion, the neurophysiological phenomenon investigated in this study has been cited as the rationale underpinning mirrored feedback therapy for patients with severe hand paresis, which restrict individuals from actively participating in training. This approach is not well established yet as a conventional therapy, but the neurophysiological mechanism of mirror feedback found in this study suggests a promising outcome of mirror therapy, specifically mirror feedback in VR. The main advantage of mirror therapy is not just its potential for enhancing brain plasticity by increasing the excitability of the sensorimotor cortex, but also as an alternative therapy for subjects who have minimal paretic hand movement and are incapable of pursuing conventional therapy.

CHAPTER 8

CONCLUSIONS

The main aim of this dissertation is to study virtual reality and its effects on brain excitability. This issue is approached in terms of 1) designing an MRI-compatible VR system (aim 1, see chapter 4) 2) exploring patterns of brain reorganization after rehabilitation intervention enriched with VR feedback (aim 2, see chapter 5), and 3) investigating the possible effects of visual discordances on enhancing brain excitability in distinct brain networks (aims 3 and 4, see chapters 6 and 7).

In terms of aim 1, the methodology to incorporate VR feedback in fMRI study proved to be successful in the experiments performed in aims 2, 3 and 4. Incorporating VR in fMRI study is novel not just for providing subjects with real time feedback, but it also makes it possible to design experiments with visual discordances without requiring additional hardware. In addition, this methodology allows tracking of subjects' performance for offline analysis.

Aim 2 (chapter 5) of this dissertation draws an outline for quantifying different forms of brain reorganization in terms of: extent of activation, intensity of activation, functional connectivity and re-lateralization. Moreover, this study provides a tool to validate interventions like robot assisted virtual reality training, a validation that goes beyond clinical measures. This study also approaches a pervasive problem related to motor control-based fMRI designs and analysis which is the inability to account for discrepancies in movement within and between fMRI sessions which would make longitudinal studies vulnerable to the confounding factors of difference in movement

performance across testing days. While two rehabilitation-based imaging studies have integrated one- degree of freedom measurement devices (e.g., force or position sensors) into fMRI (Jang et al. 2005; You et al. 2005), they were unable to model the kinematic data in the fMRI GLM (due to the blocked nature of the fMRI design). In this study, the design is event-related and it was possible to measure the complex kinematics of finger motion and model these data into the analysis. This approach could revolutionize the study of neural reorganization after stroke interventions by allowing the use of hand kinematic data acquired during scanning to account on a trial-by-trial basis for the variance explained in the BOLD signal. This significantly advances the validity of statistical inferences because analyses can be conducted at the single-subject level. It is also novel to run DCM analysis on bilateral M1 interactions, and to relate the change in coupling strength between iM1 and cM1 with motor recovery after the 2 weeks of training.

Aim 3 of this dissertation (chapter 6) shows that different forms of virtual reality-augmented feedback in real-time are able to recruit select regions of the cortex. Given the existence of rich intra-hemispheric cortico-cortical projections between occipital, parietal, and frontal cortices (Lewis and Van Essen 2000; Lewis and Van Essen 2000; Mitchell and Cauller 2001; Dum and Strick 2005; Fang et al. 2005; Lewis et al. 2005; Stepniewska et al. 2005), this study in humans supports the primate literature (Graziano and Gross 1998; Graziano and Gross 1998; Graziano 1999; Graziano and Gandhi 2000; Kakei et al. 2003), by showing that vision can be a powerful signal to sensorimotor centers. This implies a very strong promise for visual discordance in VR to become a useful tool the field of technology-assisted neurorehabilitation (Adamovich et al. 2009). A similar VR

interface providing mirrored visual feedback (aim 4, chapter 7) of non-paretic hand movement can selectively facilitate activity in topographically relevant sensorimotor areas of the ipsilesional hemisphere. These observations suggest that such neural modulation by VR visual discordance can be exploited to facilitate reorganization though Hebbian mechanisms. It also implies that visuomotor manipulations in VR may offer a tool to clinicians to facilitate functional recovery in patients. A VR study enriched with error-based visual feedback is crucial at this point to understand VR's ability to enhance the chance of motor recovery through motor learning and inducing brain reorganization. This can be approached by combining error-based feedback (amplitude manipulation, mismatched feedback, mirror visual feedback) with robot-assisted virtual reality training, and by further optimizing these interventions through the analysis of brain reorganization using the methodology in aim 3 (chapter 5). In the long term, understanding the effect of virtual reality visual feedback on motor learning might have an enormous impact on the field of neuroscience as well as on the field of rehabilitation engineering and rehabilitation medicine.

The relevance of this research stems first from the importance of the development of better procedures for rehabilitation therapy with a concentration on maximizing the chance of brain plasticity. This research is also novel in terms of combining study of movement kinematics with brain imaging. Many studies have investigated the effect of sensory feedback on brain activity and brain activity during movement, but none was able to control for the possible confounds resulting from variability in motor performance.

APPENDIX

SUPPLEMENTARY INFORMATION

Table A 6.1 Clusters of Activation in the Main Contrasts of Chapter 6 Experiment 1

Region	Side	k	x, y, z	t	z
V > G25					
mid occipital g.	L	314	[-26 -88 6]	5.62	3.78
mid temporal g.	L	645	[-46 -60 0]	5.27	3.65
sup parietal	L	57	[-22 -54 54]	3.76	2.95
G25 > V					
precentral g.	L	62	[-40 -20 68]	3.98	3.07
V>G65					
middle temporal g.	L	122	[-48 -60 -2]	5.64	3.79
G65>V					
postcentral g.	L	43	[-50 -14 50]	4.58	3.36
V > MF					
mid occipital	L	283	[-24 -98 12]	7.1	4.26
inf occipital	L	16	[-42 -70 -6]	3.34	2.72
MF > V					
inf frontal opercularis	R	80	[54 12 30]	9.82	4.92
inf frontal triangularis	L	42	[-52 16 0]	6.54	4.1
mid frontal gyrus	R	66	[36 2 58]	5.6	3.78
inf parietal g.	L	70	[-36 -46 44]	5.3	3.66
inf parietal g.	R	137	[42 -50 54]	3.69	2.91
postcentral g.	L	78	[-42 -34 42]	4.66	3.39
cerebellum	R	51	[24 -50 -36]	4.35	3.25
supplementary area	L	124	[-8 18 44]	4.34	3.25
insula	R	59	[46 18 -2]	4.34	3.25
insula	L	12	[-36 18 6]	3.81	2.98

Table A 6.1 Clusters of Activation in the Main Contrasts of Chapter 6 Experiment 1 (continued)

Region	Side	k	x, y, z	t	z
mid frontal g.	L	78	[-36 4 50]	3.77	2.96
mid frontal g.	L	69	[-54 16 36]	3.74	2.94
precentral g.	L	37	[-58 -18 42]	3.73	2.94
Decision time (+)					
supplementary motor area	R	728	[6 18 48]	6.82	4.18
insula	L	94	[-32 18 0]	6.22	3.99
sup parietal	L	185	[-22 -62 50]	5.78	3.84
sup occipital	R	73	[26 -64 44]	5.72	3.82
inf parietal	R	1237	[48 -40 46]	5.34	3.67
fusiform	R	92	[34 -78 -18]	4.57	3.35
mid frontal g.	R	69	[34 4 62]	4.54	3.34
precentral g.	L	98	[-32 2 62]	4.5	3.32
Inf parietal	L	208	[-32 -48 42]	4.27	3.21
Insula	R	212	[32 16 6]	4.22	3.19
thalamus	L	65	[-10 -20 4]	4.11	3.13
inf frontal opercularis	R	24	[44 10 24]	4	3.08
inf occipital	R	115	[38 -92 -10]	3.83	2.99
middle temporal g.	R	41	[48 -74 8]	3.62	2.88
inf parietal	L	18	[-42 -36 44]	3.4	2.75
inf frontal opercularis	L	12	[-58 10 36]	3.22	2.65
inf temporal g.	L	16	[-46 -54 -24]	3.13	2.59
postcentral g.	R	16	[58 -18 42]	2.96	2.49

Voxel-level threshold: P<0.01 uncorrected, extent threshold=10. Equivk is the cluster size of voxels, and [x, y, z] are the coordinates of the peak voxel in mm; based on the Montreal Neurological Institute (MNI) brain template. L= left; R= right; Inf= Inferior; Sup: superior; g.: gyrus.

Table A6.2 Clusters of Activation in the Main Contrasts of Chapter 6 Experiment 2

Anatomical Location	Side	equiv k	x,y,z (mm)	T	equivZ
G175>V					
caudate nucleas	L	604	-21 23 1	7.2	4.2
lingual area	L	51	-6 -64 4	6.8	4.07
inf Temporal area	L	1015	[-48 -49 -20]	6.7	4.04
mid frontal orbitalis	R	103	48 53 -2	6.2	3.9
postcentral	L	92	-30 -43 73	6.0	3.85
subgyrul	R	430	33 -25 34	5.4	3.61
fusiform	R	21	21 -82 -14	5.3	3.6
SPL	R	40	21 -67 61	4.5	3.29
superior medial frontal	R	26	6 35 46	4.3	3.18
inf frontal triangularis	L	17	-54 32 22	4.3	3.17
inf Temporal area	R	112	57 -52 -8	4.1	3.1
cerebellum	L	23	[-36 -46 -32]	3.9	2.97
precuneus	L	23	-9 -55 73	3.8	2.95
cerebellum crust	R	16	39 -58 -29	3.6	2.84
middle frontal orbitalis	R	13	15 50 -2	3.6	2.82
superior occipital	R	18	18 -91 28	3.3	2.7
Middle occipital	R	26	36 -64 34	3.3	2.68
supramarginal	R	10	66 -19 28	3.0	2.5
G25>V					
middle frontal g.	R	151	45 53 4	5.7	3.74
postcentral	L	304	-63 -19 22	5.5	3.68
precentral g.	L	262	-36 14 -17	4.7	3.36
precuneus	R	63	24 -73 52	4.7	3.35
precentral g.	L	20	-18 -16 79	4.6	3.31
lingual	L	45	[-27 -46 -8]	4.6	3.3
Postcentral g.	L	14	-27 -31 73	4.6	3.3

Table A6.2 Clusters of Activation in the Main Contrasts of Chapter 6 Experiment 2 (continued)

Anatomical Location	Side	equivk	x,y,z (mm)	T	equivZ
mid temporal g.	L	64	[-63 -55 -5]	4.2	3.14
Insula	L	15	[-42 -10 -5]	3.9	3.01
mid temporal g.	R	14	51 -37 -17	3.5	2.81
lateral ventricle	R	55	3 14 16	3.5	2.8
IPL	R	34	36 -64 46	3.4	2.74
mid frontal g.	R	14	54 26 37	3.3	2.7
superior temporal g.	R	18	54 -37 13	3.3	2.7
IPL	R	12	48 -46 49	3.2	2.63
inf frontal triangularis	R	15	48 26 25	3.2	2.63
supramarginal g.	R	30	39 -43 34	3.2	2.61

Voxel-level threshold: P<0.01 uncorrected, extent threshold=10. Equivk is the cluster size of voxels, and [x, y, z] are the coordinates of the peak voxel in mm; based on the Montreal Neurological Institute (MNI) brain template. L= left; R= right; Inf= Inferior; Sup: superior; g.: gyrus.

Table A7.2 Significantly Active Clusters in the Main Contrasts of the Study

Contrast Anatomical location	Side	T-stat	EquivZ	[x y z]	Equivk
Mirror-based activation					
Sup. and Inf. Parietal lobules	R	5.85	4.09	39 -37 49	409
Precuneus, Sup. and Inf. Parietal lobules	L	5.83	4.09	-12 -70 52	1528
Precentral g., Inf. and Middle frontal g.	L	4.74	3.6	-45 20 28	522
Precentral g. and Middle frontal g.	R	4.51	3.49	45 -4 55	92
Calcarine cortex	L	3.79	3.09	-15 -79 7	17
Inf. frontal g. (pars opercularis)	R	3.77	3.08	60 20 28	15

Table A7.2 Significantly Active Clusters in the Main Contrasts of the Study (continued)

Contrast Anatomical location	Side	T-stat	EquivZ	[x y z]	Equivk
Mirror-based activation					
Postcentral g.	R	3.61	2.99	66 -1 19	29
Inf. temporal g.	L	3.45	2.89	-51 -61 -17	115
Effective connectivity (seed: cSPL)					
Middle temporal g.	R	6.44	4.16	36 -64 22	115
	R	3.38	2.78	54 -58 -5	37
Inf. temporal g.	R	6.12	4.05	45 -40 -8	131
Middle frontal g.	R	3.69	2.96	18 -7 64	55
Postcentral g.	R	3.47	2.83	27 -31 49	20
Caudate nucleus	R	3.43	2.81	3 8 4	17
Superior frontal g.	L	3.28	2.72	-9 -4 67	16
Effective connectivity (seed: iM1)					
Inf. temporal g.	R	4.15	3.21	45 -40 -8	10
Anterior cingulate g.	L	3.69	2.96	-3 20 -5	15

Voxel-level threshold: P<0.01 uncorrected, extent threshold=10. Equivk is the cluster size of voxels, and [x, y, z] are the coordinates of the peak voxel in mm; based on the Montreal Neurological Institute (MNI) brain template. L= left; R= right; Inf= Inferior; Sup: superior; g.: gyrus.

REFERENCES

S. V. Adamovich, K. August, A. Merians and E. Tunik (2009). "A virtual reality-based system integrated with fmri to study neural mechanisms of action observation-execution: a proof of concept study." Restor Neurol Neurosci **27**(3): 209-223.

S. V. Adamovich, G. G. Fluet, A. Mathai, Q. Qiu, J. Lewis and A. S. Merians (2009). "Design of a complex virtual reality simulation to train finger motion for persons with hemiparesis: a proof of concept study." J Neuroeng Rehabil **6**: 28.

S. V. Adamovich, G. G. Fluet, E. Tunik and A. S. Merians (2009). "Sensorimotor training in virtual reality: a review." NeuroRehabilitation **25**(1): 29-44.

G. K. Aguirre, J. A. Detre, E. Zarahn and D. C. Alsop (2002). "Experimental design and the relative sensitivity of BOLD and perfusion fMRI." NeuroImage **15**(3): 488-500.

E. L. Altschuler, S. B. Wisdom, L. Stone, C. Foster, D. Galasko, D. M. Llewellyn and V. S. Ramachandran (1999). "Rehabilitation of hemiparesis after stroke with a mirror." Lancet **353**(9169): 2035-2036.

A. Antal, S. Begemeier, M. A. Nitsche and W. Paulus (2008). "Prior state of cortical activity influences subsequent practicing of a visuomotor coordination task." Neuropsychologia **46**(13): 3157-3161.

S. V. Astafiev, C. M. Stanley, G. L. Shulman and M. Corbetta (2004). "Extrastriate body area in human occipital cortex responds to the performance of motor actions." Nature neuroscience **7**(5): 542-548.

L. Aziz-Zadeh, F. Maeda, E. Zaidel, J. Mazziotta and M. Iacoboni (2002). "Lateralization in motor facilitation during action observation: a TMS study." Exp Brain Res **144**(1): 127-131.

S. Balasubramanian, J. Klein and E. Burdet (2010). "Robot-assisted rehabilitation of hand function." Curr Opin Neurol **23**(6): 661-670.

C. Begliomini, C. Nelini, A. Caria, W. Grodd and U. Castiello (2008). "Cortical activations in humans grasp-related areas depend on hand used and handedness." PLoS One **3**(10): e3388.

E. Bhatt, A. Nagpal, K. H. Greer, T. K. Grunewald, J. L. Steele, J. W. Wiemiller, S. M. Lewis and J. R. Carey (2007). "Effect of finger tracking combined with electrical stimulation on brain reorganization and hand function in subjects with stroke." Exp Brain Res **182**(4): 435-447.

C. Bosecker, L. Dipietro, B. Volpe and H. I. Krebs (2010). "Kinematic robot-based evaluation scales and clinical counterparts to measure upper limb motor performance in patients with chronic stroke." Neurorehabil Neural Repair **24**(1): 62-69.

S. Bray, S. Shimojo and J. P. O'Doherty (2007). "Direct instrumental conditioning of neural activity using functional magnetic resonance imaging-derived reward feedback." J Neurosci **27**(28): 7498-7507.

B. R. Brewer, R. Klatzky, H. Markham and Y. Matsuoka (2009). "Investigation of goal change to optimize upper-extremity motor performance in a robotic environment." Dev Med Child Neurol **51 Suppl 4**: 146-153.

B. R. Brewer, R. Klatzky and Y. Matsuoka (2008). "Visual feedback distortion in a robotic environment for hand rehabilitation." Brain Res Bull **75**(6): 804-813.

G. Buccino, A. Baumgaertner, L. Colle, C. Buechel, G. Rizzolatti and F. Binkofski (2007). "The neural basis for understanding non-intended actions." Neuroimage **36 Suppl 2**: T119-127.

C. M. Butefisch, R. Kleiser, B. Korber, K. Muller, H. J. Wittsack, V. Homberg and R. J. Seitz (2005). "Recruitment of contralesional motor cortex in stroke patients with recovery of hand function." Neurology **64**(6): 1067-1069.

A. J. Butler and S. J. Page (2006). "Mental practice with motor imagery: evidence for motor recovery and cortical reorganization after stroke." Arch Phys Med Rehabil **87**(12 Suppl 2): S2-11.

R. B. Buxton, E. C. Wong and L. R. Frank (1998). "Dynamics of blood flow and oxygenation changes during brain activation: the balloon model." Magn Reson Med **39**(6): 855-864.

C. Calautti, M. Naccarato, P. S. Jones, N. Sharma, D. D. Day, A. T. Carpenter, E. T. Bullmore, E. A. Warburton and J. C. Baron (2007). "The relationship between motor deficit and hemisphere activation balance after stroke: A 3T fMRI study." Neuroimage **34**(1): 322-331.

V. D. Calhoun, M. C. Stevens, G. D. Pearlson and K. A. Kiehl (2004). "fMRI analysis with the general linear model: removal of latency-induced amplitude bias by incorporation of hemodynamic derivative terms." Neuroimage **22**(1): 252-257.

J. R. Carey, K. R. Greer, T. K. Grunewald, J. L. Steele, J. W. Wiemiller, E. Bhatt, A. Nagpal, O. Lungu and E. J. Auerbach (2006). "Primary motor area activation during precision-demanding versus simple finger movement." Neurorehabil Neural Repair **20**(3): 361-370.

L. M. Carey, D. F. Abbott, A. Puce, G. D. Jackson, A. Syngeniotis and G. A. Donnan (2002). "Reemergence of activation with poststroke somatosensory recovery: a serial fMRI case study." Neurology **59**(5): 749-752.

S. H. Cho, H. K. Shin, Y. H. Kwon, M. Y. Lee, Y. H. Lee, C. H. Lee, D. S. Yang and S. H. Jang (2007). "Cortical activation changes induced by visual biofeedback tracking training in chronic stroke patients." NeuroRehabilitation **22**(2): 77-84.

P. A. Chouinard, G. Leonard and T. Paus (2006). "Changes in effective connectivity of the primary motor cortex in stroke patients after rehabilitative therapy." Exp Neurol **201**(2): 375-387.

C. R. Conner, T. M. Ellmore, T. A. Pieters, M. A. DiSano and N. Tandon (2011). "Variability of the relationship between electrophysiology and BOLD-fMRI across cortical regions in humans." The Journal of neuroscience : the official journal of the Society for Neuroscience **31**(36): 12855-12865.

S. A. Coombes, D. M. Corcos, L. Sprute and D. E. Vaillancourt (2010). "Selective regions of the visuomotor system are related to gain-induced changes in force error." J Neurophysiol **103**(4): 2114-2123.

J. C. Culham, S. L. Danckert, J. F. DeSouza, J. S. Gati, R. S. Menon and M. A. Goodale (2003). "Visually guided grasping produces fMRI activation in dorsal but not ventral stream brain areas." Exp Brain Res **153**(2): 180-189.

N. David, M. X. Cohen, A. Newen, B. H. Bewernick, N. J. Shah, G. R. Fink and K. Vogeley (2007). "The extrastriate cortex distinguishes between the consequences of one's own and others' behavior." Neuroimage **36**(3): 1004-1014.

M. Diers, C. Christmann, C. Koeppe, M. Ruf and H. Flor "Mirrored, imagined and executed movements differentially activate sensorimotor cortex in amputees with and without phantom limb pain." Pain **149**(2): 296-304.

M. Diers, C. Christmann, C. Koeppe, M. Ruf and H. Flor (2010). "Mirrored, imagined and executed movements differentially activate sensorimotor cortex in amputees with and without phantom limb pain." Pain **149**(2): 296-304.

C. Dohle, J. Pullen, A. Nakaten, J. Kust, C. Rietz and H. Karbe (2009). "Mirror therapy promotes recovery from severe hemiparesis: a randomized controlled trial." Neurorehabil Neural Repair **23**(3): 209-217.

R. P. Dum and P. L. Strick (2005). "Frontal lobe inputs to the digit representations of the motor areas on the lateral surface of the hemisphere." J Neurosci **25**(6): 1375-1386.

D. Ertelt, S. Small, A. Solodkin, C. Dettmers, A. McNamara, F. Binkofski and G. Buccino (2007). "Action observation has a positive impact on rehabilitation of motor deficits after stroke." Neuroimage **36 Suppl 2**: T164-173.

P. C. Fang, I. Stepniewska and J. H. Kaas (2005). "Ipsilateral cortical connections of motor, premotor, frontal eye, and posterior parietal fields in a prosimian primate, Otolemur garnetti." J Comp Neurol **490**(3): 305-333.

C. Farrer and C. D. Frith (2002). "Experiencing oneself vs another person as being the cause of an action: the neural correlates of the experience of agency." Neuroimage **15**(3): 596-603.

A. Feydy, R. Carlier, A. Roby-Brami, B. Bussel, F. Cazalis, L. Pierot, Y. Burnod and M. A. Maier (2002). "Longitudinal study of motor recovery after stroke: recruitment and focusing of brain activation." Stroke **33**(6): 1610-1617.

P. Feys, W. Helsen, M. Buekers, T. Ceux, E. Heremans, B. Nuttin, P. Ketelaer and X. Liu (2006). "The effect of changed visual feedback on intention tremor in multiple sclerosis." Neurosci Lett **394**(1): 17-21.

M. A. Finley, S. E. Fasoli, L. Dipietro, J. Ohlhoff, L. Macclellan, C. Meister, J. Whitall, R. Macko, C. T. Bever, Jr., H. I. Krebs and N. Hogan (2005). "Short-duration robotic therapy in stroke patients with severe upper-limb motor impairment." Journal of rehabilitation research and development **42**(5): 683-692.

L. Fogassi, P. F. Ferrari, B. Gesierich, S. Rozzi, F. Chersi and G. Rizzolatti (2005). "Parietal lobe: from action organization to intention understanding." Science **308**(5722): 662-667.

K. Friston, J. Daunizeau and K. E. Stephan (2011). "Model selection and gobbledygook: Response to Lohmann et al." NeuroImage.

K. Friston, J. Mattout, N. Trujillo-Barreto, J. Ashburner and W. Penny (2007). "Variational free energy and the Laplace approximation." NeuroImage **34**(1): 220-234.

K. J. Friston, C. Buechel, G. R. Fink, J. Morris, E. Rolls and R. J. Dolan (1997). "Psychophysiological and modulatory interactions in neuroimaging." Neuroimage **6**(3): 218-229.

K. J. Friston, P. Fletcher, O. Josephs, A. Holmes, M. D. Rugg and R. Turner (1998). "Event-related fMRI: characterizing differential responses." Neuroimage **7**(1): 30-40.

K. J. Friston, L. Harrison and W. Penny (2003). "Dynamic causal modelling." NeuroImage **19**(4): 1273-1302.

K. J. Friston, O. Josephs, G. Rees and R. Turner (1998). "Nonlinear event-related responses in fMRI." Magn Reson Med **39**(1): 41-52.

M. I. Garry, A. Loftus and J. J. Summers (2005). "Mirror, mirror on the wall: viewing a mirror reflection of unilateral hand movements facilitates ipsilateral M1 excitability." Exp Brain Res **163**(1): 118-122.

M. Ghilardi, C. Ghez, V. Dhawan, J. Moeller, M. Mentis, T. Nakamura, A. Antonini and D. Eidelberg (2000). "Patterns of regional brain activation associated with different forms of motor learning." Brain Res **871**(1): 127-145.

M. F. Ghilardi, M. Alberoni, M. Rossi, M. Franceschi, C. Mariani and F. Fazio (2000). "Visual feedback has differential effects on reaching movements in Parkinson's and Alzheimer's disease." Brain Res **876**(1-2): 112-123.

G. H. Glover (1999). "Deconvolution of impulse response in event-related BOLD fMRI." Neuroimage **9**(4): 416-429.

M. R. Golomb, B. C. McDonald, S. J. Warden, J. Yonkman, A. J. Saykin, B. Shirley, M. Huber, B. Rabin, M. Abdelbaky, M. E. Nwosu, M. Barkat-Masih and G. C. Burdea (2010). "In-home virtual reality videogame telerehabilitation in adolescents with hemiplegic cerebral palsy." Arch Phys Med Rehabil **91**(1): 1-8 e1.

M. S. Graziano (1999). "Where is my arm? The relative role of vision and proprioception in the neuronal representation of limb position." Proc Natl Acad Sci U S A **96**(18): 10418-10421.

M. S. Graziano and S. Gandhi (2000). "Location of the polysensory zone in the precentral gyrus of anesthetized monkeys." Exp Brain Res **135**(2): 259-266.

M. S. Graziano and C. G. Gross (1998). "Spatial maps for the control of movement." Curr Opin Neurobiol **8**(2): 195-201.

M. S. Graziano and C. G. Gross (1998). "Visual responses with and without fixation: neurons in premotor cortex encode spatial locations independently of eye position." Exp Brain Res **118**(3): 373-380.

J. Grinband, J. Savitskaya, T. D. Wager, T. Teichert, V. P. Ferrera and J. Hirsch (2011). "Conflict, error likelihood, and RT: Response to Brown & Yeung et al." Neuroimage **57**(2): 320-322.

F. Hamzei, C. Dettmers, M. Rijntjes and C. Weiller (2008). "The effect of cortico-spinal tract damage on primary sensorimotor cortex activation after rehabilitation therapy." Exp Brain Res **190**(3): 329-336.

R. Hari, S. Levanen and T. Raij (2000). "Timing of human cortical functions during cognition: role of MEG." Trends Cogn Sci **4**(12): 455-462.

R. N. Henson, C. J. Price, M. D. Rugg, R. Turner and K. J. Friston (2002). "Detecting latency differences in event-related BOLD responses: application to words versus nonwords and initial versus repeated face presentations." NeuroImage **15**(1): 83-97.

M. Huang, H. Bridge, M. J. Kemp and A. J. Parker (2011). "Human cortical activity evoked by the assignment of authenticity when viewing works of art." Front Hum Neurosci **5**: 134.

F. C. Hummel and L. G. Cohen (2006). "Non-invasive brain stimulation: a new strategy to improve neurorehabilitation after stroke?" Lancet Neurol **5**(8): 708-712.

M. Iacoboni, R. P. Woods, M. Brass, H. Bekkering, J. C. Mazziotta and G. Rizzolatti (1999). "Cortical mechanisms of human imitation." Science **286**(5449): 2526-2528.

C. S. Inman, G. A. James, S. Hamann, J. K. Rajendra, G. Pagnoni and A. J. Butler (2012). "Altered resting-state effective connectivity of fronto-parietal motor control systems on the primary motor network following stroke." Neuroimage **59**(1): 227-237.

A. Iriki (2006). "The neural origins and implications of imitation, mirror neurons and tool use." Curr Opin Neurobiol **16**(6): 660-667.

P. L. Jackson, A. N. Meltzoff and J. Decety (2006). "Neural circuits involved in imitation and perspective-taking." Neuroimage **31**(1): 429-439.

G. A. James, Z. L. Lu, J. W. VanMeter, K. Sathian, X. P. Hu and A. J. Butler (2009). "Changes in resting state effective connectivity in the motor network following rehabilitation of upper extremity poststroke paresis." Top Stroke Rehabil **16**(4): 270-281.

S. H. Jang, S. H. You, M. Hallett, Y. W. Cho, C. M. Park, S. H. Cho, H. Y. Lee and T. H. Kim (2005). "Cortical reorganization and associated functional motor recovery after virtual reality in patients with chronic stroke: an experimenter-blind preliminary study." Arch Phys Med Rehabil **86**(11): 2218-2223.

S. H. Jang, S. H. You, Y. H. Kwon, M. Hallett, M. Y. Lee and S. H. Ahn (2005). "Cortical reorganization associated lower extremity motor recovery as evidenced by functional MRI and diffusion tensor tractography in a stroke patient." Restorative neurology and neuroscience **23**(5-6): 325-329.

P. Jenmalm, C. Schmitz, H. Forssberg and H. H. Ehrsson (2006). "Lighter or heavier than predicted: neural correlates of corrective mechanisms during erroneously programmed lifts." The Journal of neuroscience : the official journal of the Society for Neuroscience **26**(35): 9015-9021.

S. Kakei, D. S. Hoffman and P. L. Strick (2003). "Sensorimotor transformations in cortical motor areas." Neurosci Res **46**(1): 1-10.

S. S. Kannurpatti and B. B. Biswal (2008). "Detection and scaling of task-induced fMRI-BOLD response using resting state fluctuations." NeuroImage **40**(4): 1567-1574.

S. S. Kannurpatti, M. A. Motes, B. Rypma and B. B. Biswal (2010). "Neural and vascular variability and the fMRI-BOLD response in normal aging." Magnetic resonance imaging **28**(4): 466-476.

S. S. Kannurpatti, M. A. Motes, B. Rypma and B. B. Biswal (2011). "Increasing measurement accuracy of age-related BOLD signal change: minimizing vascular contributions by resting-state-fluctuation-of-amplitude scaling." Human brain mapping **32**(7): 1125-1140.

C. H. Kasess, C. Windischberger, R. Cunnington, R. Lanzenberger, L. Pezawas and E. Moser (2008). "The suppressive influence of SMA on M1 in motor imagery revealed by fMRI and dynamic causal modeling." Neuroimage **40**(2): 828-837.

M. Kononen, I. M. Tarkka, E. Niskanen, M. Pihlajamaki, E. Mervaala, K. Pitkanen and R. Vanninen (2012). "Functional MRI and motor behavioral changes obtained with constraint-induced movement therapy in chronic stroke." Eur J Neurol **19**(4): 578-586.

I. Kontaris, A. J. Wiggett and P. E. Downing (2009). "Dissociation of extrastriate body and biological-motion selective areas by manipulation of visual-motor congruency." Neuropsychologia **47**(14): 3118-3124.

J. W. Lewis and D. C. Van Essen (2000). "Corticocortical connections of visual, sensorimotor, and multimodal processing areas in the parietal lobe of the macaque monkey." J Comp Neurol **428**(1): 112-137.

J. W. Lewis and D. C. Van Essen (2000). "Mapping of architectonic subdivisions in the macaque monkey, with emphasis on parieto-occipital cortex." J Comp Neurol **428**(1): 79-111.

S. J. Lewis, A. Slabosz, T. W. Robbins, R. A. Barker and A. M. Owen (2005). "Dopaminergic basis for deficits in working memory but not attentional set-shifting in Parkinson's disease." Neuropsychologia **43**(6): 823-832.

J. Liepert, F. Hamzei and C. Weiller (2004). "Lesion-induced and training-induced brain reorganization." Restorative neurology and neuroscience **22**(3-5): 269-277.

K. C. Lin, H. Y. Chung, C. Y. Wu, H. L. Liu, Y. W. Hsieh, I. H. Chen, C. L. Chen, L. L. Chuang, J. S. Liu and Y. Y. Wai (2010). "Constraint-induced therapy versus control intervention in patients with stroke: a functional magnetic resonance imaging study." Am J Phys Med Rehabil **89**(3): 177-185.

X. Liu, X. H. Zhu and W. Chen (2011). "Baseline BOLD correlation predicts individuals' stimulus-evoked BOLD responses." NeuroImage **54**(3): 2278-2286.

D. Lloyd-Jones, R. J. Adams, T. M. Brown, M. Carnethon, S. Dai, G. De Simone, T. B. Ferguson, E. Ford, K. Furie, C. Gillespie, A. Go, K. Greenlund, N. Haase, S. Hailpern, P. M. Ho, V. Howard, B. Kissela, S. Kittner, D. Lackland, L. Lisabeth, A. Marelli, M. M. McDermott, J. Meigs, D. Mozaffarian, M. Mussolino, G. Nichol, V. L. Roger, W. Rosamond, R. Sacco, P. Sorlie, R. Stafford, T. Thom, S. Wasserthiel-Smoller, N. D. Wong and J. Wylie-Rosett (2010). "Executive summary: heart disease and stroke statistics--2010 update: a report from the American Heart Association." Circulation **121**(7): 948-954.

A. R. Luft, S. McCombe-Waller, J. Whitall, L. W. Forrester, R. Macko, J. D. Sorkin, J. B. Schulz, A. P. Goldberg and D. F. Hanley (2004). "Repetitive bilateral arm training and motor cortex activation in chronic stroke: a randomized controlled trial." JAMA **292**(15): 1853-1861.

A. R. Luft, S. Waller, L. Forrester, G. V. Smith, J. Whitall, R. F. Macko, J. B. Schulz and D. F. Hanley (2004). "Lesion location alters brain activation in chronically impaired stroke survivors." Neuroimage **21**(3): 924-935.

L. R. Macclellan, D. D. Bradham, J. Whitall, B. Volpe, P. D. Wilson, J. Ohlhoff, C. Meister, N. Hogan, H. I. Krebs and C. T. Bever, Jr. (2005). "Robotic upper-limb neurorehabilitation in chronic stroke patients." Journal of rehabilitation research and development **42**(6): 717-722.

F. Maeda, G. Kleiner-Fisman and A. Pascual-Leone (2002). "Motor facilitation while observing hand actions: specificity of the effect and role of observer's orientation." J Neurophysiol **87**(3): 1329-1335.

F. Mancini, M. R. Longo, M. P. Kammers and P. Haggard (2011). "Visual distortion of body size modulates pain perception." Psychol Sci **22**(3): 325-330.

S. Manthey, R. I. Schubotz and D. Y. von Cramon (2003). "Premotor cortex in observing erroneous action: an fMRI study." Brain Res Cogn Brain Res **15**(3): 296-307.

R. S. Marshall, G. M. Perera, R. M. Lazar, J. W. Krakauer, R. C. Constantine and R. L. DeLaPaz (2000). "Evolution of cortical activation during recovery from corticospinal tract infarction." Stroke **31**(3): 656-661.

A. A. Mattar and P. L. Gribble (2005). "Motor learning by observing." Neuron **46**(1): 153-160.

K. Matthys, M. Smits, J. N. Van der Geest, A. Van der Lugt, R. Seurinck, H. J. Stam and R. W. Selles (2009). "Mirror-induced visual illusion of hand movements: a functional magnetic resonance imaging study." Arch Phys Med Rehabil **90**(4): 675-681.

D. Mclaren. (2011). "A Generalized Form of Context-Dependent Psychophysiological Interactions (gPPI)." from http://www.brainmap.wisc.edu/PPI.

A. S. Merians, G. G. Fluet, Q. Qiu, I. Lafond and S. V. Adamovich (2011). "Learning in a virtual environment using haptic systems for movement re-education: can this medium be used for remodeling other behaviors and actions?" J Diabetes Sci Technol **5**(2): 301-308.

A. S. Merians, G. G. Fluet, Q. Qiu, S. Saleh, I. Lafond, A. Davidow and S. V. Adamovich (2011). "Robotically facilitated virtual rehabilitation of arm transport integrated with finger movement in persons with hemiparesis." J Neuroeng Rehabil **8**: 27.

M. E. Michielsen, M. Smits, G. M. Ribbers, H. J. Stam, J. N. van der Geest, J. B. Bussmann and R. W. Selles (2010). "The neuronal correlates of mirror therapy: an fMRI study on mirror induced visual illusions in patients with stroke." J Neurol Neurosurg Psychiatry.

M. E. Michielsen, M. Smits, G. M. Ribbers, H. J. Stam, J. N. van der Geest, J. B. Bussmann and R. W. Selles (2011). "The neuronal correlates of mirror therapy: an fMRI study on mirror induced visual illusions in patients with stroke." J Neurol Neurosurg Psychiatry.

F. M. Miezin, L. Maccotta, J. M. Ollinger, S. E. Petersen and R. L. Buckner (2000). "Characterizing the hemodynamic response: effects of presentation rate, sampling procedure, and the possibility of ordering brain activity based on relative timing." Neuroimage **11**(6 Pt 1): 735-759.

K. L. Miller, W. M. Luh, T. T. Liu, A. Martinez, T. Obata, E. C. Wong, L. R. Frank and R. B. Buxton (2001). "Nonlinear temporal dynamics of the cerebral blood flow response." Hum Brain Mapp **13**(1): 1-12.

B. D. Mitchell and L. J. Cauller (2001). "Corticocortical and thalamocortical projections to layer I of the frontal neocortex in rats." Brain Res **921**(1-2): 68-77.

M. R. Mouawad, C. G. Doust, M. D. Max and P. A. McNulty (2011). "Wii-based movement therapy to promote improved upper extremity function post-stroke: a pilot study." J Rehabil Med **43**(6): 527-533.

J. Mount, S. R. Pierce, J. Parker, R. DiEgidio, R. Woessner and L. Spiegel (2007). "Trial and error versus errorless learning of functional skills in patients with acute stroke." NeuroRehabilitation **22**(2): 123-132.

T. Murayama, K. Numata, T. Kawakami, T. Tosaka, M. Oga, N. Oka, M. Katano, J. Takasugi and E. Shimizu (2011). "Changes in the brain activation balance in motor-related areas after constraint-induced movement therapy; a longitudinal fMRI study." Brain Inj **25**(11): 1047-1057.

S. M. Nelson, N. U. Dosenbach, A. L. Cohen, M. E. Wheeler, B. L. Schlaggar and S. E. Petersen (2010). "Role of the anterior insula in task-level control and focal attention." Brain Struct Funct **214**(5-6): 669-680.

S. Ogawa, T. M. Lee, A. R. Kay and D. W. Tank (1990). "Brain magnetic resonance imaging with contrast dependent on blood oxygenation." Proc Natl Acad Sci U S A **87**(24): 9868-9872.

S. Ogawa, R. S. Menon, D. W. Tank, S. G. Kim, H. Merkle, J. M. Ellermann and K. Ugurbil (1993). "Functional brain mapping by blood oxygenation level-dependent contrast magnetic resonance imaging. A comparison of signal characteristics with a biophysical model." Biophys J **64**(3): 803-812.

R. C. Oldfield (1971). "The assessment and analysis of handedness: the Edinburgh inventory." Neuropsychologia **9**(1): 97-113.

T. D. Parsons, A. Iyer, L. Cosand, C. Courtney and A. A. Rizzo (2009). "Neurocognitive and psychophysiological analysis of human performance within virtual reality environments." Studies in health technology and informatics **142**: 247-252.

J. L. Patton, M. Kovic and F. A. Mussa-Ivaldi (2006). "Custom-designed haptic training for restoring reaching ability to individuals with poststroke hemiparesis." Journal of rehabilitation research and development **43**(5): 643-656.

J. L. Patton, M. E. Stoykov, M. Kovic and F. A. Mussa-Ivaldi (2006). "Evaluation of robotic training forces that either enhance or reduce error in chronic hemiparetic stroke survivors." Exp Brain Res **168**(3): 368-383.

J. L. Patton, M. E. Stoykov, M. Kovic and F. A. Mussa-Ivaldi (2006). "Evaluation of robotic training forces that either enhance or reduce error in chronic hemiparetic stroke survivors." Experimental brain research. Experimentelle Hirnforschung. Experimentation cerebrale **168**(3): 368-383.

S. Patuzzo, A. Fiaschi and P. Manganotti (2003). "Modulation of motor cortex excitability in the left hemisphere during action observation: a single- and paired-pulse transcranial magnetic stimulation study of self- and non-self-action observation." Neuropsychologia **41**(9): 1272-1278.

T. Paus, S. Marrett, K. Worsley and A. Evans (1996). "Imaging motor-to-sensory discharges in the human brain: an experimental tool for the assessment of functional connectivity." Neuroimage **4**(2): 78-86.

M. V. Peelen and P. E. Downing (2005). "Is the extrastriate body area involved in motor actions?" Nature neuroscience **8**(2): 125; author reply 125-126.

W. D. Penny (2012). "Comparing dynamic causal models using AIC, BIC and free energy." NeuroImage **59**(1): 319-330.

W. D. Penny, K. E. Stephan, J. Daunizeau, M. J. Rosa, K. J. Friston, T. M. Schofield and A. P. Leff (2010). "Comparing families of dynamic causal models." PLoS computational biology **6**(3): e1000709.

W. D. Penny, K. E. Stephan, A. Mechelli and K. J. Friston (2004). "Comparing dynamic causal models." NeuroImage **22**(3): 1157-1172.

D. Perani, F. Fazio, N. A. Borghese, M. Tettamanti, S. Ferrari, J. Decety and M. C. Gilardi (2001). "Different brain correlates for watching real and virtual hand actions." Neuroimage **14**(3): 749-758.

S. Pilgramm, B. Lorey, R. Stark, J. Munzert, D. Vaitl and K. Zentgraf (2010). "Differential activation of the lateral premotor cortex during action observation." BMC Neurosci **11**: 89.

R. Pineiro, S. Pendlebury, H. Johansen-Berg and P. M. Matthews (2001). "Functional MRI detects posterior shifts in primary sensorimotor cortex activation after stroke: evidence of local adaptive reorganization?" Stroke **32**(5): 1134-1139.

D. C. Prather (1971). "Trial-and-error versus errorless learning: training, transfer, and stress." The American journal of psychology **84**(3): 377-386.

Q. Qiu, G. G. Fluet, I. Lafond, A. S. Merians and S. V. Adamovich (2009). "Coordination changes demonstrated by subjects with hemiparesis performing hand-arm training using the NJIT-RAVR robotically assisted virtual rehabilitation system." Conf Proc IEEE Eng Med Biol Soc **2009**: 1143-1146.

Q. Qiu, D. A. Ramirez, S. Saleh, G. G. Fluet, H. D. Parikh, D. Kelly and S. V. Adamovich (2009). "The New Jersey Institute of Technology Robot-Assisted Virtual Rehabilitation (NJIT-RAVR) system for children with cerebral palsy: a feasibility study." J Neuroeng Rehabil **6**: 40.

A. K. Rehme, S. B. Eickhoff, L. E. Wang, G. R. Fink and C. Grefkes (2011). "Dynamic causal modeling of cortical activity from the acute to the chronic stage after stroke." Neuroimage **55**(3): 1147-1158.

D. J. Reinkensmeyer and J. L. Patton (2009). "Can robots help the learning of skilled actions?" Exerc Sport Sci Rev **37**(1): 43-51.

N. J. Rice, E. Tunik, E. S. Cross and S. T. Grafton (2007). "On-line grasp control is mediated by the contralateral hemisphere." Brain Res **1175**: 76-84.

M. Rijntjes, F. Hamzei, V. Glauche, D. Saur and C. Weiller (2011). "Activation changes in sensorimotor cortex during improvement due to CIMT in chronic stroke." Restorative neurology and neuroscience **29**(5): 299-310.

G. Rizzolatti and L. Craighero (2004). "The mirror-neuron system." Annu Rev Neurosci **27**: 169-192.

G. Rizzolatti, P. F. Ferrari, S. Rozzi and L. Fogassi (2006). "The inferior parietal lobule: where action becomes perception." Novartis Found Symp **270**: 129-140; discussion 140-125, 164-129.

N. Rojo, J. Amengual, M. Juncadella, F. Rubio, E. Camara, J. Marco-Pallares, S. Schneider, M. Veciana, J. Montero, B. Mohammadi, E. Altenmuller, C. Grau, T. F. Munte and A. Rodriguez-Fornells (2011). "Music-supported therapy induces plasticity in the sensorimotor cortex in chronic stroke: a single-case study using multimodal imaging (fMRI-TMS)." Brain Inj **25**(7-8): 787-793.

M. F. Rushworth, T. E. Behrens and H. Johansen-Berg (2006). "Connection patterns distinguish 3 regions of human parietal cortex." Cereb Cortex **16**(10): 1418-1430.

K. Sathian, A. I. Greenspan and S. L. Wolf (2000). "Doing it with mirrors: a case study of a novel approach to neurorehabilitation." Neurorehabil Neural Repair **14**(1): 73-76.

R. Saxe, N. Jamal and L. Powell (2006). "My body or yours? The effect of visual perspective on cortical body representations." Cereb Cortex **16**(2): 178-182.

R. J. Seitz (2010). "How imaging will guide rehabilitation." Curr Opin Neurol **23**(1): 79-86.

N. Sharma, J. C. Baron and J. B. Rowe (2009). "Motor imagery after stroke: relating outcome to motor network connectivity." Ann Neurol **66**(5): 604-616.

B. Sheng and M. Lin (2009). "A longitudinal study of functional magnetic resonance imaging in upper-limb hemiplegia after stroke treated with constraint-induced movement therapy." Brain Inj **23**(1): 65-70.

S. L. Small, P. Hlustik, D. C. Noll, C. Genovese and A. Solodkin (2002). "Cerebellar hemispheric activation ipsilateral to the paretic hand correlates with functional recovery after stroke." Brain **125**(Pt 7): 1544-1557.

J. Stanley and R. C. Miall (2007). "Functional activation in parieto-premotor and visual areas dependent on congruency between hand movement and visual stimuli during motor-visual priming." Neuroimage **34**(1): 290-299.

A. Stark, Z. Meiner, R. Lefkovitz and N. Levin (2012). "Plasticity in cortical motor upper-limb representation following stroke and rehabilitation: two longitudinal multi-joint FMRI case-studies." Brain Topogr **25**(2): 205-219.

J. Steffener, M. Tabert, A. Reuben and Y. Stern (2010). "Investigating hemodynamic response variability at the group level using basis functions." Neuroimage **49**(3): 2113-2122.

I. Stepniewska, P. C. Fang and J. H. Kaas (2005). "Microstimulation reveals specialized subregions for different complex movements in posterior parietal cortex of prosimian galagos." Proc Natl Acad Sci U S A **102**(13): 4878-4883.

J. P. Szaflarski, S. J. Page, B. M. Kissela, J. H. Lee, P. Levine and S. M. Strakowski (2006). "Cortical reorganization following modified constraint-induced movement therapy: a study of 4 patients with chronic stroke." Arch Phys Med Rehabil **87**(8): 1052-1058.

W. Tominaga, J. Matsubayashi, Y. Deguchi, C. Minami, T. Kinai, M. Nakamura, T. Nagamine, M. Matsuhashi, T. Mima, H. Fukuyama and A. Mitani (2009). "A mirror reflection of a hand modulates stimulus-induced 20-Hz activity." Neuroimage **46**(2): 500-504.

P. Touzalin-Chretien and A. Dufour (2008). "Motor cortex activation induced by a mirror: evidence from lateralized readiness potentials." J Neurophysiol **100**(1): 19-23.

E. Tunik, J. C. Houk and S. T. Grafton (2009). "Basal ganglia contribution to the initiation of corrective submovements." Neuroimage **47**(4): 1757-1766.

C. Urgesi, M. Candidi, S. Ionta and S. M. Aglioti (2007). "Representation of body identity and body actions in extrastriate body area and ventral premotor cortex." Nature neuroscience **10**(1): 30-31.

A. Viau, A. G. Feldman, B. J. McFadyen and M. F. Levin (2004). "Reaching in reality and virtual reality: a comparison of movement kinematics in healthy subjects and in adults with hemiparesis." J Neuroeng Rehabil **1**(1): 11.

N. S. Ward, M. M. Brown, A. J. Thompson and R. S. Frackowiak (2003). "Neural correlates of motor recovery after stroke: a longitudinal fMRI study." Brain **126**(Pt 11): 2476-2496.

C. Weiller, S. C. Ramsay, R. J. Wise, K. J. Friston and R. S. Frackowiak (1993). "Individual patterns of functional reorganization in the human cerebral cortex after capsular infarction." Ann Neurol **33**(2): 181-189.

M. Wilke and K. Lidzba (2007). "LI-tool: a new toolbox to assess lateralization in functional MR-data." J Neurosci Methods **163**(1): 128-136.

S. P. Wise, S. L. Moody, K. J. Blomstrom and A. R. Mitz (1998). "Changes in motor cortical activity during visuomotor adaptation." Exp Brain Res **121**(3): 285-299.

G. Yavuzer, R. Selles, N. Sezer, S. Sutbeyaz, J. B. Bussmann, F. Koseoglu, M. B. Atay and H. J. Stam (2008). "Mirror therapy improves hand function in subacute stroke: a randomized controlled trial." Arch Phys Med Rehabil **89**(3): 393-398.

G. Yavuzer, A. Senel, M. B. Atay and H. J. Stam (2008). ""Playstation eyetoy games" improve upper extremity-related motor functioning in subacute stroke: a randomized controlled clinical trial." Eur J Phys Rehabil Med **44**(3): 237-244.

Y. Yomogida, M. Sugiura, Y. Sassa, K. Wakusawa, A. Sekiguchi, A. Fukushima, H. Takeuchi, K. Horie, S. Sato and R. Kawashima (2010). "The neural basis of agency: an fMRI study." Neuroimage **50**(1): 198-207.

S. H. You, S. H. Jang, Y. H. Kim, M. Hallett, S. H. Ahn, Y. H. Kwon, J. H. Kim and M. Y. Lee (2005). "Virtual reality-induced cortical reorganization and associated locomotor recovery in chronic stroke: an experimenter-blind randomized study." Stroke **36**(6): 1166-1171.